TECHNICAL REPORT
IGE–236 Revision 1

DRAGON THEORY MANUAL

PART 1: COLLISION PROBABILITY CALCULATIONS

G. MARLEAU

Institut de génie nucléaire
Département de génie physique
École Polytechnique de Montréal
October 2001

CONTENTS

LIST OF FIGURES

INTRODUCTION

This is the first part of a series of DRAGON theory manual that will be published over the next few years. The main goal here is to describe the collision probability integration techniques used in DRAGON. In order to achieve this goal we will first present in general term the collision probability method and introduce the various techniques used in DRAGON to discretize the transport equation. Note that we will not discuss here the algorithms used in DRAGON for solving the resulting system of collision probability equations. This omission is voluntary since the second part of the DRAGON theory manual will address this problem. We also avoided discussing the technique used in DRAGON to compute the directional collision probabilities. The reason in this case is that these probabilities are introduced in parallel with the leakage models which will also be described in part 2 of the DRAGON theory manual. Moreover, these are computed using a technique that follows closely that presented here for the standard probabilities and do not need a special treatment in DRAGON.

This report has been divided into 6 different sections. In Section 1 we will present a general derivation of the standard collision probability method and of some of its variants including the interface current technique and the $J_{\pm}$ approximation. This will be followed in Sections 2 to 4 by a description of the explicit form the collision probability integration relations take in 1–D, 2–D and 3–D geometries. Sections 5 and 6 illustrate how these integrations are implemented in DRAGON. In fact, the specific numerical quadrature used for various type of geometries and collision probability calculation options are first described in Section 5 while in Section 6 we discuss how this information is used in the EXCELL module of DRAGON to generate the collision probabilities themselves.

1 THE COLLISION PROBABILITY METHOD

This is one of the most widely used method for solving the integral form of the transport equation.[5–12] It is based on the fact that the flux at a given point a in space is proportional to the neutron source at any point b multiplied by an exponential attenuation factor which is proportional to the optical path that must be crossed by the neutron generated at b to reach a. This optical path τ, which is given by:

$$\tau = \int_a^b \Sigma(R)dR,$$

is defined by analogy with the problem of light transmission through an absorptive media.

In this section we will first present the general form of the integral neutron transport equation followed by a discussion of the discretization method that will lead to a definition of the collision probability method. A general definition of the collision probability matrices and their properties will also be presented. Finally, we will discuss how the boundary conditions can be applied in the context of the collision probability technique and additional approximations that can be applied to region interfaces which are compatible with the collision probability technique.

1.1 The Integral Transport Equation

The integro-differential form of the time independent neutron transport equation in the presence of a source is[1]

$$\left[\vec{\Omega}\cdot\vec{\nabla}+\Sigma(\vec{r},E)\right]\phi(\vec{r},\vec{\Omega},E)=Q(\vec{r},\vec{\Omega},E)=Q_s(\vec{r},\vec{\Omega},E)+Q_f(\vec{r},\vec{\Omega},E)+S(\vec{r},\vec{\Omega},E), \tag{1.1}$$

where the source term $Q(\vec{r},\vec{\Omega},E)$ has been decomposed into a scattering term $Q_s(\vec{r},\vec{\Omega},E)$:

$$Q_s(\vec{r},\vec{\Omega},E)=\int dE'\int d^2\Omega'\Sigma_s(\vec{r},\vec{\Omega}\,'\cdot\vec{\Omega},E'\rightarrow E)\phi(\vec{r},\vec{\Omega}\,',E'), \tag{1.2}$$

and a fission term $Q_f(\vec{r},\vec{\Omega},E)$

$$Q_f(\vec{r},\vec{\Omega},E)=\chi(E)\int dE'\nu\Sigma_f(\vec{r},E')\int d^2\Omega'\phi(\vec{r},\vec{\Omega}\,',E'), \tag{1.3}$$

that both depend on the neutron flux and a fixed source $S(\vec{r},\vec{\Omega})$ which is independent of the neutron flux. In the case where the fixed source identically vanishes, the above transport equation becomes an eigenvalue equation and the fission source can be modified to the form:

$$Q_f(\vec{r},\vec{\Omega},E)=\frac{\chi(E)}{k_{\mathit{eff}}}\int dE'\nu\Sigma_f(\vec{r},E')\int d^2\Omega'\phi(\vec{r},\vec{\Omega}\,',E'), \tag{1.4}$$

where k_{eff} is known as the multiplication constant.[12]

In order to simplify the notation we will consider in our derivation only the one velocity version of this equation namely:

$$\left[\vec{\Omega}\cdot\vec{\nabla}+\Sigma(\vec{r})\right]\phi(\vec{r},\vec{\Omega}),=\frac{1}{4\pi}q(\vec{r}), \tag{1.5}$$

where cross sections and the flux are assumed independent of the neutron energy E. We also considered the case where the source is isotropic by selecting $Q(\vec{r},\vec{\Omega})=\frac{1}{4\pi}q(\vec{r})$ such that:

$$\int_{\vec{\Omega}} d^2\Omega Q(\vec{r},\vec{\Omega})=\frac{1}{4\pi}\int_{\vec{\Omega}} d^2\Omega q(\vec{r})=q(\vec{r}),$$

where $q(\vec{r})$ represents the scalar source at point $\vec{r}$.

We would now like to evaluate the neutron flux at a point $\vec{r}$ due to neutron created at any point $\vec{r}\,'$ surrounding it. Since the neutron flux $\phi(\vec{r}\,', \vec{\Omega})$ at any point $\vec{r}\,'$ satisfies the transport equation, we can write the drift operator as $\vec{\Omega} \cdot \vec{\nabla}' = -d/dR$ for each point $\vec{r}\,' = \vec{r} - R\vec{\Omega}$ and the local transport equation becomes:[12]

$$\left[-\frac{d}{dR} + \Sigma(\vec{r} - R\vec{\Omega})\right] \phi(\vec{r} - R\vec{\Omega}, \vec{\Omega}) = \frac{1}{4\pi} q(\vec{r} - R\vec{\Omega}).$$

Now using the fact that:

$$-\frac{d}{dR} \exp\left[-\int_0^R \Sigma(\vec{r} - R'\vec{\Omega}) dR'\right] \phi(\vec{r} - R\vec{\Omega}, \vec{\Omega}) =$$
$$\exp\left[-\int_0^R \Sigma(\vec{r} - R'\vec{\Omega}) dR'\right] \left[-\frac{d}{dR} + \Sigma(\vec{r} - R\vec{\Omega})\right] \phi(\vec{r} - R\vec{\Omega}, \vec{\Omega}),$$

we obtain:

$$-\frac{d}{dR} e^{-\tau(R)} \phi(\vec{r} - R\vec{\Omega}, \vec{\Omega}) = \frac{1}{4\pi} e^{-\tau(R)} q(\vec{r} - R\vec{\Omega}),$$

where

$$\tau(R) = \int_0^R \Sigma(\vec{r} - R'\vec{\Omega}) dR'. \tag{1.6}$$

The above equation can be transformed to:[8]

$$\phi(\vec{r}, \vec{\Omega}) = e^{-\tau(R_S)} \phi(\vec{r}_S, \vec{\Omega}) + \frac{1}{4\pi} \int_0^R e^{-\tau(R')} q(\vec{r}\,') dR', \tag{1.7}$$

where $\vec{r}_S$ represents a point on the surface S where boundary conditions will be applied. Integrating over all angular directions the transport equation becomes:

$$\phi(\vec{r}) = \int_S \frac{e^{-\tau(R_S)}}{R_S^2} (\vec{\Omega} \cdot \vec{N}_-) \phi_-(\vec{r}_S, \vec{\Omega}\,') d^2 r' + \int_V \frac{e^{-\tau(R)}}{4\pi R^2} q(\vec{r}\,') d^3 r', \tag{1.8}$$

where we have used

$$d^3 r = R^2 d^2\Omega dR, \tag{1.9}$$
$$(\vec{\Omega} \cdot \vec{N}_-) d^2 r = R_S^2 d^2\Omega, \tag{1.10}$$
$$\tau(x) = \int_0^x \Sigma(R) dR, \tag{1.11}$$

with $R = |\vec{r} - \vec{r}\,'|$, $R_S = |\vec{r} - \vec{r}_S|$, and where

$$\phi(\vec{r}) = \int d^2\Omega' \phi(\vec{r}, \vec{\Omega}\,'),$$

represents the scalar flux while $\phi_-(\vec{r}_S, \vec{\Omega}\,')$ is the incoming angular flux at surface S. Similarly, one can obtain an equation for the outgoing angular flux $\phi_+(\vec{r}_S, \vec{\Omega}\,')$ at S by taking the limit $\vec{r} = \vec{r}_S$ in equation Eq. (1.7):

$$\phi_+(\vec{r}_S, \vec{\Omega}) = e^{-\tau(R_S)} \phi_-(\vec{r}\,'_S, \vec{\Omega}) + \int_0^R e^{-\tau(R')} q(\vec{r}\,') dR'. \tag{1.12}$$

1.2 The Boundary Conditions

In order to ensure the closure of the above system of equations, namely Eqs. (1.8) and (1.12), boundary conditions are required. Typically, two types of boundary conditions will be considered.

In the case where there is a direct relation between the outgoing and incoming angular flux on the surface S, one uses the so-called albedo boundary condition

$$\phi_-(\vec{r}_S, \vec{\Omega} - 2(\vec{N}_S \cdot \vec{\Omega})) = \beta(\vec{r}_S, \vec{\Omega})\phi_+(\vec{r}_S, \vec{\Omega}), \tag{1.13}$$

where the albedo $\beta(\vec{r}_S, \vec{\Omega})$ represents the reflection coefficient at surface S and $\vec{\Omega} - 2(\vec{N}_S \cdot \vec{\Omega})$ is the final direction of the neutron after a mirror-like (specular) reflection. Note that vacuum boundary conditions correspond to the special case where the albedo vanishes identically.

The second type of boundary conditions we will consider are the periodic boundary conditions. In this case the neutron leaving a surface S will re-enter the cell by a different surface S' and the boundary conditions will take the form

$$\phi_-(\vec{r}_{S'}, \vec{\Omega}) = T(\vec{r}_S \rightarrow \vec{r}_{S'}, \vec{\Omega})\phi_+(\vec{r}_{S'}, \vec{\Omega}), \tag{1.14}$$

with $T(\vec{r}_S \rightarrow \vec{r}_{S'}, \vec{\Omega})$ the transmission operator.

Each of these boundary conditions can be applied in two different ways. The trivial option is to solve the transport equation for the scalar and angular flux on a finite cell, and apply directly the above relations to the angular flux at the cell limits.[2,8] An alternative is to unfold the cell to infinity using the boundary conditions and solve the transport equation only for the scalar flux. Note that in order for the second method to work, an analytical relation for summing the contribution from the sources at infinity is needed. We will discuss later the consequences of using each of these techniques in the collision probability method as well as present the summation relations required to take into account the sources at infinity.[22–24,28]

1.3 The Discretized Flux Equation

In order to obtain the discretized flux equations, we will divide the domain into N_V regions of volume V_i and assume that the cross sections and the source inside each region are constant:

$$\begin{aligned} \Sigma(\vec{r}) &= \Sigma_j \qquad \text{for } \vec{r} \in V_j, \\ q(\vec{r}) &= q_j \qquad \text{for } \vec{r} \in V_j. \end{aligned}$$

We will also consider the external boundary S to be composed of N_S surfaces of area S_α. The angular flux on these surfaces we will approximated by a limited series expansion in terms of half-range spherical harmonics $\psi^\nu(\vec{\Omega}, \vec{N}_\pm)$, namely:

$$\phi_\pm(\vec{r}_S, \vec{\Omega}) = \frac{1}{4\pi} \sum_{\nu=0}^{N_\nu} \phi_\pm^\nu(\vec{r}_S)\psi^\nu(\vec{\Omega}, \vec{N}_\pm), \tag{1.15}$$

where:[8,27]

$$\psi^\nu(\vec{\Omega}, \vec{N}_\pm) = \begin{cases} 1 & \text{for } \nu = 0 \\ \sqrt{2}(3\vec{\Omega} \cdot \vec{N}_\pm^1 - 2) & \text{for } \nu = 1 \\ 2\vec{\Omega} \cdot \vec{N}_\pm^2 & \text{for } \nu = 2 \\ 2\vec{\Omega} \cdot \vec{N}_\pm^3 & \text{for } \nu = 3 \end{cases}, \tag{1.16}$$

such that $\vec{N}_\pm^1 = \vec{N}_\pm$ with the vectors $\vec{N}_\pm^1$, $\vec{N}_\pm^2$ and $\vec{N}_\pm^3$ forming a three dimensional unit vector basis on the surface S_α. Here we considered the case where the series expansion in spherical harmonics is limited to $N_\nu = 4$. The half-range spherical harmonics satisfy the following orthogonality relations

$$\int_{(\vec{\Omega} \cdot \vec{N}_\pm) > 0} (\vec{\Omega} \cdot \vec{N}_\pm)\psi^\nu(\vec{\Omega}, \vec{N}_\pm)\psi^\mu(\vec{\Omega}, \vec{N}_\pm) d^2\Omega = \pi\delta_{\nu\mu}, \tag{1.17}$$

where $\delta_{\nu\mu}$ is the Kronecker δ.

We will also define the average scalar flux inside each region as:

$$\phi_i = \frac{1}{V_i}\int_{V_i}\phi(\vec{r})d^3r, \tag{1.18}$$

while the various components of the average angular flux on each surface will be written as:

$$\phi^{\nu}_{\pm,\alpha} = \frac{4}{S_\alpha}\int_{S_\alpha} d^2r \int_{(\vec{\Omega}\cdot\vec{N}_\pm)>0} d^2\Omega(\vec{\Omega}\cdot\vec{N}_-)\psi^\nu(\vec{\Omega},\vec{N}_\pm)\phi_\pm(\vec{r}_S,\vec{\Omega}). \tag{1.19}$$

Here we may note that the case where the flux is uniform in volume V_i correspond to $\phi(\vec{r}) = \phi_i$. On the other hand, a uniform angular flux on surface S_α corresponds to:

$$\phi_\pm(\vec{r}_S,\vec{\Omega}) = \frac{1}{4\pi}\sum_{\nu=0}^{N_\nu}\phi^\nu_{\pm,\alpha}\psi^\nu(\vec{\Omega},\vec{N}_\pm). \tag{1.20}$$

We can now integrate Eq. (1.8) over each volume V_i. Using Eqs. (1.18) and (1.20) we get the following relation for the average flux in region i:

$$\begin{aligned} V_i\phi_i = &\sum_{\alpha=1}^{N_S}\sum_{\nu=0}^{N_\nu}\int_{V_i}\int_{S_\alpha}\frac{e^{-\tau(R_S)}}{4\pi R_S^2}(\vec{\Omega}\cdot\vec{N}_-)\phi^\nu_{-,\alpha}\psi^\nu(\vec{\Omega},\vec{N}_-)d^3rd^2r' \\ &+\sum_{j=1}^{N_V}\int_{V_i}\int_{V_j}\frac{e^{-\tau(R)}}{4\pi R^2}q_j d^3r'd^3r, \end{aligned} \tag{1.21}$$

where we assumed that the components of the angular flux $\phi^\nu_-(\vec{r}_S)$ are constant and equal to $\phi^\nu_{-,\alpha}$ on each surface S_α.

We can also obtain an equation for the average outgoing angular flux on surface α in the form:

$$\begin{aligned} \frac{S_\alpha}{4}\phi^\nu_{+,\alpha} = &\sum_{\beta=1}^{N_S}\sum_{\mu=0}^{N_\nu}\int_{S_\alpha}\int_{S_\beta}\frac{e^{-\tau(R_S)}}{4\pi R_S^2}(\vec{\Omega}\cdot\vec{N}_+)\psi^\nu(\vec{\Omega},\vec{N}_+)(\vec{\Omega}\cdot\vec{N}_-)\psi^\mu(\vec{\Omega},\vec{N}_-)\phi^\mu_{-,\beta}d^2rd^2r' \\ &+\sum_{j=1}^{N_V}\int_{S_\alpha}\int_{V_j}\frac{e^{-\tau(R)}}{4\pi R^2}(\vec{\Omega}\cdot\vec{N}_+)\psi^\nu(\vec{\Omega},\vec{N}_+)q_j d^3r'd^2r. \end{aligned} \tag{1.22}$$

A final comment concerns the discretization of the boundary conditions described in Eqs. (1.13) and (1.14). Using the approximations described above, we will have

$$\phi^\nu_{-,\alpha} = \phi^\nu_{0,\alpha} + \sum_{\beta=1}^{N_S}\sum_{\mu=1}^{N_\nu}A^{\nu,\mu}_{\alpha,\beta}\phi^\mu_{+,\beta}, \tag{1.23}$$

where $\phi^\mu_{0,\alpha}$ represents the fixed incoming angular flux and $A^{\mu,\nu}_{\alpha,\beta}$ is the boundary condition matrix which gives a relation between the outgoing current on a given surface and the incoming angular flux on different surfaces. Typically for purely reflective boundary conditions this matrix will be equivalent to the product of two Kronecker delta functions $\delta_{\alpha,\beta}$ and $\delta_{\mu,\nu}$. Finally note that if one relies on an unfolding of the geometry to apply the boundary conditions on the problem, one can in general avoid the use of the above approximation on the angular flux at the cell boundary.

1.4 General Definition of Collision Probabilities

Based on Eqs. (1.21) and (1.22) we can now define four types of collision probabilities:

$$\tilde{p}_{ij} = V_i p_{ij} = \int_{V_i}\int_{V_j} \frac{e^{-\tau(R)}}{4\pi R^2} d^3r' d^3r, \tag{1.24}$$

$$\tilde{p}^{\nu}_{i\alpha} = V_i p^{\nu}_{i\alpha} = \int_{V_i}\int_{S_\alpha} \frac{e^{-\tau(R_S)}}{4\pi R_S^2} (\vec{\Omega}\cdot\vec{N}_-)\psi^{\nu}(\vec{\Omega},\vec{N}_-) d^3r' d^2r, \tag{1.25}$$

$$\tilde{p}^{\nu}_{\alpha i} = \frac{S_\alpha}{4} p^{\nu}_{\alpha i} = \int_{S_\alpha}\int_{V_i} \frac{e^{-\tau(R)}}{4\pi R^2} (\vec{\Omega}\cdot\vec{N}_+)\psi^{\nu}(\vec{\Omega},\vec{N}_+) d^2r' d^3r, \tag{1.26}$$

$$\tilde{p}^{\nu\mu}_{\alpha\beta} = \frac{S_\alpha}{4} p^{\nu\mu}_{\alpha\beta} = \int_{S_\alpha}\int_{S_\beta} \frac{e^{-\tau(R_S)}}{4\pi R_S^2} (\vec{\Omega}\cdot\vec{N}_-)\psi^{\nu}(\vec{\Omega},\vec{N}_-)(\vec{\Omega}\cdot\vec{N}_+)\psi^{\mu}(\vec{\Omega},\vec{N}_+) d^2r d^2r', \tag{1.27}$$

in terms of which the transport equation becomes:

$$\phi_i = \sum_{\alpha=1}^{N_S}\sum_{\mu=0}^{N_\nu} p^{\mu}_{i\alpha}\phi^{\mu}_{-,\alpha} + \sum_{j=1}^{N_V} p_{ij} q_j, \tag{1.28}$$

$$\phi^{\nu}_{+,\alpha} = \sum_{\beta=1}^{N_S}\sum_{\mu=0}^{N_\nu} p^{\nu\mu}_{\alpha\beta}\phi^{\mu}_{-,\beta} + \sum_{j=1}^{N_V} p^{\nu}_{\alpha j} q_j, \tag{1.29}$$

or in matrix notation:

$$\vec{\phi} = \mathbf{P}_{vs}\vec{J}_- + \mathbf{P}_{vv}\vec{q}, \tag{1.30}$$

$$\vec{J}_+ = \mathbf{P}_{ss}\vec{J}_- + \mathbf{P}_{sv}\vec{q}, \tag{1.31}$$

where $\vec{\phi}$, $\vec{J}_\pm$ and $\vec{q}$ are vectors containing respectively ϕ_i, ϕ^{ν}_{α} and q_i. Similarly, the matrices $\mathbf{P}_{vv}$, $\mathbf{P}_{vs}$, $\mathbf{P}_{sv}$ and $\mathbf{P}_{ss}$ contain respectively the elements p_{ij}, $p^{\nu}_{i\alpha}$, $p^{\nu}_{\alpha i}$ and $p^{\nu\mu}_{\alpha\beta}$.

1.5 Properties of the Collision Probability Matrices

From the symmetry of the optical path τ, we can derive directly the following reciprocity relations:

$$V_i p_{ij} = \tilde{p}_{ij} = \tilde{p}_{ji} = V_j p_{ji}, \tag{1.32}$$

$$V_i p^{\nu}_{i\alpha} = \tilde{p}^{\nu}_{i\alpha} = \tilde{p}^{\nu}_{\alpha i} = \frac{S_\alpha}{4} p^{\nu}_{\alpha i}, \tag{1.33}$$

$$\frac{S_\alpha}{4} p^{\nu\mu}_{\alpha\beta} = \tilde{p}^{\nu\mu}_{\alpha\beta} = \tilde{p}^{\mu\nu}_{\beta\alpha} = \frac{S_\beta}{4} p^{\mu\nu}_{\beta\alpha}. \tag{1.34}$$

These collision probabilities also satisfy classical conservation relations that can be derived easily using the integro-differential transport equation. Integrating Eq. (1.5) over all neutron directions and over the total volume V one obtains using Stoke's theorem:

$$\int_S \vec{N}\cdot\vec{J}(\vec{r}) d^2r + \int_V \Sigma(\vec{r})\phi(\vec{r}) d^3r = \int_V q(\vec{r}) d^3r, \tag{1.35}$$

where we have used the fact that:

$$\vec{J}(\vec{r}) = \int_{\vec{\Omega}} \vec{\Omega}\phi(\vec{r},\vec{\Omega}) d^2\Omega.$$

The above equation can also be written in the following discretized form:

$$\sum_{\alpha=1}^{N_\alpha} S_\alpha \phi^0_{+,\alpha} + \sum_{i=1}^{N_i} \Sigma_i V_i \phi_i = \sum_{i=1}^{N_i} V_i q_i. \tag{1.36}$$

Now, let us assume that the source is isotropic and uniform in volume V_j and vanishes everywhere else, namely:

$$q_i = \begin{cases} 1 & \text{for } \vec{r} \in V_i \\ 0 & \text{elsewhere} \end{cases},$$

then we obtain, using Eqs. (1.28) and (1.29), the following expressions for the scalar flux and outgoing angular current:

$$\phi_i = p_{ij},$$
$$\phi^{\nu}_{+,\alpha} = p^{\nu}_{\alpha j},$$

which after substituting into Eq. (1.36) lead to:

$$\sum_{\alpha=1}^{N_\alpha} \frac{S_\alpha}{4} p^0_{\alpha j} + \sum_{i=1}^{N_i} \Sigma_i V_i p_{ij} = V_j, \tag{1.37}$$

or using the symmetry relations:

$$\sum_{\alpha=1}^{N_\alpha} p^0_{j\alpha} + \sum_{j=1}^{N_j} p_{ij} \Sigma_j = 1. \tag{1.38}$$

Similarly, if one considers the case where the incoming current is uniform on surface S_β in direction μ and zero elsewhere:

$$\phi^{\mu}_{-,\beta} = \begin{cases} 1 & \text{for } \vec{r} \in S_\beta \\ 0 & \text{elsewhere} \end{cases},$$

we will have, using the collision probabilities equation:

$$\phi_i = p^0_{i\beta},$$
$$\phi^0_{+,\alpha} = p^{0\mu}_{\alpha\beta},$$

which can be substituted in Eq. (1.36) to produce:

$$\sum_{\alpha=1}^{N_\alpha} \frac{S_\alpha}{4} p^{0\mu}_{\alpha\beta} + \sum_{i=1}^{N_i} \Sigma_i V_i p^0_{i\beta} = \frac{S_\beta}{4} \delta_{0\mu}, \tag{1.39}$$

or using the symmetry relations:

$$\sum_{\beta=1}^{N_\alpha} p^{\nu 0}_{\alpha\beta} + \sum_{i=1}^{N_i} p^0_{\alpha i} \Sigma_i = \delta_{0\nu}. \tag{1.40}$$

1.6 Multi-Region Collision Probabilities

In the case where the neutron source is identical for each region $i \in I$ (namely $q_i = q_I$ for $i \in I$), it is possible to obtain directly the average neutron flux ϕ_I in region I without having to compute the individual local components of the flux ϕ_i. Since the averaged neutron flux in region I is given by

$$\phi_I = \frac{1}{V_I} \sum_{i \in I} V_i \phi_i$$

we can write using Eq. (1.28):

$$\phi_I = \frac{1}{V_I} \sum_{i \in I} \sum_{\alpha=1}^{N_S} \sum_{\mu=0}^{N_\nu} V_i p^{\mu}_{i\alpha} \phi^{\mu}_{-,\alpha} + \frac{1}{V_I} \sum_{i \in I} \sum_{J} \sum_{j \in J}^{N_V} V_i p_{ij} q_J,$$

where we have assumed that $q_j = q_J$ for each region $j \in J$. We can therefore write

$$\phi_I = \sum_{\alpha=1}^{N_S} \sum_{\mu=0}^{N_\nu} p_{I\alpha}^{\mu} \phi_{-,\alpha}^{\mu} + \sum_J p_{IJ} q_J, \tag{1.41}$$

where we have defined:

$$V_I p_{IJ} = \tilde{p}_{IJ} = \sum_{i \in I} \sum_{j \in I} \tilde{p}_{ij} = \sum_{i \in I} \int_{V_i} \sum_{j \in I} \int_{V_j} \frac{e^{-\tau(R)}}{4\pi R^2} d^3r' d^3r, \tag{1.42}$$

$$V_I p_{I\alpha}^{\mu} = \tilde{p}_{I\alpha}^{\mu} = \sum_{i \in I} \tilde{p}_{i\alpha}^{\mu} = \sum_{i \in I} \int_{V_i} \int_{S_\alpha} \frac{e^{-\tau(R_S)}}{4\pi R_S^2} (\vec{\Omega} \cdot \vec{N}_-) \psi^{\nu}(\vec{\Omega}, \vec{N}_-) d^3r' d^2r. \tag{1.43}$$

Finally note that if region I is made up of n_I regions of identical volumes V_i, the above set of relations can be further simplified to the form:

$$p_{IJ} = \frac{1}{n_I} \sum_{i \in I} \sum_{j \in I} p_{ij} \tag{1.44}$$

$$p_{I\alpha}^{\mu} = \frac{1}{n_I} \sum_{i \in I} p_{i\alpha}^{\mu} \tag{1.45}$$

1.7 Using Boundary Conditions in the Collision Probability Method

The boundary conditions we will use here are in the form of a relation between the average outgoing angular flux $\phi_{+,\beta}^{\mu}$ on a surface S_β and the average incoming angular flux $\phi_{-,\alpha}^{\nu}$ on a different surface S_α (see Eq. (1.23)). Here we will write the boundary conditions in the following matrix form:

$$\vec{J}_- = \mathbf{A}\vec{J}_+. \tag{1.46}$$

After multiplying Eq. (1.31) by A one obtains:

$$\vec{J}_- = \mathbf{A}\mathbf{P}_{ss}\vec{J}_- + \mathbf{A}\mathbf{P}_{sv}\vec{q},$$

which, after inversion yields:

$$\vec{J}_- = (\mathbf{I} - \mathbf{A}\mathbf{P}_{ss})^{-1}\mathbf{A}\mathbf{P}_{sv}\vec{q},$$

where $\mathbf{I}$ is the identity matrix. After substitution in Eq. (1.30) one gets

$$\vec{\phi} = \left(\mathbf{P}_{vv} + \mathbf{P}_{vs}(\mathbf{I} - \mathbf{A}\mathbf{P}_{ss})^{-1}\mathbf{A}\mathbf{P}_{sv}\right)\vec{q} = \mathbf{P}_{vv}^{c}\vec{q}, \tag{1.47}$$

where

$$\begin{aligned} \mathbf{P}_{vv}^{c} &= \left(\mathbf{P}_{vv} + \mathbf{P}_{vs}(\mathbf{I} - \mathbf{A}\mathbf{P}_{ss})^{-1}\mathbf{A}\mathbf{P}_{sv}\right) \\ &= \left(\mathbf{P}_{vv} + \mathbf{P}_{vs}\mathbf{A}(\mathbf{I} - \mathbf{P}_{ss}\mathbf{A})^{-1}\mathbf{P}_{sv}\right) \\ &= \left(\mathbf{P}_{vv} + \mathbf{P}_{vs}(\mathbf{A}^{-1} - \mathbf{P}_{ss})^{-1}\mathbf{P}_{sv}\right), \end{aligned} \tag{1.48}$$

is known as the complete collision probability matrix.

In the case of albedo boundary conditions, the general form of $A_{\alpha\beta}^{\nu\mu}$ is:

$$A_{\alpha\beta}^{\nu\mu} = \beta_\alpha \delta_{\alpha\beta} \delta^{\nu\mu},$$

where β_α is the reflection coefficient at surface α. In the case of vacuum boundary conditions $\beta_\alpha = 0$ while for a total reflection on surface α we will use $\beta_\alpha = 1$. Accordingly for a totally reflected cell we will have:

$$\mathbf{P}_{vv}^{c} = \left(\mathbf{P}_{vv} + \mathbf{P}_{vs}(\mathbf{I} - \mathbf{P}_{ss})^{-1}\mathbf{P}_{sv}\right), \tag{1.49}$$

while for a cell fully surrounded by vacuum we will use:

$$\mathbf{P}_{vv}^{c} = \mathbf{P}_{vv}. \tag{1.50}$$

Finally consider a cell with one region and two external surfaces and assume that the spherical harmonics series expansion for the angular flux is limited to $N_\nu = 0$. Assuming that the various collision probability matrices take the form:

$$\begin{aligned}
\mathbf{P}_{vv} &= a, \\
\mathbf{P}_{vs} &= \begin{bmatrix} b & c \end{bmatrix}, \\
\mathbf{P}_{sv} &= \begin{bmatrix} d \\ e \end{bmatrix}, \\
\mathbf{P}_{ss} &= \begin{bmatrix} r & s \\ t & u \end{bmatrix},
\end{aligned}$$

and that periodic boundary conditions are to be imposed on the cell, namely:

$$\mathbf{A} = \begin{bmatrix} 0 & 1 \\ 1 & 0 \end{bmatrix},$$

we obtain the following result for the complete collision probability matrix:

$$\mathbf{P}_{vv}^{c} = \frac{1}{(1 - s - t + st - ru)}(a + d(br + c(1 - s)) + e(b(1 - t) + cu)).$$

One final comment on the boundary conditions. Because we use limited series expansions for the angular flux at the outer surfaces, the general form of the boundary condition matrix described above is also limited to the same expansion order. In the case where the interface between two regions is not treated explicitly as a boundary condition, the above approximation is not used which is equivalent to using an infinite, rather than a finite series expansion for the angular flux at these surfaces. We will return to this problem in the next section when we discuss the interface current method.

1.8 Interface Current Approximation

The interface current method involves a further approximation to the collision probability method.[2,8] In addition to using a limited spherical harmonics series expansion for the angular flux on the external surfaces, one also uses such an expansion at specific surfaces inside the cell. As an example, consider the case of a 1–D Cartesian cell located between $z = a$ and $z = b$, and subdivided into an even number of subregions (N_V) such that:

$$z_{i-\frac{1}{2}} \leq z \leq z_{i+\frac{1}{2}},$$

with

$$\begin{aligned}
a &= z_{-\frac{1}{2}}, \\
b &= z_{N_V+\frac{1}{2}}.
\end{aligned}$$

We may wish to use the collision probability method on the full cell, in which case the limited series expansion for the angular flux will be applied only on the two external surfaces. This represents the standard collision probability method described before. Alternatively, we could have divided the problem in two parts, namely a first cell (L) containing the first $N_V/2$ regions and a second cell (R) containing the last $N_V/2$ regions. As a result two sets of transport equations would be produced namely:

$$\vec{\phi}^{L} = \mathbf{P}_{vs}^{L}\vec{J}_{-}^{L} + \mathbf{P}_{vv}^{L}\vec{d}^{L}, \tag{1.51}$$

$$\vec{J}_{+}^{L} = \mathbf{P}_{ss}^{L}\vec{J}_{-}^{L} + \mathbf{P}_{sv}^{L}\vec{q}^{L}, \tag{1.52}$$

for the first sub-cell and

$$\vec{\phi}^R = \mathbf{P}^R_{vs}\vec{J}^R_- + \mathbf{P}^R_{vv}\vec{q}^R, \tag{1.53}$$

$$\vec{J}^R_+ = \mathbf{P}^R_{ss}\vec{J}^R_- + \mathbf{P}^R_{sv}\vec{q}^R, \tag{1.54}$$

for the second sub-cell. The two sets of collision probability matrices denoted $\mathbf{P}^L_{vv}$, $\mathbf{P}^L_{sv}$, $\mathbf{P}^L_{vs}$ and $\mathbf{P}^L_{ss}$ for the first sub-cell and $\mathbf{P}^R_{vv}$, $\mathbf{P}^R_{sv}$, $\mathbf{P}^R_{vs}$ and $\mathbf{P}^R_{ss}$ for the second sub-cell would then be computed assuming each cell to be isolated in space. Since a neutron leaving the left surface of the second sub-cell enters directly the first sub-cell by its right surface, and vice versa, there is a direct relation between the corresponding components of the $\vec{J}^R_+$ and $\vec{J}^L_-$ vectors (and $\vec{J}^R_-$ and $\vec{J}^L_+$). Defining an extended current vector as $\vec{J}^E_\pm = (\vec{J}^L_\pm, \vec{J}^R_\pm)$ we can combine Eqs. (1.52) and (1.54) to the form:

$$\vec{J}^E_+ = \mathbf{P}^E_{ss}\vec{J}^E_- + \mathbf{P}^E_{sv}\vec{q}^E, \tag{1.55}$$

where $\vec{q}^E = (\vec{q}^L, \vec{q}^R)$ and

$$\mathbf{P}^E_{ss} = \begin{bmatrix} \mathbf{P}^L_{ss} & 0 \\ 0 & \mathbf{P}^R_{ss} \end{bmatrix},$$

$$\mathbf{P}^E_{sv} = \begin{bmatrix} \mathbf{P}^L_{sv} & 0 \\ 0 & \mathbf{P}^R_{sv} \end{bmatrix}.$$

Similarly, by defining $\vec{\phi}^E = (\vec{\phi}^L, \vec{\phi}^R)$ Eqs. (1.51) and (1.53) can be combined to the form:

$$\vec{\phi}^E = \mathbf{P}^E_{vs}\vec{J}^E_- + \mathbf{P}^E_{vv}\vec{q}^E, \tag{1.56}$$

where

$$\mathbf{P}^E_{vs} = \begin{bmatrix} \mathbf{P}^L_{vs} & 0 \\ 0 & \mathbf{P}^R_{vs} \end{bmatrix},$$

$$\mathbf{P}^E_{vv} = \begin{bmatrix} \mathbf{P}^L_{vv} & 0 \\ 0 & \mathbf{P}^R_{vv} \end{bmatrix}.$$

We can now close this system of equations using boundary conditions for the outer surfaces and the angular flux continuity relation for the inner surface. Combining these condition into matrix $\mathbf{A}$ we obtain after some algebra the following final form for the interface current transport equation:

$$\vec{\phi}^E = \mathbf{P}^c_{vv}\vec{q}^E, \tag{1.57}$$

where

$$\mathbf{P}^c_{vv} = \left(\mathbf{P}^E_{vv} + \mathbf{P}^E_{vs}(\mathbf{I} - \mathbf{A}\mathbf{P}^E_{ss})^{-1}\mathbf{A}\mathbf{P}^E_{sv}\right), \tag{1.58}$$

which are identical to Eqs. (1.47) and (1.48) except that the matrix $\mathbf{A}$ now involves in addition to the original boundary conditions, angular flux continuity relations at the interfaces. Assuming that the current expansion is limited to the isotropic component for the four surfaces, as is the case for the two sub-cells problem we considered above, the matrix $\mathbf{A}$ takes the form:

$$\mathbf{A} = \begin{bmatrix} \beta_a & 0 & 0 & 0 \\ 0 & 0 & 1 & 0 \\ 0 & 1 & 0 & 0 \\ 0 & 0 & 0 & \beta_b \end{bmatrix},$$

where external albedo boundary conditions are used on surfaces a and b while internal current transmission is assumed at the interface of the two sub-cells.

Finally note that one of the perverse effects of using the interface current method in general 2 and 3–D geometries is the so-called *refraction* effect where a neutron, which would be traveling in a straight line when the full collision probability method is used, may return to its point of creation after crossing interfaces where angular flux homogenization takes place.[18,27]

1.9 The $J_{\pm}$ approximation

The so-called $J_{\pm}$ method represents the special case of the interface current method, where each individual region in a cell is considered independently.[2,16,19,25,27] As a result, the restricted spherical harmonics series expansion for the angular flux is used at each zone interface. For the 1–D case presented in Section 1.8, the number of surfaces on which the current is approximated is $2N_V$ rather than 2 for the collision probability method or 4 for the interface current method described above. The main advantage of treating each region individually is that modifying the properties in a single region does not affect the collision probabilities associated with the other regions. However, this is at the expense of using an approximate angular flux distribution on all interfaces.

One last comment on the $J_{\pm}$ method concerns the number of collision probabilities to evaluate. Since the collision probability matrix $\mathbf{P}$ associated with each region contains a single term, namely p_{11} we will have using Eq. (1.38) the relation:

$$p_{11} = \frac{1}{\Sigma_1}\left(1 - \sum_{\alpha=1}^{N_\alpha} p_{1\alpha}^0\right), \tag{1.59}$$

namely, knowledge of the leakage probabilities is sufficient to evaluate the collision probability. Similarly using Eqs. (1.33) and (1.40) we will have:

$$p_{1\alpha}^0 = \frac{S_\alpha}{4V_1\Sigma_1}\left(\delta_{0\nu} - \sum_{\beta=1}^{N_\alpha} p_{\alpha\beta}^{\nu 0}\right), \tag{1.60}$$

that is the leakage probabilities are related directly to the transmission probabilities. We will therefore have:

$$p_{11} = \frac{1}{4V_1\Sigma_1^2}\left[1 - \sum_{\alpha=1}^{N_\alpha}\left(S_\alpha\delta_{0\nu} - S_\alpha\sum_{\beta=1}^{N_\alpha} p_{\alpha\beta}^{\nu 0}\right)\right]. \tag{1.61}$$

As a result, when using the $J_{\pm}$ method, the evaluation of the transmission probabilities associated with each isolated cell is sufficient to determine the full set of collision probabilities associated with this cell.

2 COLLISION PROBABILITY IN 1–D GEOMETRIES

The collision probability definitions presented in Section 1 are all given in terms of 3–D volume and 2–D surface integrals. We will now discuss how these relations can be simplified when a 1–D Cartesian geometry is considered. Here by 1–D Cartesian geometry we mean a 3–D cell which is uniform and infinite in both the X and Y directions. This cell will generally be heterogeneous in the Z direction but not necessarily infinite. The typical 1–D Cartesian geometry we will consider is that presented in Figure 1 where each region V_k is defined as:

$$-\infty \leq x \leq \infty, \qquad -\infty \leq y \leq \infty, \qquad z_{k-\frac{1}{2}} \leq z \leq z_{k-\frac{1}{2}},$$

for $1 \leq k \leq N_V$. As a result we will have for a surface S_α perpendicular to the Z-axis ($1 \leq \alpha \leq N_S = 2$):

$$\frac{1}{S_\alpha}\int_{S_\alpha} d^2r' F(\vec{r},z') = \frac{1}{S_\alpha}\int_{-\infty}^{\infty} dx' \int_{-\infty}^{\infty} dy' F(\vec{r},z'_\alpha) = F(\vec{r},z'_\alpha), \tag{2.1}$$

while a volume integral of a function of $F(z)$ will take the form:

$$\frac{1}{V_k}\int_{V_k} d^3r' F(\vec{r},z') = \frac{1}{V_k}\int_{-\infty}^{\infty} dx' \int_{-\infty}^{\infty} dy' \int_{z_{k-\frac{1}{2}}}^{z_{k+\frac{1}{2}}} dz' F(\vec{r},z') = \frac{1}{V_k^{1D}}\int_{z_{k-\frac{1}{2}}}^{z_{k+\frac{1}{2}}} dz' F(\vec{r},z'), \tag{2.2}$$

with $V_k^{1D} = \Delta z_k = z_{k+\frac{1}{2}} - z_{k-\frac{1}{2}}$, the width of region k and the points $z_{\frac{1}{2}}$ and $z_{N_V+\frac{1}{2}}$ are associated with surfaces S_1 and S_2 respectively. For the final surface or volume integrals over $\vec{r}$ we will use spherical coordinates and write:

$$\begin{aligned}\int_{S_\beta} (\vec{\Omega}\cdot\vec{N}_-)\frac{F(\vec{r},z')}{R^2}d^2r &= \int_0^{2\pi} d\varphi \int_{-\frac{\pi}{2}}^{\frac{\pi}{2}} \sin\theta d\theta F(\varphi,\theta,R_\beta,z') \\ &= \int_0^{2\pi} d\varphi \int_0^1 du F(\varphi,u,z_\beta,z'), \end{aligned}\tag{2.3}$$

$$\begin{aligned}\int_{V_i} \frac{F(\vec{r},z')}{R^2}d^3r &= \int_0^{2\pi} d\varphi \int_{-\frac{\pi}{2}}^{\frac{\pi}{2}} \sin\theta d\theta \int_{R_{i-\frac{1}{2}}}^{R_{i+\frac{1}{2}}} dR F(\varphi,\theta,R,z') \\ &= \int_0^{2\pi} d\varphi \int_0^1 \frac{du}{u} \int_{z_{i-\frac{1}{2}}}^{z_{i+\frac{1}{2}}} dz F(\varphi,u,z,z'), \end{aligned}\tag{2.4}$$

where we have used the definition for d^3r and d^2r given respectively in Eqs. (1.9) and (1.10) and the notation $z = R\cos\theta$ and $u = \cos\theta$.

As a result the various probabilities will be defined as:

$$V_i^{1D} p_{ij} = \tilde{p}_{ij} = \frac{1}{4\pi}\int_{z_{i-\frac{1}{2}}}^{z_{i+\frac{1}{2}}} dz' \int_0^{2\pi} d\varphi \int_0^1 \frac{du}{u} \int_{z_{j-\frac{1}{2}}}^{z_{j+\frac{1}{2}}} dz\, e^{-\tau(\varphi,u,z,z')}, \tag{2.5}$$

$$V_i^{1D} p_{i\alpha}^{\nu} = \tilde{p}_{i\alpha}^{\nu} = \frac{1}{4\pi}\int_{z_{i-\frac{1}{2}}}^{z_{i+\frac{1}{2}}} dz' \int_0^{2\pi} d\varphi \int_0^1 du\, \psi^\nu(\vec{\Omega},\vec{N}_-)\, e^{-\tau(\varphi,u,z_\alpha,z')}, \tag{2.6}$$

$$\frac{1}{4}p_{\alpha i}^{\nu} = \tilde{p}_{\alpha i}^{\nu} = \frac{1}{4\pi}\int_0^{2\pi} d\varphi \int_0^1 \frac{du}{u} \int_{z_{i-\frac{1}{2}}}^{z_{i+\frac{1}{2}}} dz\, (\vec{\Omega}\cdot\vec{N}_+)\psi^\nu(\vec{\Omega},\vec{N}_+)\, e^{-\tau(\varphi,u,z,z'_\alpha)}, \tag{2.7}$$

$$\frac{1}{4}p_{\alpha\gamma}^{\nu\mu} = \tilde{p}_{\alpha\gamma}^{\nu\mu} = \frac{1}{4\pi}\int_0^{2\pi} d\varphi \int_0^1 du\, (\vec{\Omega}\cdot\vec{N}_+)\psi^\mu(\vec{\Omega},\vec{N}_+)\psi^\nu(\vec{\Omega},\vec{N}_-)\, e^{-\tau(\varphi,u,z_\gamma,z'_\gamma)}. \tag{2.8}$$

2.1 Finite Cells Collision Probabilities

Here we will consider the 1–D cell presented in Figure 1. We will first assume that it is isolated in space, namely, vacuum boundary conditions are to be applied on the external surfaces (S_1 and S_2) associated with this cell.

2.1.1 The collision probability $\tilde{p}_{ij}$

Let us consider the expression for $\tilde{p}_{ij}$ given in Eq. (2.5). According to the notation given in Figure 1 we can write:

$$\tau(R) = \begin{cases} \frac{1}{u}\left((z_{i+\frac{1}{2}} - z')\Sigma_i + \sum_{k=i+1}^{j-1}\Delta z_k\Sigma_k + (z - z_{j-\frac{1}{2}})\Sigma_j\right) & \text{for } i < j \\ \frac{1}{u}\left((z_{j+\frac{1}{2}} - z')\Sigma_j + \sum_{k=j+1}^{i-1}\Delta z_k\Sigma_k + (z - z_{i-\frac{1}{2}})\Sigma_i\right) & \text{for } i > j \\ \frac{1}{u}(z - z')\Sigma_i & \text{for } i = j \text{ and } z' \le z \\ \frac{1}{u}(z' - z)\Sigma_i & \text{for } i = j \text{ and } z' \ge z \end{cases}, \tag{2.9}$$

where we have used the fact that $R = z/u$. In the case where $i < j$ and both Σ_i and Σ_j are not 0 we will need to evaluate the following integrals over z and z'. :

$$\begin{aligned} I(z,z') &= \int_{z_{i-\frac{1}{2}}}^{z_{i+\frac{1}{2}}} dz' \int_{z_{j-\frac{1}{2}}}^{z_{j+\frac{1}{2}}} dz\, \exp\left(-\frac{1}{u}\left((z_{i+\frac{1}{2}} - z')\Sigma_i + \sum_{k=i+1}^{j-1}\Delta z_k\Sigma_k + (z - z_{j-\frac{1}{2}})\Sigma_j\right)\right] \\ &= \exp\left(-\frac{1}{u}\sum_{k=i+1}^{j-1}\Delta z_k\Sigma_k\right)\left[\int_{z_{i-\frac{1}{2}}}^{z_{i+\frac{1}{2}}} dz' e^{-\frac{\Sigma_i}{u}(z_{i+\frac{1}{2}} - z')}\right]\left[\int_{z_{j-\frac{1}{2}}}^{z_{j+\frac{1}{2}}} dz e^{-\frac{\Sigma_j}{u}(z - z_{j-\frac{1}{2}})}\right] \end{aligned} \tag{2.10}$$

These integrals are trivial and yield:

$$\begin{aligned} I(z,z') &= \frac{u^2}{\Sigma_i\Sigma_j}\left[\exp\left(-\frac{1}{u}\sum_{k=i+1}^{j-1}\Delta z_k\Sigma_k\right) - \exp\left(-\frac{1}{u}\sum_{k=i}^{j-1}\Delta z_k\Sigma_k\right)\right. \\ &\quad \left. - \exp\left(-\frac{1}{u}\sum_{k=i+1}^{j}\Delta z_k\Sigma_k\right) + \exp\left(-\frac{1}{u}\sum_{k=i}^{j}\Delta z_k\Sigma_k\right)\right] \\ &= \frac{u^2}{\Sigma_i\Sigma_j}\left[F_{i-\frac{1}{2},j+\frac{1}{2}}(u) - F_{i-\frac{1}{2},j-\frac{1}{2}}(u) - F_{i+\frac{1}{2},j+\frac{1}{2}}(u) + F_{i+\frac{1}{2},j-\frac{1}{2}}(u)\right] \end{aligned} \tag{2.11}$$

where

$$F_{i\pm\frac{1}{2},j\pm\frac{1}{2}}(u) = \exp\left[-\left(\frac{\tau_{i\pm\frac{1}{2},j\pm\frac{1}{2}}}{u}\right)\right], \tag{2.12}$$

and

$$\tau_{i\pm\frac{1}{2},j\pm\frac{1}{2}} = \Sigma_i(z_{i+\frac{1}{2}} - z_{i\pm\frac{1}{2}}) + \sum_{k=i+1}^{j-1}\Sigma_k(z_{k+\frac{1}{2}} - z_{k-\frac{1}{2}}) + \Sigma_j(z_{j\pm\frac{1}{2}} - z_{j-\frac{1}{2}}). \tag{2.13}$$

After the integration over φ has been performed we are then left with the following expression for $\tilde{p}_{ij}$

$$\tilde{p}_{ij} = \frac{1}{2\Sigma_i\Sigma_j}\int_0^1 u\, du\left[F_{i-\frac{1}{2},j+\frac{1}{2}}(u) - F_{i-\frac{1}{2},j-\frac{1}{2}}(u) - F_{i+\frac{1}{2},j+\frac{1}{2}}(u) + F_{i+\frac{1}{2},j-\frac{1}{2}}(u)\right], \tag{2.14}$$

Now, using the definition of the exponential integral (see Appendix A):

$$E_n(x) = \int_0^1 \exp\left(\frac{-x}{u}\right) u^{n-2} du, \tag{2.15}$$

we obtain:

$$\tilde{p}_{ij} = \frac{1}{2\Sigma_i\Sigma j}\left[E_3(\tau_{i-\frac{1}{2},j+\frac{1}{2}}) - E_3(\tau_{i-\frac{1}{2},j-\frac{1}{2}}) - E_3(\tau_{i+\frac{1}{2},j+\frac{1}{2}}) + E_3(\tau_{i+\frac{1}{2},j-\frac{1}{2}})\right]. \tag{2.16}$$

Three other cases may be considered. First, the case where $\Sigma_i = 0$ which leads to:

$$\tilde{p}_{ij} = \frac{V_i^{1D}}{2\Sigma_j} \int_0^1 du \left[-F_{i+\frac{1}{2},j+\frac{1}{2}}(u) + F_{i+\frac{1}{2},j-\frac{1}{2}}(u) \right],$$

since the exponential is now independent of z'. This result in:

$$\tilde{p}_{ij} = \frac{V_i^{1D}}{2\Sigma j} \left[E_2(\tau_{i+\frac{1}{2},j-\frac{1}{2}}) - E_2(\tau_{i+\frac{1}{2},j+\frac{1}{2}}) \right]. \tag{2.17}$$

We may also have $\Sigma_j = 0$ which yields:

$$\tilde{p}_{ij} = \frac{V_j^{1D}}{2\Sigma_i} \left[E_2(\tau_{i+\frac{1}{2},j-\frac{1}{2}}) - E_2(\tau_{i-\frac{1}{2},j-\frac{1}{2}}) \right], \tag{2.18}$$

since the exponential is now independent of z. Finally in the case where Σ_i and Σ_j both vanishes, the exponential function becomes independent of z and z' and we obtain

$$\tilde{p}_{ij} = \frac{V_i^{1D} V_j^{1D}}{2} E_1(\tau_{i+\frac{1}{2},j-\frac{1}{2}}). \tag{2.19}$$

In the case where $i = j$ the integral over z in Eq. (2.5) must be divided into two different parts since the expression for $\tau(R)$ with $z \leq z'$ is different from that one gets when $z > z'$. As a result we will write

$$\tilde{p}_{ii} = \frac{1}{2} \int_0^1 \left(\frac{du}{u} \right) \int_{z_{i-\frac{1}{2}}}^{z_{i+\frac{1}{2}}} dz' \left[\int_{z_{i-\frac{1}{2}}}^{z'} dz \exp\left(-\frac{\Sigma_i (z' - z)}{u} \right) + \int_{z'}^{z_{i+\frac{1}{2}}} dz \exp\left(-\frac{\Sigma_i (z - z')}{u} \right) \right].$$

The first integral over z and z' yields:

$$\int_{z_{i-\frac{1}{2}}}^{z_{i+\frac{1}{2}}} dz' \int_{z_{i-\frac{1}{2}}}^{z'} dz \exp\left(-\frac{\Sigma_i (z' - z)}{u} \right) = \frac{u^2}{\Sigma_i^2} \left[\frac{\Sigma_i V_i^{1D}}{u} + F_{i-\frac{1}{2},i+\frac{1}{2}}(u) - 1 \right]$$

while for the second integral we obtain:

$$\int_{z_{i-\frac{1}{2}}}^{z_{i+\frac{1}{2}}} dz' \int_{z'}^{z_{i+\frac{1}{2}}} dz \exp\left(-\frac{\Sigma_i (z - z')}{u} \right) = \frac{u^2}{\Sigma_i^2} \left[\frac{\Sigma_i V_i^{1D}}{u} + F_{i-\frac{1}{2},i+\frac{1}{2}}(u) - 1 \right],$$

and we will have:

$$\tilde{p}_{ii} = \frac{1}{\Sigma_i^2} \int_0^1 u du \left[\frac{\tau_{i-\frac{1}{2},i+\frac{1}{2}}}{u} + u\, F_{i-\frac{1}{2},i+\frac{1}{2}}(u) - u \right], \tag{2.20}$$

which results in:

$$\tilde{p}_{ii} = \frac{1}{2\Sigma_i^2} \left[2\tau_{i-\frac{1}{2},i+\frac{1}{2}} + 2E_3(\tau_{i-\frac{1}{2},i+\frac{1}{2}}) - 1 \right] = \frac{1}{\Sigma_i^2} \left[\tau_{i-\frac{1}{2},i+\frac{1}{2}} + E_3(\tau_{i-\frac{1}{2},i+\frac{1}{2}}) - E_3[0] \right]. \tag{2.21}$$

Finally for the case where $\Sigma_i = 0$ we obtain:

$$\tilde{p}_{ii} = \frac{1}{2} \int_0^1 \frac{1}{u} du \int_{z_{i-\frac{1}{2}}}^{z_{i+\frac{1}{2}}} dz' \int_{z_{i-\frac{1}{2}}}^{z_{i+\frac{1}{2}}} dz = \frac{(V_i^{1D})^2}{2} \int_0^1 \left(\frac{du}{u} \right), \tag{2.22}$$

which diverges.

2.1.2 The leakage probability $\tilde{p}^{\nu}_{i\alpha}$

The leakage probability $\tilde{p}^{\nu}_{i\alpha}$ is defined in Eq. (2.6). Using the notation of Figure 1 we can write:

$$\tau(R) = \begin{cases} \frac{1}{u}\left((z_{i+\frac{1}{2}} - z')\Sigma_i + \sum_{k=i+1}^{N_V} \Delta z_k \Sigma_k\right) & \text{for } i \text{ to the left of } S_\alpha \\ \frac{1}{u}\left(\sum_{k=1}^{i-1} \Delta z_k \Sigma_k + (z' - z_{i-\frac{1}{2}})\Sigma_i\right) & \text{for } i \text{ to the right of } S_\alpha \end{cases}, \tag{2.23}$$

for the optical path associated with $\tilde{p}_{i\alpha}$. We will also have $(\vec{\Omega} \cdot \vec{N}_-) = u$ with

$$\psi^{\nu}(\vec{\Omega}, \vec{N}_-) = \begin{cases} 1 & \text{for } \nu = 0 \\ \sqrt{2}(3u-2) & \text{for } \nu = 1 \\ 2\sin\theta\sin\varphi & \text{for } \nu = 2 \\ 2\sin\theta\cos\varphi & \text{for } \nu = 3 \end{cases}.$$

Accordingly, the leakage probabilities for region V_i to the left of S_α becomes after integration over z':

$$\begin{aligned} \tilde{p}^0_{i\alpha} &= \frac{1}{2\Sigma_i}\int_0^1 u\,du\left[F_{i+\frac{1}{2},\alpha}(u) - F_{i-\frac{1}{2},\alpha}(u)\right], \\ \tilde{p}^1_{i\alpha} &= \frac{\sqrt{2}}{2\Sigma_i}\int_0^1 (3u-2)u\,du\left[F_{i+\frac{1}{2},\alpha}(u) - F_{i-\frac{1}{2},\alpha}(u)\right], \\ \tilde{p}^2_{i\alpha} &= 0, \\ \tilde{p}^3_{i\alpha} &= 0, \end{aligned}$$

where the last two terms vanishes because of the integration over φ. Here we have used Eq. (4.9) for the definition of $F_{i\pm\frac{1}{2},\alpha}(u)$ and

$$\tau_{i\pm\frac{1}{2},\alpha} = \Sigma_i(z_{i+\frac{1}{2}} - z_{i\pm\frac{1}{2}}) + \sum_{k=i+1}^{N_v} \Sigma_k(z_{k+\frac{1}{2}} - z_{k-\frac{1}{2}}). \tag{2.24}$$

Integrating over u yields:

$$\tilde{p}^0_{i\alpha} = \frac{1}{2\Sigma_i}\left[E_3(\tau_{i+\frac{1}{2},\alpha}) - E_3(\tau_{i-\frac{1}{2},\alpha})\right], \tag{2.25}$$

$$\tilde{p}^1_{i\alpha} = \frac{\sqrt{2}}{2\Sigma_i}\left[3E_4(\tau_{i+\frac{1}{2},\alpha}) - 3E_4(\tau_{i-\frac{1}{2},\alpha}) - 2E_3(\tau_{i+\frac{1}{2},\alpha}) + 2E_3(\tau_{i-\frac{1}{2},\alpha})\right]. \tag{2.26}$$

In the case where V_i is to the right of S_α, the second form for $\tau(R)$ in Eq. (2.23) must be considered and we obtain:

$$\tilde{p}^0_{i\alpha} = \frac{1}{2\Sigma_i}\left[E_3(\tau_{\alpha,i-\frac{1}{2}}) - E_3(\tau_{\alpha,i+\frac{1}{2}})\right], \tag{2.27}$$

$$\tilde{p}^1_{i\alpha} = \frac{\sqrt{2}}{2\Sigma_i}\left[3E_4(\tau_{\alpha,i-\frac{1}{2}}) - 3E_4(\tau_{\alpha,i+\frac{1}{2}}) - 2E_3(\tau_{\alpha,i-\frac{1}{2}}) + 2E_3(\tau_{\alpha,i+\frac{1}{2}})\right], \tag{2.28}$$

where

$$\tau_{\alpha,j\pm\frac{1}{2}} = \sum_{k=1}^{j-1} \Sigma_k(z_{k+\frac{1}{2}} - z_{k-\frac{1}{2}}) + \Sigma_j(z_{j\pm\frac{1}{2}} - z_{j-\frac{1}{2}}). \tag{2.29}$$

Finally in the case where $\Sigma_i = 0$ the expression for $\tau(R)$ becomes independent of z' and we obtain:

$$\begin{aligned}
\tilde{p}^0_{i\alpha} &= \frac{V_i^{1D}}{2}\int_0^1 du\, F_{i+\frac{1}{2},\alpha}(u),\\
\tilde{p}^1_{i\alpha} &= \frac{\sqrt{2}V_i^{1D}}{2}\int_0^1 (3u-2)du\, F_{i+\frac{1}{2},\alpha}(u),\\
\tilde{p}^2_{i\alpha} &= 0,\\
\tilde{p}^3_{i\alpha} &= 0,
\end{aligned}$$

which leads to:

$$\tilde{p}^0_{i\alpha} = \frac{V_i^{1D}}{2}E_2(\tau_{i+\frac{1}{2},\alpha}), \tag{2.30}$$

$$\tilde{p}^1_{i\alpha} = \frac{\sqrt{2}V_i^{1D}}{2}\left[3E_3(\tau_{i+\frac{1}{2},\alpha}) - 2E_2(\tau_{i+\frac{1}{2},\alpha})\right], \tag{2.31}$$

and

$$\tilde{p}^0_{i\alpha} = \frac{V_i^{1D}}{2}E_2(\tau_{\alpha,i-\frac{1}{2}}), \tag{2.32}$$

$$\tilde{p}^1_{i\alpha} = \frac{\sqrt{2}V_i^{1D}}{2}\left[3E_3(\tau_{\alpha,i-\frac{1}{2}}) - 2E_2(\tau_{\alpha,i-\frac{1}{2}})\right]. \tag{2.33}$$

in the cases where V_i is to the left or right of S_α respectively.

2.1.3 The transmission probability $\tilde{p}^{\nu\mu}_{\alpha\gamma}$

Finally, the transmission probability $\tilde{p}^{\nu\mu}_{\alpha\gamma}$ is defined in Eq. (2.8). Following the notation of Figure 1 we can write:

$$\tau(R) = \frac{1}{u}\sum_{k=1}^{N_V}\Delta z_k \Sigma_k, \tag{2.34}$$

for the optical path associated with $\tilde{p}^{\nu\mu}_{\alpha\gamma}$. We will also have:

$$(\vec{\Omega}\cdot\vec{N}_-) = (\vec{\Omega}\cdot\vec{N}_+) = u,$$

with

$$\psi^\nu(\vec{\Omega},\vec{N}_\pm) = \begin{cases} 1 & \text{for } \nu = 0\\ \sqrt{2}(3u-2) & \text{for } \nu = 1\\ 2\sin\theta\sin\varphi & \text{for } \nu = 2\\ 2\sin\theta\cos\varphi & \text{for } \nu = 3 \end{cases}.$$

After integration over φ, the transmission probabilities from surface S_α to S_γ become:

$$\begin{aligned}
\tilde{p}^{00}_{\alpha\gamma} &= \frac{1}{2}\int_0^1 u\,du\,F_{\alpha,\gamma}(u),\\
\tilde{p}^{01}_{\alpha\gamma} &= \frac{\sqrt{2}}{2}\int_0^1 (3u-2)u\,du\,F_{\alpha,\gamma}(u),\\
\tilde{p}^{10}_{\alpha\gamma} &= \frac{\sqrt{2}}{2}\int_0^1 (3u-2)u\,du\,F_{\alpha,\gamma}(u),\\
\tilde{p}^{11}_{\alpha\gamma} &= \int_0^1 (9u^2-12u+4)u\,du\,F_{\alpha,\gamma}(u),\\
\tilde{p}^{22}_{\alpha\gamma} &= 2\int_0^1 (1-u^2)u\,du\,F_{\alpha,\gamma}(u),\\
\tilde{p}^{33}_{\alpha\gamma} &= 2\int_0^1 (1-u^2)u\,du\,F_{\alpha,\gamma}(u),
\end{aligned}$$

where the terms not given explicitly vanish identically. Again $F_{\alpha,\gamma}(u)$ is given by Eq. (4.9) with

$$\tau_{\alpha\gamma} = \sum_{k=1}^{N_V} \Delta z_k \Sigma_k. \tag{2.35}$$

Integrating over u yields:

$$\tilde{p}^{00}_{\alpha\gamma} = \frac{1}{2}E_3(\tau_{\alpha,\gamma}), \tag{2.36}$$

$$\tilde{p}^{01}_{\alpha\gamma} = -2\sqrt{2}\tilde{p}^{00}_{\alpha\gamma} + \frac{3\sqrt{2}}{2}E_4(\tau_{\alpha,\gamma}), \tag{2.37}$$

$$\tilde{p}^{10}_{\alpha\gamma} = \tilde{p}^{01}_{\alpha\gamma}, \tag{2.38}$$

$$\tilde{p}^{11}_{\alpha\gamma} = -8\tilde{p}^{00}_{\alpha\gamma} - 4\sqrt{2}\tilde{p}^{01}_{\alpha\gamma} + 9E_5(\tau_{\alpha,\gamma}), \tag{2.39}$$

$$\tilde{p}^{22}_{\alpha\gamma} = 2\left[E_3(\tau_{\alpha,\gamma}) - E_5(\tau_{\alpha,\gamma})\right], \tag{2.40}$$

$$\tilde{p}^{33}_{\alpha\gamma} = 2\left[E_3(\tau_{\alpha,\gamma}) - E_5(\tau_{\alpha,\gamma})\right]. \tag{2.41}$$

2.2 Infinite Cells Collision Probabilities

As we have stated in Section 1.2 two different techniques can be used to implement the boundary conditions, one of which consists in unfolding the cell to infinity. In principle using the collision probability method on an infinite cell is impossible since it involves an infinite sum of contribution. Here, we will show that this sum can be written in a closed form and the collision probability can be evaluated explicitly to the expense of replacing the exponential integral functions by a numerical quadrature.

2.2.1 Periodic boundary conditions

In this case the cell unfolding results in an infinite lattice with a periodicity corresponding to the cell pitch (N_V regions). Each cell i in the initial geometry will therefore appear an infinite number of times (see Figure 2). According to Eq. (1.44), the total collision probability will then be represented by the sum of the individual probabilities $\tilde{p}_{ij_k}$. The optical path from region i to j will be given by:

$$\tau_{p,m}(R) = \begin{cases} \frac{1}{u}\left((z_{i+\frac{1}{2}} - z')\Sigma_i + \sum_{k=i+1}^{j-1}\Delta z_k\Sigma_k + (z - z_{j-\frac{1}{2}})\Sigma_j + m\tau_p\right) & \text{for } i < j \\ \frac{1}{u}\left((z-z')\Sigma_i + m\tau_p\right) & \text{for } i = j \end{cases}, \tag{2.42}$$

where m represents the number of original cells the neutron must cross before reaching region j. For the case where an isolated cell is to be considered, only the term $m = 0$ is permitted and the result is identical to that obtained in Eq. (2.9). In the above $\tau_p = \tau_{\alpha\gamma}$ (see Eq. (2.35)) is independent of z and z' and represents the optical path traveled by a neutron for a full lattice period.

The contribution to the collision probability matrix coming from a neutron which has traveled an optical path $\tau_{p,m}(R)$ is:

$$\begin{aligned}(\tilde{p}_{ij})_{p,m} = \frac{1}{2\Sigma_i\Sigma_j}\int_0^1 u\,du\left[F_{i-\frac{1}{2},j+\frac{1}{2}}(u) - F_{i-\frac{1}{2},j-\frac{1}{2}}(u) - F_{i+\frac{1}{2},j+\frac{1}{2}}(u) + F_{i+\frac{1}{2},j-\frac{1}{2}}(u)\right] \\ \times (\beta_p)^m \exp\left(-\frac{m\tau_p}{u}\right).\end{aligned}$$

The coefficient β_p is the product of the transmission coefficient for each interface combination (S_α, S_γ):

$$\beta_p = A_{12}A_{21}, \tag{2.43}$$

where A_{12} and A_{21} are the transmission coefficients from surface $S_1 \rightarrow S_2$ and $S_2 \rightarrow S_1$ respectively (see Eq. (1.46)). The factor β_p represents the attenuation of the neutron flux due to the boundary condition for a neutron travelling through a single cell. After summing over all possible values of m we can write

$$\begin{aligned}\tilde{p}_{ij} = \frac{1}{2\Sigma_i\Sigma_j}\int_0^1 u\,du\left[F_{i-\frac{1}{2},j+\frac{1}{2}}(u) - F_{i-\frac{1}{2},j-\frac{1}{2}}(u) - F_{i+\frac{1}{2},j+\frac{1}{2}}(u) + F_{i+\frac{1}{2},j-\frac{1}{2}}(u)\right] \\ \times \left[1 - \beta_p \exp\left(-\frac{\tau_p}{u}\right)\right]^{-1},\end{aligned} \tag{2.44}$$

using the fact that

$$\sum_{m=0}^{\infty}(\beta_p)^m \exp\left(-\frac{m\tau_p}{u}\right) = \sum_{m=0}^{\infty}\left[\beta_p \exp\left(-\frac{\tau_p}{u}\right)\right]^m = \left[1 - \beta_p \exp\left(-\frac{\tau_p}{u}\right)\right]^{-1}. \tag{2.45}$$

Here the last integration over u can no longer be expressed in terms of exponential functions and will require a numerical integration.

Note that in order to complete this evaluation one should sum the above expression over the $M = \infty$ possible location of region i in the unfolded lattice and then divide by M as specified by Eq. (1.44). Since the individual $\tilde{p}_{ij}$ are identical, the final relation for the total collision probability is identical to that presented in Eq. (2.44).

2.2.2 Albedo boundary conditions

In the case where albedo (reflection) boundary conditions are considered, the problem is more complex since the periodicity of the infinite lattice is now equal to two lattice pitches ($2 \times N_V$ instead of N_V). Moreover, each cell i will need to be considered twice inside the elementary periodic lattice (see Figure 3). In this case the optical path from region i to j will be given by:

$$\tau_{r,m}(R) = \begin{cases}\frac{1}{u}\left((z_{i+\frac{1}{2}} - z')\Sigma_i + \sum_{k=i+1}^{j-1}\Delta z_k\Sigma_k + (z - z_{j-\frac{1}{2}})\Sigma_j + m\tau_r\right) & \text{for } i < j \\ \frac{1}{u}\left((z - z')\Sigma_i + m\tau_r\right) & \text{for } i = j\end{cases}, \tag{2.46}$$

with

$$\tau_r = 2\tau_p = 2\tau_{\alpha\gamma}$$

Here we assumed that region j is located in a cell $2m$ lattice pitch away from region j in the initial cell. In the case where i is located in the initial cell and j is in a reflected cell we obtain:

$$\tau_{2,m}(R) = \begin{cases}\frac{1}{u}\left((z_{i+\frac{1}{2}} - z')\Sigma_i + \tau_2 + (z - z_{j-\frac{1}{2}})\Sigma_j + m\tau_r\right) & \text{for } i < j \\ \frac{1}{u}\left((z_{i+\frac{1}{2}} - z')\Sigma_i + \tau_2 + (z - z_{i-\frac{1}{2}})\Sigma_i + m\tau_r\right) & \text{for } i = j\end{cases}, \tag{2.47}$$

where the index 2 reflects the fact that the neutron will have to cross surface S_2 in order to reach region j. For the situation where i is in the reflected cell and j is in the direct cell (surface S_1 is then crossed) we obtain:

$$\tau_{1,m}(R) = \begin{cases} \frac{1}{u}\left((z_{i+\frac{1}{2}} - z')\Sigma_i + \tau_1 + (z - z_{j-\frac{1}{2}})\Sigma_j + m\tau_r\right) & \text{for } i < j \\ \frac{1}{u}\left((z_{i+\frac{1}{2}} - z')\Sigma_i + \tau_1 + (z - z_{i-\frac{1}{2}})\Sigma_i + m\tau_r\right) & \text{for } i = j \end{cases}, \tag{2.48}$$

where τ_2 (τ_1) is the minimum distance between region i in the original (reflected) cell and region j in the reflected (original) cell:

$$\tau_2 = \sum_{k=i+1}^{N_V} \Delta z_k \Sigma_k + \sum_{k=j+1}^{N_V} \Delta z_k \Sigma_k,$$
$$\tau_1 = \sum_{k=1}^{i-1} \Delta z_k \Sigma_k + \sum_{k=1}^{j-1} \Delta z_k \Sigma_k.$$

In the above, τ_r, τ_1 and τ_2 are all independent of z and z'. Neutrons traveling through a distance τ_r will therefore cross surfaces S_2 and S_1 successively. As a result, the neutron flux will be attenuated by a factor

$$\beta_r = \beta_2 \beta_1, \tag{2.49}$$

after each such crossing according to the boundary conditions. Accordingly, the neutron attenuation factors β_1 and β_2 will be associated with τ_1 and τ_2 respectively.

Substituting the above relation into the collision probability equation and summing all the possible contributions to region j one obtains the following results after the integration over z and z' has been performed:

$$\tilde{p}_{ij} = \frac{1}{2\Sigma_i \Sigma_j} \int_0^1 u\, du \left[F_{i-\frac{1}{2},j+\frac{1}{2}}(u) - F_{i-\frac{1}{2},j-\frac{1}{2}}(u) - F_{i+\frac{1}{2},j+\frac{1}{2}}(u) + F_{i+\frac{1}{2},j-\frac{1}{2}}(u)\right]$$
$$\times \left[1 + \beta_2 \exp\left(-\frac{\tau_2}{u}\right)\right]\left[1 - \beta_r \exp\left(-\frac{\tau_r}{u}\right)\right]^{-1}. \tag{2.50}$$

if i is located in the initial cell or

$$\tilde{p}_{ij} = \frac{1}{2\Sigma_i \Sigma_j} \int_0^1 u\, du \left[F_{i-\frac{1}{2},j+\frac{1}{2}}(u) - F_{i-\frac{1}{2},j-\frac{1}{2}}(u) - F_{i+\frac{1}{2},j+\frac{1}{2}}(u) + F_{i+\frac{1}{2},j-\frac{1}{2}}(u)\right]$$
$$\times \left[1 + \beta_1 \exp\left(-\frac{\tau_1}{u}\right)\right]\left[1 - \beta_r \exp\left(-\frac{\tau_r}{u}\right)\right]^{-1}. \tag{2.51}$$

if region i is located in the reflected cell.

As one can see, in the case where β_1 and β_2 both vanish, the result one obtains using Eqs. (2.50) and (2.51) is identical to that provided in Eq. (2.14). Even if only one of β_1 or β_2 vanishes the last term in Eqs. (2.50) and (2.51) disappears and we are left with an integral of the form given in Eq. (2.14).

2.3 Verification of the Conservation Relations for Finite Cells Collision Probabilities

Here for completeness we will prove that the expressions described above for the collision probabilities satisfy the conservation relations described in Eqs. (1.38) and (1.40) of Section 1. We will first write Eq. (2.5) as:

$$\sum_{j=1}^{N_j} p_{ij}\Sigma_j = \sum_{j=1}^{i-1} p_{ij}\Sigma_j + p_{ii}\Sigma_j + \sum_{j=i+1}^{N_j} p_{ij}\Sigma_j.$$

Using Eqs. (2.16) and (2.20) and the fact that i is to the left of surface α and to the right of surface γ we can write:

$$\sum_{j=1}^{N_j} p_{ij}\Sigma_j = \frac{1}{2\Sigma_i V_i^{1D}}\left[E_3(\tau_{i-\frac{1}{2},\alpha}) - E_3(\tau_{i+\frac{1}{2},\alpha})) - E_3(\tau_{\gamma,i-\frac{1}{2}}) + E_3(\tau_{\gamma,i+\frac{1}{2}})) + 2\tau_{i-\frac{1}{2},i+\frac{1}{2}}\right].$$

where we have used:

$$\tau_{i\pm\frac{1}{2},N_V+\frac{1}{2}} = \tau_{i\pm\frac{1}{2},\alpha},$$
$$\tau_{1-\frac{1}{2},i\pm\frac{1}{2}} = \tau_{\gamma+i\pm\frac{1}{2}},$$
$$E_n(\tau_{i\pm\frac{1}{2},i\pm\frac{1}{2}}) = E_n(0) = \frac{1}{n-1}$$

Similarly, using Eqs. (2.25) and (2.27) we can write

$$\sum_{\alpha=1}^{N_\alpha} p^0_{i\alpha} = \frac{2}{\Sigma_i V_i^{1D}} \left[E_3(\tau_{i+\frac{1}{2},\alpha}) - E_3(\tau_{i-\frac{1}{2},\alpha}) + E_3(\tau_{\gamma,i-\frac{1}{2}}) - E_3(\tau_{\gamma,i+\frac{1}{2}}) \right].$$

Adding these two terms yields:

$$\frac{1}{2\Sigma_i V_i^{1D}} \left[2\tau_{i-\frac{1}{2},i+\frac{1}{2}} \right] = 1.$$

as expected.

3 COLLISION PROBABILITY IN 2–D GEOMETRIES

Let us first discuss how the 3–D volume and 2–D surface integrals required in the evaluation of the collision probabilities can be simplified when a 2–D geometry is considered. We will assume that the geometries we wish to consider are infinite and uniform in the Z direction while their extension in a plane perpendicular to this axis is finite and identified by a two dimensional vector $\vec{\rho}$ as illustrated Figures 4 and 5.

For the final volume or surface integrals over $\vec{r}$, we will use spherical coordinates. From the definition for d^3r and d^2r given respectively in Eqs. (1.9) and (1.10) we will write:

$$\int_{V_i} \frac{F(\vec{r})}{R^2} d^3r = \int_0^{2\pi} d\varphi \int_{-\frac{\pi}{2}}^{\frac{\pi}{2}} \sin\theta d\theta \int_{R_{i-\frac{1}{2}}}^{R_{i+\frac{1}{2}}} dR F(\varphi, \theta, R),$$

$$\int_{V_i} (\vec{\Omega} \cdot \vec{N}_-) \frac{F(\vec{r})}{R^2} d^2r = \int_0^{2\pi} d\varphi \int_{-\frac{\pi}{2}}^{\frac{\pi}{2}} \sin\theta d\theta F(\varphi, \theta, R_S),$$

which become:

$$\int_{V_i} \frac{F(\vec{r})}{R^2} d^3r = \int_0^{2\pi} d\varphi \int_{-1}^{1} \left(\frac{du}{\sqrt{1-u^2}} \right) \int_{\rho_{i-\frac{1}{2}}}^{\rho_{i+\frac{1}{2}}} d\rho F(\varphi, u, \rho), \tag{3.1}$$

$$\int_{V_i} (\vec{\Omega} \cdot \vec{N}_-) \frac{F(\vec{r})}{R^2} d^2r = \int_0^{2\pi} d\varphi \int_{-1}^{1} du F(\varphi, u, \rho_S), \tag{3.2}$$

when we use the notation $\rho = R\sin(\theta)$ with $u = \cos(\theta)$. In the case where $F(\varphi, u, \rho_S) = F(\varphi, -u, \rho_S)$, namely the integral over u is symmetric, we can write:

$$\int_{V_i} \frac{F(\vec{r})}{R^2} d^3r = 2\int_0^{2\pi} d\varphi \int_{0}^{1} \left(\frac{du}{\sqrt{1-u^2}} \right) \int_{\rho_{i-\frac{1}{2}}}^{\rho_{i+\frac{1}{2}}} d\rho F(\varphi, u, \rho), \tag{3.3}$$

$$\int_{V_i} (\vec{\Omega} \cdot \vec{N}_-) \frac{F(\vec{r})}{R^2} d^2r = 2\int_0^{2\pi} d\varphi \int_{0}^{1} du F(\varphi, u, \rho_S), \tag{3.4}$$

while we will have:

$$\int_{V_i} \frac{F(\vec{r})}{R^2} d^3r = 0, \tag{3.5}$$

$$\int_{V_i} (\vec{\Omega} \cdot \vec{N}_-) \frac{F(\vec{r})}{R^2} d^2r = 0, \tag{3.6}$$

for an anti-symmetric integrand ($F(\varphi, u, \rho_S) = -F(\varphi, -u, \rho_S)$).

The volume integral over $\vec{r}\,'$ will take the form

$$\int_{-\infty}^{\infty} dz \int_{\vec{\rho'} \in V_k} d^2\rho' = \int_{-\infty}^{\infty} dz \int_{h' \in V_k} dh' \int_{\rho' \in V_k} d\rho' = V_k.$$

Defining V_k^{2D} as:

$$\int_{h' \in V_k} dh' \int_{\rho' \in V_k} d\rho' = V_k^{2D},$$

and using the fact that the properties of the cell are uniform in the Z direction, namely $\tau(R) = \tau(h', \rho')$, we can write:

$$\frac{1}{V_k} \int_{V_k} d^3r' F(\vec{r}\,') = \frac{1}{V_k^{2D}} \int_{h' \in V_k} dh' \int_{\rho' \in V_k} d\rho' F(h', \rho'),$$

where V_k^{2D} is the surface of the region V_k projected on the 2–D plane defined by $\vec{\rho}' = (h', \rho')$. Similarly, the surface integral of a function $F(h', \rho')$ will take the form:

$$\frac{1}{S_\alpha}\int_{S_\alpha} d^2r'(\vec{\Omega}\cdot\vec{N}_+)F(h',\rho') = \frac{1}{S_\alpha^{2D}}\int_{h'\in S_\alpha} dh'(\vec{\Omega}\cdot\vec{N}_+)F(h',\rho'(h'))\frac{|\vec{\rho'}|}{|\vec{\rho'}\cdot\vec{N}_+|},$$

where S_α^{2D} represents the part of the perimeter of surface V_k^{2D} associated with S_α. Using the fact that

$$(\vec{\Omega}\cdot\vec{N}_\pm) = \sin(\theta)\frac{|\vec{\rho'}\cdot\vec{N}_\pm|}{|\vec{\rho'}|} = \sqrt{1-u^2}\frac{|\vec{\rho'}\cdot\vec{N}_\pm|}{|\vec{\rho'}|} \tag{3.7}$$

where u is defined above, we will have

$$\frac{1}{S_\alpha}\int_{S_\alpha} d^2r'(\vec{\Omega}\cdot\vec{N}_+)F(h',\rho') = \frac{1}{S_\alpha^{2D}}\int_{h'\in S_\alpha} dh'\sqrt{1-u^2}F(h',\rho'(h')).$$

Accordingly, the various probabilities will be written as:

$$V_i^{2D}p_{ij} = \tilde{p}_{ij} = \frac{1}{2\pi}\int_0^{2\pi} d\varphi\int_{h'\in V_i} dh'\int_0^1\left(\frac{du}{\sqrt{1-u^2}}\right)\int_{\rho_{i-\frac{1}{2}}}^{\rho_{i+\frac{1}{2}}} d\rho'\int_{\rho_{j-\frac{1}{2}}}^{\rho_{j+\frac{1}{2}}} d\rho\, e^{-\tau(R)}, \tag{3.8}$$

$$V_i^{2D}p_{i\alpha}^\nu = \tilde{p}_{i\alpha}^\nu = \frac{1}{2\pi}\int_0^{2\pi} d\varphi\int_{h'\in V_i} dh'\int_0^1 du\int_{\rho_{i-\frac{1}{2}}}^{\rho_{i+\frac{1}{2}}} d\rho'\,\psi^\nu(\vec{\Omega},\vec{N}_-)e^{-\tau(R_S)}, \tag{3.9}$$

$$\frac{S_\alpha^{2D}}{4}p_{\alpha j}^\nu = \tilde{p}_{\alpha j}^\nu = \frac{1}{2\pi}\int_0^{2\pi} d\varphi\int_{h'\in S_\alpha} dh'\int_0^1 du\int_{\rho_{j-\frac{1}{2}}}^{\rho_{j+\frac{1}{2}}} d\rho\,\psi^\nu(\vec{\Omega},\vec{N}_+)e^{-\tau(R)}, \tag{3.10}$$

$$\frac{S_\alpha^{2D}}{4}p_{\alpha\gamma}^{\nu\mu} = \tilde{p}_{\alpha\gamma}^{\nu\mu} = \frac{1}{2\pi}\int_0^{2\pi} d\varphi\int_{h'\in S_\alpha} dh'\int_0^1 du\sqrt{1-u^2}\,\psi^\nu(\vec{\Omega},\vec{N}_+)\psi^\mu(\vec{\Omega},\vec{N}_-)e^{-\tau(R)}, \tag{3.11}$$

for the case where the various integrand are symmetric. These vanish for anti-symmetric integrand. Note that by definition $e^{-\tau(R)}$ is always symmetric in u since:

$$R = \frac{\rho}{\sqrt{1-u^2}}.$$

The parity of the integrand will therefore only depend on that of the half-range spherical harmonics $\psi^\nu(\vec{\Omega},\vec{N}_\pm)$.

3.1 Finite Cells Collision Probabilities

Again, we will first consider a cell or an assembly isolated in space.

3.1.1 The collision probability $\tilde{p}_{ij}$

Let us consider the expression for $\tilde{p}_{ij}$ given in Eq. (3.8). According to the notation given in Figure 5 we can write:

$$\tau(R) = \begin{cases} \frac{1}{\sqrt{1-u^2}}\left((\rho_{i+\frac{1}{2}}-\rho')\Sigma_i + \sum_{k=i+1}^{j-1}\Delta\rho_k\Sigma_k + (\rho-\rho_{j-\frac{1}{2}})\Sigma_j\right) & \text{for } i<j \\ \frac{1}{\sqrt{1-u^2}}(\rho-\rho')\Sigma_i & \text{for } i=j \end{cases}, \tag{3.12}$$

where

$$\Delta\rho_k = \rho_{k+\frac{1}{2}} - \rho_{k-\frac{1}{2}},$$

Here the various $\rho_{k\pm\frac{1}{2}}$ are functions of φ. Moreover, the integrand is symmetric in u as expected.

In the case where $i < j$ and $\Sigma_i \neq 0$ and $\Sigma_j \neq 0$, the integrations over ρ and ρ' are similar to the z and z' integrations found in Eq. (2.10). These can again be evaluated in terms of the function $F_{i\pm\frac{1}{2},j\pm\frac{1}{2}}$ defined in Eq. (4.9) where we now use:

$$\tau_{i\pm\frac{1}{2},j\pm\frac{1}{2}} = \Sigma_i(\rho_{i+\frac{1}{2}} - \rho_{i\pm\frac{1}{2}}) + \sum_{k=i+1}^{j-1} \Sigma_k(\rho_{k+\frac{1}{2}} - \rho_{k-\frac{1}{2}}) + \Sigma_j(\rho_{j\pm\frac{1}{2}} - \rho_{j-\frac{1}{2}}), \tag{3.13}$$

We are then left with the following expression for $\tilde{p}_{ij}$

$$\begin{aligned}\tilde{p}_{ij} =& \frac{1}{2\pi\Sigma_i\Sigma_j}\int_0^{2\pi} d\varphi \int_{h'\in V_i} dh' \int_0^1 \sqrt{1-u^2}du \\ & \left[F_{i-\frac{1}{2},j+\frac{1}{2}}(\sqrt{1-u^2}) - F_{i-\frac{1}{2},j-\frac{1}{2}}(\sqrt{1-u^2}) - F_{i+\frac{1}{2},j+\frac{1}{2}}(\sqrt{1-u^2}) + F_{i+\frac{1}{2},j-\frac{1}{2}}(\sqrt{1-u^2})\right],\end{aligned}$$

Using the definition of the Bickley Nayler function (see Appendix B):[32]

$$\mathrm{Ki}_n(x) = \int_0^1 \exp\left(\frac{-x}{\sqrt{1-u^2}}\right)\left(\sqrt{1-u^2}\right)^{n-2} du, \tag{3.14}$$

we obtain:

$$\begin{aligned}\tilde{p}_{ij} =& \frac{1}{2\pi\Sigma_i\Sigma_j}\int_0^{2\pi} d\varphi \int_{h'\in V_i} dh' \\ & \left[\mathrm{Ki}_3(\tau_{i-\frac{1}{2},j+\frac{1}{2}}) - \mathrm{Ki}_3(\tau_{i-\frac{1}{2},j-\frac{1}{2}}) - \mathrm{Ki}_3(\tau_{i+\frac{1}{2},j+\frac{1}{2}}) + \mathrm{Ki}_3(\tau_{i+\frac{1}{2},j-\frac{1}{2}})\right].\end{aligned} \tag{3.15}$$

Three other cases may be considered. First, the case where $\Sigma_i = 0$ which leads to:

$$\begin{aligned}\tilde{p}_{ij} =& \frac{1}{2\pi\Sigma_j}\int_0^{2\pi} d\varphi \int_{h'\in V_i} dh'\Delta\rho_i \int_0^1 du \\ & \left[-F_{i+\frac{1}{2},j+\frac{1}{2}}(\sqrt{1-u^2}) + F_{i+\frac{1}{2},j-\frac{1}{2}}(\sqrt{1-u^2})\right],\end{aligned}$$

since the exponential is now independent of ρ'. This result in:

$$\begin{aligned}\tilde{p}_{ij} =& \frac{1}{2\pi\Sigma j}\int_0^{2\pi} d\varphi \left[\mathrm{Ki}_2(\tau_{i+\frac{1}{2},j-\frac{1}{2}}) - \mathrm{Ki}_2(\tau_{i+\frac{1}{2},j+\frac{1}{2}})\right]\int_{h'\in V_i} dh'\Delta\rho_i. \\ =& \frac{V_j^{2D}}{2\pi\Sigma j}\int_0^{2\pi} d\varphi \left[\mathrm{Ki}_2(\tau_{i+\frac{1}{2},j-\frac{1}{2}}) - \mathrm{Ki}_2(\tau_{i+\frac{1}{2},j+\frac{1}{2}})\right].\end{aligned} \tag{3.16}$$

We may also have $\Sigma_j = 0$ which gives:

$$\tilde{p}_{ij} = \frac{V_j^{2D}}{2\pi\Sigma_i}\int_0^{2\pi} d\varphi \left[\mathrm{Ki}_2(\tau_{i+\frac{1}{2},j-\frac{1}{2}}) - \mathrm{Ki}_2(\tau_{i-\frac{1}{2},j-\frac{1}{2}})\right]. \tag{3.17}$$

since the exponential is now independent of ρ. Finally in the case where Σ_i and Σ_j both vanish, the exponential becomes independent on both ρ and ρ' and we obtain

$$\tilde{p}_{ij} = \frac{1}{2\pi}\int_0^{2\pi} d\varphi \int_{h'\in V_i} dh'\Delta\rho_i\Delta\rho_j \mathrm{Ki}_1(\tau_{i+\frac{1}{2},j-\frac{1}{2}}). \tag{3.18}$$

In the case where $i = j$ the integral over ρ in Eq. (3.8) must be divided into two different parts since the expression for $\tau(R)$ with $\rho \leq \rho'$ is different from that one gets when $\rho > \rho'$. As a result we will write

$$\begin{aligned}\tilde{p}_{ii} =& \frac{1}{2\pi}\int_0^{2\pi} d\varphi \int_{h'\in V_i} dh' \int_0^1 \left(\frac{du}{\sqrt{1-u^2}}\right) \int_{\rho_{i-\frac{1}{2}}}^{\rho_{i+\frac{1}{2}}} d\rho' \\ & \left[\int_{\rho_{i-\frac{1}{2}}}^{\rho'} d\rho \exp\left(-\frac{\Sigma_i(\rho'-\rho)}{\sqrt{1-u^2}}\right) + \int_{\rho'}^{\rho_{i+\frac{1}{2}}} d\rho \exp\left(-\frac{\Sigma_i(\rho-\rho')}{\sqrt{1-u^2}}\right)\right].\end{aligned}$$

The integral over ρ and ρ' yields:

$$\frac{1}{\sqrt{1-u^2}}\int_{\rho_{i-\frac{1}{2}}}^{\rho_{i+\frac{1}{2}}} d\rho' \int_{\rho_{i-\frac{1}{2}}}^{\rho'} d\rho \exp\left(-\frac{\Sigma_i(\rho'-\rho)}{\sqrt{1-u^2}}\right) = \frac{\tau_{i-\frac{1}{2},i+\frac{1}{2}}}{\Sigma_i^2} + \frac{\sqrt{1-u^2}}{\Sigma_i^2}\left[F_{i-\frac{1}{2},i+\frac{1}{2}}(\sqrt{1-u^2})-1\right],$$

$$\frac{1}{\sqrt{1-u^2}}\int_{\rho_{i-\frac{1}{2}}}^{\rho_{i+\frac{1}{2}}} d\rho' \int_{\rho'}^{\rho_{i+\frac{1}{2}}} d\rho \exp\left(-\frac{\Sigma_i(\rho-\rho')}{\sqrt{1-u^2}}\right) = \frac{\tau_{i-\frac{1}{2},i+\frac{1}{2}}}{\Sigma_i^2} + \frac{\sqrt{1-u^2}}{\Sigma_i^2}\left[F_{i-\frac{1}{2},i+\frac{1}{2}}(\sqrt{1-u^2})-1\right],$$

Using

$$\int_0^1 du = 1 = \mathrm{Ki}_2(0),$$

$$\int_0^1 \sqrt{1-u^2}du = \frac{1}{2}\left(u\sqrt{1-u^2}+\arcsin(u)\right)\Big|_0^1 = \frac{\pi}{4} = \mathrm{Ki}_3(0) = \frac{\mathrm{Ki}_1(0)}{2},$$

we then obtain:

$$\begin{aligned}\tilde{p}_{ii} &= \frac{1}{\pi\Sigma_i^2}\int_0^{2\pi} d\varphi \int_{h'\in V_i} dh' \left[\tau_{i-\frac{1}{2},i+\frac{1}{2}} + \mathrm{Ki}_3(\tau_{i-\frac{1}{2},i+\frac{1}{2}}) - \frac{\pi}{4}\right] \\ &= \frac{1}{\pi\Sigma_i^2}\int_0^{2\pi} d\varphi \int_{h'\in V_i} dh' \left[\mathrm{Ki}_2(0)\tau_{i-\frac{1}{2},i+\frac{1}{2}} + \mathrm{Ki}_3(\tau_{i-\frac{1}{2},i+\frac{1}{2}}) - \mathrm{Ki}_3(0)\right] \end{aligned} \tag{3.19}$$

Finally for the case where $\Sigma_i = 0$ the above expression can be simplified to the form:

$$\tilde{p}_{ii} = \frac{1}{4}\int_0^{2\pi} d\varphi \int_{h'\in V_i} dh' \left(\Delta\rho_i\right)^2 = \frac{\mathrm{Ki}_1(0)}{2\pi}\int_0^{2\pi} d\varphi \int_{h'\in V_i} dh' \left(\Delta\rho_i\right)^2, \tag{3.20}$$

which is finite.

3.1.2 The leakage probability $\tilde{p}^{\nu}_{i\alpha}$

Using the notation of Figure 5 we can write:

$$\tau(R) = \frac{1}{\sqrt{1-u^2}}\left((\rho_{i+\frac{1}{2}}-\rho')\Sigma_i + \sum_{k=i+1}^{N_V}\Delta\rho_k\Sigma_k\right), \tag{3.21}$$

for the optical path associated with $\tilde{p}_{i\alpha}$. We will have according to Eq. (3.7):

$$(\vec{\Omega}\cdot\vec{N}_-) = \sqrt{1-u^2}\frac{|\vec{\rho}\cdot\vec{N}_-|}{|\vec{\rho}|} = \sqrt{1-u^2}\cos[\varepsilon(\varphi)] = \sqrt{1-u^2}v(\varphi), \tag{3.22}$$

where ε is generally a function of φ and

$$v(\varphi) = \cos[\varepsilon(\varphi)].$$

We will therefore use

$$\psi^{\nu}(\vec{\Omega},\vec{N}_-) = \begin{cases} 1 & \text{for } \nu = 0 \\ \sqrt{2}(3\sqrt{1-u^2}v(\varphi)-2) & \text{for } \nu = 1 \\ 2u\sqrt{1-v^2(\varphi)} & \text{for } \nu = 2 \\ 2uv(\varphi) & \text{for } \nu = 3 \end{cases}.$$

Using the notation for the surface integral presented in Eq. (3.9) for the zero order leakage probabilities ($\nu = 0$), one obtains after integration over ρ':

$$\tilde{p}^0_{i\alpha} = \frac{1}{2\pi\Sigma_i}\int_0^{2\pi} d\varphi \int_{h'\in V_i} dh' \int_0^1 \sqrt{1-u^2}du \left[F_{i+\frac{1}{2},\alpha}(\sqrt{1-u^2}) - F_{i-\frac{1}{2},\alpha}(\sqrt{1-u^2})\right].$$

Using again the definition of the Bickley Nayler function, the integral over u yields:

$$\tilde{p}^0_{i\alpha} = \frac{1}{2\pi\Sigma_i}\int_0^{2\pi} d\varphi \int_{h'\in V_i} dh' \left[\mathrm{Ki}_3(\tau_{i+\frac{1}{2},\alpha}) - \mathrm{Ki}_3(\tau_{i-\frac{1}{2},\alpha})\right]. \tag{3.23}$$

In the case where $\Sigma_i = 0$ the expression for $\tau(R)$ becomes independent of ρ' and we obtain

$$\tilde{p}^0_{i\alpha} = \frac{1}{2\pi}\int_0^{2\pi} d\varphi \int_{h'\in V_i} dh' \Delta\rho_i \mathrm{Ki}_2(\tau_{i+\frac{1}{2},\alpha}). \tag{3.24}$$

For $\tilde{p}^1_{i\alpha}$, the integrand remains symmetric in u ($\psi^1(u) = \psi^1(-u)$) and we obtain:

$$\tilde{p}^1_{i\alpha} = -2\sqrt{2}\tilde{p}^0_{i\alpha} + 3\sqrt{2}\frac{1}{2\pi\Sigma_i}\int_0^{2\pi} d\varphi \int_{h'\in V_i} dh' v\varphi \left[\mathrm{Ki}_4(\tau_{i+\frac{1}{2},\alpha}) - \mathrm{Ki}_4(\tau_{i-\frac{1}{2},\alpha})\right], \tag{3.25}$$

while $\tilde{p}^2_{i\alpha} = \tilde{p}^3_{i\alpha} = 0$ from Eq. (3.6) since $\psi^2(u) = -\psi^2(-u)$ and $\psi^3(u) = -\psi^3(-u)$.

3.1.3 The transmission probability $\tilde{p}^{\nu\mu}_{\alpha\gamma}$

Finally, for the transmission probability we can write:

$$\tau(R) = \frac{1}{\sqrt{1-u^2}}\sum_{k=1}^{N_V}\Delta\rho_k\Sigma_k = \frac{\tau_{\alpha,\gamma}}{\sqrt{1-u^2}}, \tag{3.26}$$

for the optical path associated with $\tilde{p}^{\nu\mu}_{\alpha\gamma}$. We will also use:

$$(\vec{\Omega}\cdot\vec{N}_+) = \sqrt{1-u^2}\frac{|\vec{\rho}\cdot\vec{N}_+|}{|\vec{\rho}|} = \sqrt{1-u^2}\cos[\eta(\varphi)] = \sqrt{1-u^2}w(\varphi), \tag{3.27}$$

where η is generally a function of φ and

$$w(\varphi) = \cos[\eta(\varphi)],$$

with

$$\psi^\nu(\vec{\Omega},\vec{N}_+) = \begin{cases} 1 & \text{for } \nu = 0 \\ \sqrt{2}(3\sqrt{1-u^2}w(\varphi) - 2) & \text{for } \nu = 1 \\ 2u\sqrt{1-w^2(\varphi)} & \text{for } \nu = 2 \\ 2uw(\varphi) & \text{for } \nu = 3 \end{cases}.$$

Using the notation for the surface integral presented in Eq. (3.11), the transmission probabilities from surface S_α to S_γ become:

$$\tilde{p}^{00}_{\alpha\gamma} = \frac{1}{2\pi}\int_0^{2\pi} d\varphi \int_{h'\in V_i} dh' \mathrm{Ki}_3(\tau_{\alpha,\gamma}), \tag{3.28}$$

$$\tilde{p}^{01}_{\alpha\gamma} = -2\sqrt{2}\tilde{p}^{00}_{\alpha\gamma} + \frac{3\sqrt{2}}{2\pi}\int_0^{2\pi} d\varphi \int_{h'\in V_i} dh' v(\varphi)\mathrm{Ki}_4(\tau_{\alpha,\gamma}), \tag{3.29}$$

$$\tilde{p}^{10}_{\alpha\gamma} = -2\sqrt{2}\tilde{p}^{00}_{\alpha\gamma} + \frac{3\sqrt{2}}{2\pi}\int_0^{2\pi} d\varphi \int_{h'\in V_i} dh' w(\varphi)\mathrm{Ki}_4(\tau_{\alpha,\gamma}), \tag{3.30}$$

$$\tilde{p}^{11}_{\alpha\gamma} = -8\tilde{p}^{00}_{\alpha\gamma} - 2\sqrt{2}\left(\tilde{p}^{10}_{\alpha\gamma} + \tilde{p}^{01}_{\alpha\gamma}\right) + \frac{9}{\pi}\int_0^{2\pi} d\varphi \int_{h'\in V_i} dh' w(\varphi)v(\varphi)\mathrm{Ki}_5(\tau_{\alpha,\gamma}), \tag{3.31}$$

$$\tilde{p}^{22}_{\alpha\gamma} = \frac{2}{\pi}\int_0^{2\pi} d\varphi \int_{h'\in V_i} dh' \sqrt{(1-w^2(\varphi)}\sqrt{(1-v^2(\varphi)}\left[\mathrm{Ki}_3(\tau_{\alpha,\gamma}) - \mathrm{Ki}_5(\tau_{\alpha,\gamma})\right], \tag{3.32}$$

$$\tilde{p}^{23}_{\alpha\gamma} = \frac{2}{\pi}\int_0^{2\pi} d\varphi \int_{h'\in V_i} dh' \sqrt{(1-w^2(\varphi)}v(\varphi)\left[\mathrm{Ki}_3(\tau_{\alpha,\gamma}) - \mathrm{Ki}_5(\tau_{\alpha,\gamma})\right], \tag{3.33}$$

$$\tilde{p}^{32}_{\alpha\gamma} = \frac{2}{\pi}\int_0^{2\pi} d\varphi \int_{h'\in V_i} dh' w(\varphi)\sqrt{(1-v^2(\varphi)}\left[\mathrm{Ki}_3(\tau_{\alpha,\gamma}) - \mathrm{Ki}_5(\tau_{\alpha,\gamma})\right], \tag{3.34}$$

$$\tilde{p}^{33}_{\alpha\gamma} = \frac{2}{\pi}\int_0^{2\pi} d\varphi \int_{h'\in V_i} dh' w(\varphi)v(\varphi)\left[\mathrm{Ki}_3(\tau_{\alpha,\gamma}) - \mathrm{Ki}_5(\tau_{\alpha,\gamma})\right], \tag{3.35}$$

where the terms not given explicitly vanish identically.

3.2 Infinite Cells Collision Probabilities

Here we will consider the case where the boundary conditions are applied directly on the cell geometry. Note that this technique can only be applied to cells having Cartesian surfaces. As a result one ends up with the need to compute the collision probabilities associated with an infinite cell that involves an infinite sum of path length contribution. We will show that this sum can also be written in a closed form for 2–D collision probabilities provided a cyclic tracking procedure can be selected.

3.2.1 Full periodic boundary conditions

In this case the cell unfolding results in an infinite cell with a periodicity of one lattice pitch (N_V cells) along each Cartesian direction where the periodic boundary condition is applied. Accordingly, each cell j in the initial geometry will appear an infinite number of times (see Figure 6). The optical path for a neutron traveling in direction φ along the line defined by h' from a point ρ' in region i to a point ρ in region j will be given by:

$$\tau_{p,m}(R) = \begin{cases} \frac{1}{\sqrt{1-u^2}}\left((\rho_{i+\frac{1}{2}} - \rho')\Sigma_i + \sum_{k=i+1}^{j-1}\Delta\rho_k\Sigma_k + (\rho - \rho_{j-\frac{1}{2}})\Sigma_j + m\tau_p\right) & \text{for } i < j \\ \frac{1}{\sqrt{1-u^2}}\left((\rho-\rho')\Sigma_i + m\tau_p\right) & \text{for } i = j \end{cases}, \tag{3.36}$$

where for an isolated cell $m = 0$ and the result is identical to that obtained in Eq. (3.12). In the above τ_p, which is independent of ρ' and ρ, represents the minimal optical path that a neutron, starting at a position ρ in region j, must travel in direction φ along line h' in order to reach a second time the point ρ in j after traveling through the infinite lattice. In principle, τ_p may be infinite since the neutron starting at ρ in j may never be able to reach a second time this position in j. In practice we will assume that for each value of ρ, the neutron will always be able to return to its starting point after crossing a number $j(\varphi, h')$ of cells:

$$\tau_p = \sum_{l=1}^{j(\varphi,h')} \Delta\rho_l\Sigma_l.$$

We will also define the effective transmission coefficient β_p as the product of the individual transmission coefficient $A_{\alpha\beta}$ for each pair of surfaces (S_α, S_γ) crossed by the neutron while traveling through the optical path τ_p:

$$\beta_p = \prod_\alpha A_{\alpha\gamma}, \tag{3.37}$$

where we assumed that $A_{\alpha\gamma} = A_{\gamma\alpha}$ is an element of the boundary condition matrix defined in Eq. (1.46).

We will therefore obtain after integrating over ρ' and ρ and summing over all possible value of m the following expression for the collision probability:

$$\begin{aligned}\tilde{p}_{ij} =& \frac{1}{2\pi\Sigma_i\Sigma_j}\int_0^{2\pi} d\varphi \int_{h'\in V_i} dh' \int_0^1 \sqrt{1-u^2}\left[1-\beta_p \exp\left(-\frac{\tau_p}{\sqrt{1-u^2}}\right)\right]^{-1} du \\ & \left[1-\exp\left(-\frac{\tau_{i-\frac{1}{2},i+\frac{1}{2}}}{\sqrt{1-u^2}}\right)\right]\exp\left(-\frac{\tau_{i+\frac{1}{2},j-\frac{1}{2}}}{\sqrt{1-u^2}}\right)\left[1-\exp\left(-\frac{\tau_{j-\frac{1}{2},j+\frac{1}{2}}}{\sqrt{1-u^2}}\right)\right],\end{aligned} \tag{3.38}$$

where the last integration over u can no longer be expressed in terms of Bickley Nayler functions and will require a numerical integration.

3.2.2 Full albedo boundary conditions

In the case where albedo boundary conditions are considered, the problem is more complex since the periodicity of the infinite lattice is now twice the initial lattice pitch in each direction ($4 \times N_V$ instead of N_V cells). Moreover, each cell i will need to be considered four times inside the elementary periodic lattice (see Figure 7). In this case the optical path from region i to j will be given by:

$$\tau_{r,m}(R) = \begin{cases} \frac{1}{\sqrt{1-u^2}}\left((\rho_{i+\frac{1}{2}}-\rho')\Sigma_i + \tau_s + (\rho-\rho_{j-\frac{1}{2}})\Sigma_j + m\tau_r\right) & \text{for } i<j \\ \frac{1}{\sqrt{1-u^2}}\left((\rho_{i+\frac{1}{2}}-\rho')\Sigma_i + \tau_s + (\rho-\rho_{i-\frac{1}{2}})\Sigma_i + m\tau_r\right) & \text{for } i=j \end{cases}, \tag{3.39}$$

where τ_r is defined in much the same way as τ_p but for a periodic lattice containing $4N_V$ cells and τ_s is defined as the minimal optical path the neutron must travel before it reaches the point ρ in the lattice corresponding to a reflection of the original lattice along the X, the Y or both axis. In the above τ_s and τ_r are both independent of ρ and ρ'. As before we will define the surface attenuation factors β_r and β_s as the product of the albedo at the surfaces crossed while traveling the optical path τ_r and τ_s respectively.

Substituting the above relation in Eq. (3.8) and summing over all possible final values of m yields:

$$\begin{aligned}\tilde{p}_{ij} =& \frac{1}{2\pi\Sigma_i\Sigma_j}\int_0^{2\pi} d\varphi \int_{h'\in V_i} dh' \int_0^1 \sqrt{1-u^2}du\ \beta_s \exp\left(-\frac{\tau_s}{\sqrt{1-u^2}}\right)\left[1-\beta_r \exp\left(-\frac{\tau_r}{\sqrt{1-u^2}}\right)\right]^{-1} \\ & \left[1-\exp\left(-\frac{\tau_{i-\frac{1}{2},i+\frac{1}{2}}}{\sqrt{1-u^2}}\right)\right]\exp\left(-\frac{\tau_{i+\frac{1}{2},j-\frac{1}{2}}}{\sqrt{1-u^2}}\right)\left[1-\exp\left(-\frac{\tau_{j-\frac{1}{2},j+\frac{1}{2}}}{\sqrt{1-u^2}}\right)\right],\end{aligned} \tag{3.40}$$

The technique described above also works for the case where one mixes both periodic and albedo boundary conditions, namely the cell is periodic in one direction and symmetric in the other. However, in this case the periodicity of the infinite lattice is twice the initial lattice pitch in the reflected direction and equal to the original lattice pitch in the other direction ($2 \times N_V$ instead of N_V cells).

4 COLLISION PROBABILITY IN 3–D GEOMETRIES

We will assume that the geometry we wish to consider is that which is illustrated in Figure 8. For the final volume or surface integrals over $\vec{r}$, we will consider spherical coordinates. Using the definition for d^3r and d^2r given respectively in Eqs. (1.9) and (1.10) we will write:

$$\int_{V_i} \frac{F(\vec{r})}{R^2} d^3r = \int_0^{4\pi} d^2\Omega \int_{R_{i-\frac{1}{2}}}^{R_{i+\frac{1}{2}}} dR F(\vec{\Omega}, R), \tag{4.1}$$

$$\int_{V_i} (\vec{\Omega} \cdot \vec{N}_-) \frac{F(\vec{r})}{R^2} d^2r = \int_0^{4\pi} d^2\Omega F(\vec{\Omega}, R_S), \tag{4.2}$$

when $\vec{\Omega}$ is a solid angle which represents the neutron direction of travel.

The initial volume integral will be represented as

$$\int_{x' \in V_k} dx' \int_{y' \in V_k} dy' \int_{R' \in V_k} dR' = V_k^{3D} = V_k,$$

where R' is the distance traveled by the neutron in the region k on a line parallel to the direction $\vec{\Omega}$ while x' and y' define a plane in three dimensions normal to this direction. Accordingly for a function $F(\vec{r}') = F(x', y', R')$, we will write:

$$\frac{1}{V_k} \int_{V_k} d^3r' F(\vec{r}') = \frac{1}{V_k^{3D}} \int_{x' \in V_k} dx' \int_{y' \in V_k} dy' \int_{R' \in V_k} dR' F(x', y', R').$$

Similarly, the surface integral of a function $F(x', y', R')$ will take the form:

$$\frac{1}{S_\alpha} \int_{S_\alpha} d^2r' (\vec{\Omega} \cdot \vec{N}_+) F(x', y', R') = \frac{1}{S_\alpha^{3D}} \int_{x' \in S_\alpha} dx' \int_{y' \in S_\alpha} dy' (\vec{\Omega} \cdot \vec{N}_+) F(x', y', R'(x', y')) \frac{|\vec{R}'|}{|\vec{R}' \cdot \vec{N}_+|},$$

where S_α^{3D} represents the part of surface V_k^{3D} associated with S_α. Using the fact that

$$(\vec{\Omega} \cdot \vec{N}_\pm) = \frac{|\vec{R}' \cdot \vec{N}_\pm|}{|\vec{R}'|}, \tag{4.3}$$

we will have

$$\frac{1}{S_\alpha} \int_{S_\alpha} d^2r' (\vec{\Omega} \cdot \vec{N}_+) F(x', y', R') = \frac{1}{S_\alpha^{3D}} \int_{x' \in S_\alpha} dx' \int_{y' \in S_\alpha} dy' F(x', y', R'(x', y')).$$

Accordingly we will define the various probabilities as:

$$V_i^{3D} p_{ij} = \tilde{p}_{ij} = \frac{1}{4\pi} \int_0^{4\pi} d^2\Omega \int_{x' \in V_i} dx' \int_{y' \in V_i} dy' \int_{R_{i-\frac{1}{2}}}^{R_{i+\frac{1}{2}}} dR' \int_{R_{j-\frac{1}{2}}}^{R_{j+\frac{1}{2}}} dR\, e^{-\tau(R)}, \tag{4.4}$$

$$V_i^{3D} p_{i\alpha}^\nu = \tilde{p}_{i\alpha}^\nu = \frac{1}{4\pi} \int_0^{4\pi} d^2\Omega \int_{x' \in V_i} dx' \int_{y' \in V_i} dy' \int_{R_{i-\frac{1}{2}}}^{R_{i+\frac{1}{2}}} dR'\, \psi^\nu(\vec{\Omega}, \vec{N}_-) e^{-\tau(R_S)}, \tag{4.5}$$

$$\frac{S_\alpha^{3D}}{4} p_{\alpha j}^\nu = \tilde{p}_{\alpha j}^\nu = \frac{1}{4\pi} \int_0^{4\pi} d^2\Omega \int_{x' \in S_\alpha} dx' \int_{y' \in S_\alpha} dy' \int_{R_{j-\frac{1}{2}}}^{R_{j+\frac{1}{2}}} dR\, \psi^\nu(\vec{\Omega}, \vec{N}_+) e^{-\tau(R)}, \tag{4.6}$$

$$\frac{S_\alpha^{3D}}{4} p_{\alpha\gamma}^{\nu\mu} = \tilde{p}_{\alpha\gamma}^{\nu\mu} = \frac{1}{4\pi} \int_0^{4\pi} d^2\Omega \int_{x' \in S_\alpha} dx' \int_{y' \in S_\alpha} dy'\, \psi^\nu(\vec{\Omega}, \vec{N}_-) \psi^\mu(\vec{\Omega}, \vec{N}_+) e^{-\tau(R_S)}. \tag{4.7}$$

4.1 Finite Cells Collision Probabilities

Again, we will first analyze the case where a cell or an assembly is isolated in space.[17,18]

4.1.1 The collision probability $\tilde{p}_{ij}$

Let us consider the expression for $\tilde{p}_{ij}$ given in Eq. (4.4). According to the notation given in Figure 8 we can write:

$$\tau(R) = \begin{cases} (R_{i+\frac{1}{2}} - R')\Sigma_i + \sum_{k=i+1}^{j-1} \Delta R_k \Sigma_k + (R - R_{j-\frac{1}{2}})\Sigma_j & \text{for } i < j \\ (R - R')\Sigma_i & \text{for } i = j \end{cases}, \tag{4.8}$$

where ΔR_k is given by,

$$\Delta R_k = R_{k+\frac{1}{2}} - R_{k-\frac{1}{2}}.$$

In the case where $i < j$ and $\Sigma_i \neq 0$ and $\Sigma_j \neq 0$ we are left with the following expression for $\tilde{p}_{ij}$ after the integration over R and R' have been performed:

$$\begin{aligned} \tilde{p}_{ij} =& \frac{1}{4\pi\Sigma_i\Sigma_j} \int_0^{4\pi} d^2\Omega \int_{x' \in V_i} dx' \int_{y' \in V_i} dy' \\ & \left[F_{i-\frac{1}{2},j+\frac{1}{2}}(1) - F_{i-\frac{1}{2},j-\frac{1}{2}}(1) - F_{i+\frac{1}{2},j+\frac{1}{2}}(1) + F_{i+\frac{1}{2},j-\frac{1}{2}}(1) \right], \end{aligned}$$

where F is defined as

$$F_{i\pm\frac{1}{2},j\pm\frac{1}{2}}(u) = \exp\left[-\left(\frac{\tau_{i\pm\frac{1}{2},j\pm\frac{1}{2}}}{u} \right) \right], \tag{4.9}$$

and

$$\begin{aligned} \tau_{i\pm\frac{1}{2},j\pm\frac{1}{2}} =& \Sigma_i(R_{i+\frac{1}{2}} - R_{i\pm\frac{1}{2}}) + \sum_{k=i+1}^{j-1} \Sigma_k(R_{k+\frac{1}{2}} - R_{k-\frac{1}{2}}) + \Sigma_j(R_{j\pm\frac{1}{2}} - R_{j-\frac{1}{2}}) \\ =& \Sigma_i(R_{i+\frac{1}{2}} - R_{i\pm\frac{1}{2}}) + \tau_{i+\frac{1}{2},j-\frac{1}{2}} + \Sigma_j(R_{j\pm\frac{1}{2}} - R_{j-\frac{1}{2}}). \end{aligned} \tag{4.10}$$

Factoring the term in $\tau_{i+\frac{1}{2},j-\frac{1}{2}}$ from the above equation we obtain:

$$\begin{aligned} \tilde{p}_{ij} =& \frac{1}{4\pi\Sigma_i\Sigma_j} \int_0^{4\pi} d^2\Omega \int_{x' \in V_i} dx' \int_{y' \in V_i} dy' \\ & \left[1 - \exp\left(-\tau_{i-\frac{1}{2},i+\frac{1}{2}} \right) \right] \exp\left(-\tau_{i+\frac{1}{2},j-\frac{1}{2}} \right) \left[1 - \exp\left(-\tau_{j-\frac{1}{2},j+\frac{1}{2}} \right) \right]. \end{aligned} \tag{4.11}$$

Three other cases may be considered, namely $\Sigma_i = 0$ which leads to:

$$\tilde{p}_{ij} = \frac{1}{4\pi\Sigma_j} \int_0^{4\pi} d^2\Omega \int_{x' \in V_i} dx' \int_{y' \in V_i} dy' \Delta R_i \exp(-\tau_{i+\frac{1}{2},j-\frac{1}{2}}) \left[1 - \exp(-\tau_{j-\frac{1}{2},j+\frac{1}{2}}) \right], \tag{4.12}$$

since the exponential is now independent of $R', \Sigma_j = 0$ which gives:

$$\tilde{p}_{ij} = \frac{1}{4\pi\Sigma_i} \int_0^{4\pi} d^2\Omega \int_{x' \in V_i} dx' \int_{y' \in V_i} dy' \Delta R_j \exp(-\tau_{i+\frac{1}{2},j-\frac{1}{2}}) \left[1 - \exp(-\tau_{i-\frac{1}{2},i+\frac{1}{2}}) \right], \tag{4.13}$$

since the exponential is now independent of R. Finally when both Σ_i and Σ_j vanish, the exponential function becomes independent on both R and R' and we obtain

$$\tilde{p}_{ij} = \frac{1}{4\pi} \int_0^{4\pi} d^2\Omega \int_{x' \in V_i} dx' \int_{y' \in V_i} dy' \Delta R_i \Delta R_j \exp(-\tau_{i+\frac{1}{2},j-\frac{1}{2}}). \tag{4.14}$$

In the case where $i = j$, the expression for $\tilde{p}_{ii}$ can be written as

$$\tilde{p}_{ii} = \frac{1}{4\pi}\int_0^{4\pi} d^2\Omega \int_{x'\in V_i} dx' \int_{y'\in V_i} dy' \left[\int_{R_{i-\frac{1}{2}}}^{R_{i+\frac{1}{2}}} dR' \int_{R_{i-\frac{1}{2}}}^{R'} dR \exp(-\Sigma_i(R'-R))\right]$$
$$+\frac{1}{4\pi}\int_0^{4\pi} d^2\Omega \int_{x'\in V_i} dx' \int_{y'\in V_i} dy' \left[\int_{R_{i-\frac{1}{2}}}^{R_{i+\frac{1}{2}}} dR' \int_{R'}^{R_{i+\frac{1}{2}}} dR \exp(-\Sigma_i(R-R'))\right].$$

The integrals over R and R' then yields:

$$\int_{R_{i-\frac{1}{2}}}^{R_{i+\frac{1}{2}}} dR' \int_{R_{i-\frac{1}{2}}}^{R'} dR \exp(-\Sigma_i(R'-R)) = \frac{\tau_{i-\frac{1}{2},i+\frac{1}{2}}}{\Sigma_i^2} - \frac{1}{\Sigma_i^2}\left[1-\exp(-\tau_{i-\frac{1}{2},i+\frac{1}{2}})\right],$$
$$\int_{R_{i-\frac{1}{2}}}^{R_{i+\frac{1}{2}}} dR' \int_{R'}^{R_{i-\frac{1}{2}}} dR \exp(-\Sigma_i(R-R')) = \frac{\tau_{i-\frac{1}{2},i+\frac{1}{2}}}{\Sigma_i^2} - \frac{1}{\Sigma_i^2}\left[1-\exp(-\tau_{i-\frac{1}{2},i+\frac{1}{2}})\right],$$

and we obtain:

$$\tilde{p}_{ii} = \frac{1}{2\pi\Sigma_i^2}\int_0^{4\pi} d^2\Omega \int_{x'\in V_i} dx' \int_{y'\in V_i} dy' \left[\tau_{i-\frac{1}{2},i+\frac{1}{2}} - \left(1-\exp(-\tau_{i-\frac{1}{2},i+\frac{1}{2}})\right)\right]. \tag{4.15}$$

Finally for the case where $\Sigma_i = 0$ we obtain:

$$\tilde{p}_{ii} = \frac{1}{4\pi}\int_0^{4\pi} d^2\Omega \int_{x'\in V_i} dx' \int_{y'\in V_i} dy' \left(\Delta R_i\right)^2, \tag{4.16}$$

which is finite as in the 2–D case.

4.1.2 The leakage probability $\tilde{p}^0_{i\alpha}$

The leakage probability $\tilde{p}^{\nu}_{i\alpha}$ is defined in Eq. (4.5). Here we will consider only the case where $N_\nu = 0$, namely the isotropic leakage probability. Using the notation of Figure 8 we can write:

$$\tau(R) = (R_{i+\frac{1}{2}} - R')\Sigma_i + \sum_{k=i+1}^{N_V} \Delta R_k \Sigma_k, \tag{4.17}$$

for the optical path associated with $\tilde{p}_{i\alpha}$. We will also have:

$$\psi^0(\vec{\Omega}, \vec{N}_-) = 1.$$

Using the notation for the surface integral presented in Eq. (4.2), one obtains after integration over R':

$$\tilde{p}^0_{i\alpha} = \frac{1}{4\pi\Sigma_i}\int_0^{4\pi} d^2\Omega \int_{x'\in V_i} dx' \int_{y'\in V_i} dy' \exp(-\tau_{i+\frac{1}{2},\alpha})\left[1-\exp(-\tau_{j-\frac{1}{2},j+\frac{1}{2}})\right]. \tag{4.18}$$

In the case where $\Sigma_i = 0$ the expression for $\tau(R)$ becomes independent of R' and we obtain

$$\tilde{p}^0_{i\alpha} = \frac{1}{4\pi}\int_0^{4\pi} d^2\Omega \int_{x'\in V_i} dx' \int_{y'\in V_i} dy' \Delta R_i \exp(-\tau_{i+\frac{1}{2},\alpha}). \tag{4.19}$$

4.1.3 The transmission probability $\tilde{p}^{\nu\mu}_{\alpha\gamma}$

Finally, for the transmission probability we will have:

$$\tau(R) = \sum_{k=1}^{N_V} \Delta R_k \Sigma_k = \tau_{\alpha,\gamma}, \tag{4.20}$$

for the optical path associated with $\tilde{p}^{\nu\mu}_{\alpha\gamma}$. Using the notation for the surface integral presented in Eq. (4.2) the transmission probabilities from surface S_α to S_γ become:

$$\tilde{p}^{00}_{\alpha\gamma} = \frac{1}{4\pi} \int_0^{4\pi} d^2\Omega \int_{x' \in V_i} dx' \int_{y' \in V_i} dy' \exp(-\tau_{\alpha,\gamma}). \tag{4.21}$$

For the other components of $\tilde{p}^{\nu\mu}_{\alpha\gamma}$ the final relations will be similar to Eq. (4.21) except for the added presence of the half-range spherical harmonic.

5 COLLISION PROBABILITY TRACKING IN DRAGON

The code DRAGON can be used to evaluate numerically the collision probability matrix associated with a large number of different types of geometries.[14,15] However because of the complexity of the required calculation procedure, this work is generally divided between two different DRAGON modules. The first module, called the tracking module, consist in selecting the specific numerical quadrature scheme that will be used to analyze a given geometry and to generate the integration points and weights required for a specific problem. In the second module, called the assembly module, the summation process associated with the numerical quadrature is performed. Here, we will first present the specific numerical quadrature technique used for each possible type of geometries for the various tracking options available in the code. The discussion on how the assembly module uses this information to generate the required collision probability matrices will be presented in the next section.

5.1 Cartesian 1–D Geometries

The Cartesian 1–D geometries are generally used to simulate plate reactors in the case where the extension of the plates in two directions can be assumed infinite while their extension in the third direction is finite. There are two different tracking modules that can be used to analyze these 1–D geometries in DRAGON, namely `JPM:` and `SYBIL:`. Both modules relies on the finite cell collision probability expressions even if, as we will see, the `SYBIL` module simulates approximately an infinite cell.

5.1.1 The $J_\pm$ model

We will first discuss the $J_\pm$ model (module `JPM:`) where each individual region in the cell is considered isolated in space (see Section 1.9). In this case, the collision probabilities can be evaluated by directly using Eq. (2.20) (see Appendix A.4) and no additional numerical quadrature is required. For the cases where one region in the cell to be analyzed is completely voided, a finite result of 1×10^{20} will be arbitrarily associated to the collision probability even if this probability is theoretically divergent according to Eq. (2.22). The isotropic leakage and transmission probabilities are evaluated using Eq. (2.25) or Eq. (2.27) and Eq. (2.36). When the more precise DP_1 approximation is required (order $N_\nu = 4$ expansion in the angular flux) the anisotropic components of the leakage and transmission probabilities are also evaluated using Eq. (2.26) and Eqs. (2.36) to (2.39). On the other hand, the contributions to $\tilde{p}^{22}_{\alpha\gamma}$ and $\tilde{p}^{33}_{\alpha\gamma}$ are never considered since they are not required to solve the transport equation for the flux. This is because the terms coupling the $\nu = 2, 3$ components of the angular flux to the scalar flux vanish, namely $\tilde{p}^{2}_{i\gamma} = \tilde{p}^{3}_{i\gamma} = 0$.

In DRAGON, the `JPM` tracking module (subroutine `READ3D`) essentially evaluates the regional 1–D volume and associates with each region and surface an identification index. It also builds the boundary condition matrix that includes the surface coupling terms and the external boundary conditions.

5.1.2 The standard model

For 1–D geometries, the `SYBIL` module of DRAGON is a hybrid between the standard collision probability technique and the infinite cell collision probability method. It unfolds the geometry to infinity using the external boundary conditions, but instead of using the summation relation described in Eq. (2.45), it evaluates explicitly each path contribution to the collision probability using Eq. (2.16) and then performs the required summation. This infinite sum can be evaluated because the exponential integral function decreases rapidly with increasing optical path length. As a result, the contributions to the collision probability coming from neutron crossing an optical path longer than a fixed cutoff τ_C (with $\tau_C = 10$ in the `SYBIL` module) are neglected. One of the advantages of this technique is to bypass the explicit numerical integration of the collision probabilities dictated by Eq. (2.44) while avoiding the use of the approximate boundary conditions resulting from the treatment of a finite cell. The `SYBIL`

tracking module will essentially perform the same functions as the `JPM` tracking module (subroutine `READ3D` is used again).

5.1.3 The specular model

Because `SYBIL` already takes into account explicitly the effect of unfolding the cell to infinity, there is no module of DRAGON that uses Eq. (2.44). However, for the sake of completeness, we will present a quadrature technique that would ensure an adequate numerical integration of this equation.

Because of the apparent singularity of the integrand

$$F_{i\pm\frac{1}{2},j\pm\frac{1}{2}}(u) = \exp\left[-\left(\frac{\tau_{i\pm\frac{1}{2},j\pm\frac{1}{2}}}{u}\right)\right],$$

at $u = 0$, applying a direct trapezoidal or Gaussian quadrature is not recommended. A better choice consists in using a double Gauss–Legendre quadrature with $2 \times N_G$ points u_i such that:[22]

$$u_i = \begin{cases} 1-\mu_i & \text{for } 1 \leq i \leq N_G \\ 1-\mu_{2N_G-i+1} & \text{for } N_G+1 \leq i \leq 2N_G \end{cases},$$

with quadrature weight W_i:

$$W_i = \begin{cases} \omega_i & \text{for } 1 \leq i \leq N_G \\ \omega_{2N_G-i+1} & \text{for } N_G+1 \leq i \leq 2N_G \end{cases},$$

where μ_i and ω_i are the standard the Gauss–Legendre quadrature points and weights (see Appendix C).[31]

5.2 Annular 1–D Geometries

The annular 1–D geometries represent infinite 3–D cylindric cells with properties that are angularly uniform in a 2–D plane and vary only as a function of the radial distance from the center of the cell. The collision probabilities associated with these geometries will be computed using the relations provided in Section 3 for 2–D geometries. Because of the inherent symmetry of this problem, the one dimensional integration over φ described in Eqs. (3.8) to (3.11) is generally evaluated analytically. On the other hand, the integration over h' will be evaluated numerically, this integration taking different forms depending on the tracking technique used. Note that for annular cells an explicit treatment of the boundary conditions via cell unfolding is not possible.

5.2.1 The $J_\pm$ model

As we noted in Section 1.9 both the collision and leakage probabilities associated with an isolated cell can be derived from the transmission probabilities using the reciprocity and conservation equations. Accordingly, in the application of the $J_\pm$ model to annular 1–D geometries, we will only need to consider the integration of Eqs. (3.28) to (3.35). As we noted above we will carry out the φ integration analytically. As for the h' integration we will consider the following change of variable (see Figure 9):

$$h' = R_\alpha \sin(\epsilon),$$

where R_α represents the radius of the annulus associated with surface S_α and ϵ is the angle between the track direction and a radii to the same surface. The distance $\Delta\rho_{\alpha\alpha}$ traveled by the neutron inside this region before reaching surface S_α will be given by:

$$\Delta\rho_{\alpha\alpha} = 2R_\alpha \cos(\epsilon),$$

with the angular integration limits being:

$$\arcsin(\frac{R_\gamma}{R_\alpha}) \leq \epsilon \leq \frac{\pi}{2} \qquad \text{and} \qquad -\frac{\pi}{2} \leq \epsilon \leq -\arcsin(\frac{R_\gamma}{R_\alpha}).$$

For a neutron reaching the internal surface S_γ we will have:

$$\Delta\rho_{\alpha\gamma} = R_\alpha \cos(\epsilon) - \sqrt{R_\gamma^2 - R_\alpha^2 \sin^2(\epsilon)},$$

with

$$-\arcsin(\frac{R_\gamma}{R_\alpha}) \leq \epsilon \leq \arcsin(\frac{R_\gamma}{R_\alpha}).$$

Typically, for the numerical integration over ϵ, one could select a standard Gauss–Legendre quadrature. The problem with this choice is that both the integrand and its derivatives must be finite over all the integration range. This is not the case here since high order derivatives of the Bickley Nayler functions $\mathrm{Ki}_n(x)$ diverge when evaluated at $x = 0$ ($\epsilon = \pi/2$ for $\Delta\rho_{\alpha\alpha}$). We will therefore use a second change of variable:

$$u = \sqrt{1 - \sin(\epsilon)},$$

such that

$$\cos(\epsilon)d\epsilon = -2udu.$$

The general form of the integral will finally be such that it can be evaluated using a Gauss–Jacobi quadrature of the form (see Appendix C):

$$\int F(u)udu = \sum_{i=1}^{N} w_i F(u_i),$$

where u_i and w_i are respectively the quadrature points and weights.[31]

5.2.2 The standard model

Again we can carry out the φ integration analytically. For the remaining h' integration we will first use the fact that for any direction φ, if one defines the origin of the h' axis as the center of the concentric annular cell, the integration becomes symmetric under a transformation from $h' \rightarrow -h'$. Accordingly, $\tilde{p}_{ij}$ will be given by (see Figure 10):

$$\tilde{p}_{ij} = \frac{2}{\Sigma_i \Sigma_j} \int_0^{R_i} dh' \left[\mathrm{Ki}_3(\tau_{i-\frac{1}{2},j+\frac{1}{2}}) - \mathrm{Ki}_3(\tau_{i-\frac{1}{2},j-\frac{1}{2}}) - \mathrm{Ki}_3(\tau_{i+\frac{1}{2},j+\frac{1}{2}}) + \mathrm{Ki}_3(\tau_{i+\frac{1}{2},j-\frac{1}{2}}) \right],$$

for the contribution of neutron in region i and j both located in the first quadrant (upper right quadrant) while the neutron generated in the part of region i located in the second quadrant (upper left quadrant) will produce an additional contribution to the collision probability given by:

$$\tilde{p}_{ij} = \frac{2}{\Sigma_i \Sigma_j} \int_0^{R_i} dh' \left[\mathrm{Ki}_3(\tau_{-i-\frac{1}{2},j+\frac{1}{2}}) - \mathrm{Ki}_3(\tau_{-i-\frac{1}{2},j-\frac{1}{2}}) - \mathrm{Ki}_3(\tau_{-i+\frac{1}{2},j+\frac{1}{2}}) + \mathrm{Ki}_3(\tau_{-i+\frac{1}{2},j-\frac{1}{2}}) \right],$$

where R_i represents the outer radius of the annulus associated with region V_i and

$$\tau_{-i-\frac{1}{2},j\pm\frac{1}{2}} = 2\sum_{k=l}^{i} \Sigma_k \delta R_k(h') + \tau_{i+\frac{1}{2},j\pm\frac{1}{2}}, \tag{5.1}$$

$$\tau_{-i+\frac{1}{2},j\pm\frac{1}{2}} = 2\sum_{k=l}^{i-1} \Sigma_k \delta R_k(h') + \tau_{i-\frac{1}{2},j\pm\frac{1}{2}}, \tag{5.2}$$

$$\tau_{i\pm\frac{1}{2},j\pm\frac{1}{2}} = \delta_{i-\frac{1}{2},i\pm\frac{1}{2}} \Sigma_i \delta R_i(h') + \sum_{k=i+}^{j-1} \Sigma_k \delta R_k(h') + \delta_{j+\frac{1}{2},j\pm\frac{1}{2}} \Sigma_j \delta R_j(h'), \tag{5.3}$$

where

$$\delta R_k = \begin{cases} \sqrt{R_k^2 - h^2} - \sqrt{R_{k-1}^2 - h^2} & \text{for } R_{k-1} \geq h' \\ \sqrt{R_k^2 - h^2} & \text{for } R_{k-1} < h' \end{cases}.$$

If one classifies the regions from the inside to the outside of the cell consecutively, then the above relation becomes:

$$\tilde{p}_{ij} = \frac{2}{\Sigma_i \Sigma_j} \sum_{k=1}^{i} \int_{R_{k-1}}^{R_k} dh' \Big[\mathrm{Ki}_3(\tau_{i-\frac{1}{2},j+\frac{1}{2}}) - \mathrm{Ki}_3(\tau_{i-\frac{1}{2},j-\frac{1}{2}}) - \mathrm{Ki}_3(\tau_{i+\frac{1}{2},j+\frac{1}{2}}) + \mathrm{Ki}_3(\tau_{i+\frac{1}{2},j-\frac{1}{2}}) + \mathrm{Ki}_3(\tau_{-i-\frac{1}{2},j+\frac{1}{2}}) - \mathrm{Ki}_3(\tau_{-i-\frac{1}{2},j-\frac{1}{2}}) - \mathrm{Ki}_3(\tau_{-i+\frac{1}{2},j+\frac{1}{2}}) + \mathrm{Ki}_3(\tau_{-i+\frac{1}{2},j-\frac{1}{2}}) \Big], \tag{5.4}$$

where $R_0 = 0$. Since the integrand is a function of $\sqrt{R_k^2 - h^2}$, its first derivative will be singular when $h = R_k$ and consequently a Gauss–Legendre quadrature is not recommended. Here we will perform a second change of variable of the form:[3]

$$h' = t^2 + R_{k-1}^2,$$

and rewrite Eq. (5.4) as

$$\tilde{p}_{ij} = \frac{4}{\Sigma_i \Sigma_j} \sum_{k=1}^{i} \int_{0}^{\sqrt{R_k^2 - R_{k-1}^2}} t dt \Big[\mathrm{Ki}_3(\tau_{i-\frac{1}{2},j+\frac{1}{2}}) - \mathrm{Ki}_3(\tau_{i-\frac{1}{2},j-\frac{1}{2}}) - \mathrm{Ki}_3(\tau_{i+\frac{1}{2},j+\frac{1}{2}}) + \mathrm{Ki}_3(\tau_{i+\frac{1}{2},j-\frac{1}{2}}) + \mathrm{Ki}_3(\tau_{-i-\frac{1}{2},j+\frac{1}{2}}) - \mathrm{Ki}_3(\tau_{-i-\frac{1}{2},j-\frac{1}{2}}) - \mathrm{Ki}_3(\tau_{-i+\frac{1}{2},j+\frac{1}{2}}) + \mathrm{Ki}_3(\tau_{-i+\frac{1}{2},j-\frac{1}{2}}) \Big], \tag{5.5}$$

This can now be integrated without problem using a Gauss–Jacobi quadrature.

In this module we will assume that there is a single external surface associated with the geometry. We will also limit the half-range spherical harmonic expansion for the angular flux to order $N_\nu = 0$. Accordingly, the leakage and transmission probabilities will be obtained directly from the collision probabilities using the reciprocity and conservation relations.

5.3 Spherical 1–D Geometries

A spherical 1–D geometry represent a 3–D cell that has properties which are angularly uniform and vary only as a function of the radial distance from the center of the cell. The collision probabilities associated with such geometries will be computed based the relations described in Section 4 for 3–D geometries. Because of the inherent symmetry of this problem, the angular integration over $d^2\Omega$ described in Eqs. (4.4) to (4.7) is generally evaluated analytically. On the other hand, the integration over x' and y' will be evaluated numerically, this integration taking different forms depending on the calculation option considered. Note that for these cells an explicit treatment of the boundary conditions via cell unfolding is not possible.

5.3.1 The $J_\pm$ model

In our application of the $J_\pm$ model to spherical 1–D geometries, we will only discuss here the integration of Eq. (4.21). The final expressions for the anisotropic components of the transmission probability which are similar to those obtained for the isotropic component will not be presented here.[19] As we noted above we will carry out the $d^2\Omega$ integration analytically. As for the x' and y' integration we will consider the following change of variables (see Figure 11):

$$\int dx' \int dy' F(x', y') = R^2 \int d\varphi' \int \sin(\theta') d\theta' F(\varphi', \theta')$$

which will lead to:

$$\int_{4\pi} d^2\Omega \int dx' \int dy' F(x',y') = S_\alpha^{3D} \int_0^\pi d\varphi' \int_{\varphi_b}^{\varphi_t} \sin(\theta') d\theta' \left[F(\varphi',\theta') + F(-\varphi',\theta')\right]$$

For the contributions to $\tilde{p}^{00}_{\alpha\alpha}$ we will have:

$$\begin{aligned}\Delta R =& 2R_\alpha \cos(\theta') \\ \varphi_b =& \arcsin\left(\frac{R_\gamma}{R_\alpha}\right) \\ \varphi_t =& \frac{\pi}{2}\end{aligned}$$

while

$$\begin{aligned}\Delta R =& R_\alpha \cos(\theta') - \sqrt{R_\gamma^2 - R_\alpha^2 \sin^2(\theta')} \\ \varphi_b =& 0 \\ \varphi_t =& \arcsin\left(\frac{R_\gamma}{R_\alpha}\right)\end{aligned}$$

for contributions to $\tilde{p}^{00}_{\alpha\gamma}$ and we assumed that $R_\gamma < R_\alpha$.

Because of the form of $F(\varphi',\theta')$ the final two integrations can always be evaluated numerically.[19] As an example for $\tilde{p}^{00}_{\alpha\alpha}$ we will obtain:

$$\tilde{p}^{00}_{\alpha\alpha} = \frac{\pi}{2\Sigma_i^2}\left(1 - \exp(-2\Sigma_i z)[1 + 2\Sigma_i z]\right)$$

with $z = \sqrt{R_\alpha^2 - R_\gamma^2}$

5.3.2 The standard model

Again we will carry out analytically the $d^2\Omega$ integration. For the remaining x' and y' integration we will use (see Figure 12):

$$\int dx' \int dy' F(x',y') = \int_0^{2\pi} d\varphi' \int_0^{R_i} h' dh' F(h') = 2\pi \int_0^{R_i} h' dh' F(h')$$

with the origin of the h' axis taken as the center of the concentric spherical shells. Accordingly, $\tilde{p}_{ij}$ will be given by:[3]

$$\begin{aligned}\tilde{p}_{ij} =& \frac{2\pi}{\Sigma_i \Sigma_j} \int_0^{R_i} h' dh' \exp(-\tau_{i+\frac{1}{2},j-\frac{1}{2}}) \\ & \left[1 - \exp(-\tau_{i-\frac{1}{2},i+\frac{1}{2}}) - \exp(-\tau_{j-\frac{1}{2},j+\frac{1}{2}}) + \exp(-\tau_{i-\frac{1}{2},i+\frac{1}{2}}) \exp(-\tau_{j-\frac{1}{2},j+\frac{1}{2}})\right] \\ & + \frac{2\pi}{\Sigma_i \Sigma_j} \int_0^{R_i} h' dh' \exp(-\tau_{-i+\frac{1}{2},j-\frac{1}{2}}) \\ & \left[1 - \exp(-\tau_{-i-\frac{1}{2},-i+\frac{1}{2}}) - \exp(-\tau_{j-\frac{1}{2},j+\frac{1}{2}}) + \exp(-\tau_{-i-\frac{1}{2},-i+\frac{1}{2}}) \exp(-\tau_{j-\frac{1}{2},j+\frac{1}{2}})\right]\end{aligned}$$

where R_i represents the outer radius of the annulus associated with region V_i and the optical path lengths are identical to those defined in Eqs. (5.1) to (5.3). If one classifies the regions from the inside to the outside of the

cell, then the above relation becomes:

$$\begin{aligned}\tilde{p}_{ij} =&\frac{4\pi}{\Sigma_i\Sigma_j}\sum_{k=1}^{i}\int_0^{\sqrt{R_k^2-R_{k-1}^2}} t(t^2+R_{k-1}^2)dt\\ &\left(e^{-(\tau_{i+\frac{1}{2},j-\frac{1}{2}})}\left[1-e^{-(\tau_{-i-\frac{1}{2},-i+\frac{1}{2}})}-e^{-(\tau_{j-\frac{1}{2},j+\frac{1}{2}})}+e^{-(\tau_{-i-\frac{1}{2},-i+\frac{1}{2}}+\tau_{j-\frac{1}{2},j+\frac{1}{2}})}\right]\right.\\ &\left.+e^{-(\tau_{-i+\frac{1}{2},j-\frac{1}{2}})}\left[1-e^{-(\tau_{-i-\frac{1}{2},-i+\frac{1}{2}})}-e^{-(\tau_{j-\frac{1}{2},j+\frac{1}{2}})}+e^{-(\tau_{-i-\frac{1}{2},-i+\frac{1}{2}}+\tau_{j-\frac{1}{2},j+\frac{1}{2}})}\right]\right)\end{aligned} \tag{5.6}$$

where the same change of variable as in the annular case was performed to avoid the divergence in the second derivative of the integrand at $h = R_k$. Each sub-integral can will then be performed using, as before, a Gauss–Jacobi quadrature.

5.4 Cartesian 2–D Geometries with embedded annular regions

Here we will consider the case where a rectangular region in 2–D can be subdivided into a number $N_x \times N_y$ of smaller rectangles over which the cross sections are assumed uniform. The size of each of these rectangles does not need to be identical, however, they must be arranged to form a regular mesh in both the X and Y direction (see Figure 13). In addition these Cartesian regions can also contain annular sub-regions similar to those described in Figure 14. To each Cartesian region will be associated 4 surfaces denoted respectively as $x_\pm$ and $y_\pm$ as described in Figure 15. Because of the symmetry of this problem, both the integration over φ and h' described in Eqs. (3.8) to (3.11) will generally be evaluated numerically (except for the $J_\pm$ model where the h' integration is evaluated analytically), these integration taking different forms depending on the tracking method considered. Note that for such geometries an explicit treatment of the boundary conditions via cell unfolding is permitted.

5.4.1 The $J_\pm$ model

Here we will first concentrate on the evaluation of $\tilde{p}^{00}_{\alpha\gamma}$ for purely Cartesian geometries which is given by Eq. (3.28). For the geometry described in Figure 15 only three contributions are independent, namely $\tilde{p}^{00}_{x_-,x_+}$, $\tilde{p}^{00}_{x_-,y_+}$ and $\tilde{p}^{00}_{y_-,y_+}$. The transmission from surface S_{x_-} to S_{x_+} is possible only if $0 \leq \varphi \leq \varphi_x^t$ where

$$\varphi_x^t = \arctan\left(\frac{\Delta y}{\Delta x}\right)$$

and Δx and Δy are the dimensions of the rectangle in the x and y directions respectively. In addition, for each angle in this range the neutron will be able to reach the surface x_+ only when $0 \leq h' \leq H^t$ such that:

$$H^t(\varphi) = \Delta y\cos(\varphi) - \Delta x\sin(\varphi).$$

The optical path traveled by the neutron is independent of h' and given by:

$$\tau_{x,x}(\varphi) = \frac{\Sigma\Delta x}{\cos(\varphi)}.$$

Accordingly we will have:

$$\tilde{p}^{00}_{x_-,x_+} = \frac{1}{2\pi}\int_0^{\varphi_x^t} d\varphi\,(\Delta y\cos(\varphi) - \Delta x\sin(\varphi))\,\mathrm{Ki}_3\left(\frac{\Sigma\Delta x}{\cos(\varphi)}\right), \tag{5.7}$$

For the higher order contributions to $\tilde{p}^{\nu\mu}_{x_-,x_+}$, the main difference is the presence of the factors $v(\varphi) = w(\varphi) = \cos(\varphi)$. A similar relation can be obtained for $\tilde{p}^{00}_{y_-,y_+}$ by rotating the rectangle by $-\pi/2$, namely

$$\tilde{p}^{00}_{y_-,y_+} = \frac{1}{2\pi}\int_0^{\varphi_y^t} d\varphi\,(\Delta x\cos(\varphi) - \Delta y\sin(\varphi))\,\mathrm{Ki}_3\left(\frac{\Sigma\Delta y}{\cos(\varphi)}\right), \tag{5.8}$$

with $\varphi_y^t = \arctan(\Delta x/\Delta y)$.

The second term we wish to consider is $\tilde{p}^{00}_{x_-,y_+}$. According to Figure 15, the limits of integration over φ and h' now become:

$$\varphi_x^t \leq \varphi \leq \frac{\pi}{2}$$
$$0 \leq h' \leq \Delta x \sin(\varphi)$$

However, in this case, the optical path remains a function of h':

$$\tau_{x,y}(\varphi, h') = \frac{\Sigma}{\cos(\varphi)\sin(\varphi)} \left(\Delta x \sin(\varphi) - h'\right).$$

We can now integrate the expression for the collision probability over h' and obtain:

$$\tilde{p}^{00}_{x_-,y_+} = \frac{1}{2\pi\Sigma} \int_{\varphi_x^t}^{\pi/2} d\varphi \cos(\varphi)\sin(\varphi) \left[\mathrm{Ki}_4(0) - \mathrm{Ki}_4\left(\frac{\Sigma\Delta x}{\cos(\varphi)}\right)\right], \tag{5.9}$$

For higher order contribution to this transmission probability, we will use $v(\varphi) = \sin(\varphi)$ and $w(\varphi) = \cos(\varphi)$. Finally, since the above function and their derivatives are all finite for the whole φ integration range we can use directly a Gauss–Legendre quadrature.

In the case where Cartesian cells containing annular regions are considered, the problem is more complex since there are additional restrictions on the specific geometries that can be considered. In fact, for these cases, the geometry must be such that one can represent the cell by an assembly of Cartesian sub-cells with the annular regions located at the center of one Cartesian sub-cell. Moreover, the annular regions must be totally located inside a specific cell. Finally, the Cartesian sub-cells containing an annular region cannot be subdivided along the X and Y axis. In this case the collision probabilities are computed in the following way. For the annular regions, the results of Section 5.2.1 are used while for the Cartesian ring one uses a technique similar to that described in Section 5.4.2 with opaque annular regions (infinite cross sections in the annular regions) to compute the collision probability associated with the ring. Once this collision probability has been obtained it is simple, using the conservation and symmetry relations described in Section 1.8 to obtain the required transmission probabilities.

5.4.2 The standard model

In this case we will evaluate $\tilde{p}_{ij}$, $\tilde{p}^0_{i\alpha}$ and $\tilde{p}^{00}_{\alpha\gamma}$ using Eq. (3.15), Eq. (3.23) and Eq. (3.28) directly. As one can see this involves a 2–D integration which will be performed numerically. For the φ integration, we will limit the range of integration to $0 \leq \varphi \leq \pi$ since the contributions to the integral arising from angles in the range $\pi \leq \varphi \leq 2\pi$ will be associated with the probability $\tilde{p}_{ji}$ which are symmetric to $\tilde{p}_{ij}$. For a N^φ points angular quadrature the weights and points w_i^φ and u_i^φ will be selected as follows:

$$w_i^\varphi = \frac{\pi}{N^\varphi} \tag{5.10}$$
$$u_i^\varphi = \left(\frac{2i-1}{2}\right) w_i^\varphi \tag{5.11}$$

For the h' integral, we will select a trapezoidal quadrature set. Moreover this set can be made independent of the angular set in the following way. Assuming that the center of the cell is located at (x_c, y_c), then one will have $-h_+ \leq h' \leq h_+$ where h_+ is the radius of the smallest circle centered at (x_c, y_c) surrounding the cell (see Figure 16). Selecting a tracking density of d_h will be equivalent to selecting N^h spatial points such that:

$$N^h = (2d_h h_+) + 1 \tag{5.12}$$

As a result the effective spacing between the tracks is given by:

$$\delta^h = \frac{2h_+}{N^h} \tag{5.13}$$

and the quadrature weights and points will be given by:

$$w_i^h = \delta^h \tag{5.14}$$

$$u_i^h = \left(\frac{2i-1}{2}\right)\delta^h \tag{5.15}$$

A tracking line will then be associated with each quadrature point (u_i^φ, u_i^h) and followed as it travels through the cell. One will then identify the successive external surfaces and regions crossed by this line and evaluate the distance the neutron will travel inside each region. Note that there will also be a track length of 1.0 associated with each external surface. This information will then be saved on a binary tracking file in the format described in Appendix D.1. In DRAGON, `XELTI2` is the main tracking routine associated with this type of geometry.

5.4.3 The specular model

In this case we will evaluate $\tilde{p}_{ij}$ using Eqs. (3.38) or (3.40). As one can see this involves a 3–D integration which will be performed numerically.[22–24,28] For the u integration we will use a simple Gauss–Legendre quadrature. For the φ and h' numerical integration, the problem is more complex than for the standard collision probability method. As we discuss in Section 3.2, in order for the infinite line contribution proportional to τ_p to exist, a neutron starting at a point (φ_i, h'_i) in the integration plane must be able to cross this same point again after a finite number of cell crossing. Two options can be considered to reach this goal. One can select the angles and adjust the h' integral or the reverse. Here we have considered the first option. Since both reflective and periodic boundary conditions can be selected, the set of angles we choose should reflect this possibility. Accordingly, for each quadrature angle $0 \leq \varphi_i \leq \pi$ there must exist a symmetric angle φ_j which represents the mirror reflection of the initial angle on an external surface. In the case where $2N^\varphi$ angles are selected, we will have the following integration points:

$$v_i^\varphi = \cos(\varphi_i) = \frac{(i-1)\Delta y}{\sqrt{(i-1)^2(\Delta y)^2 + (N^\varphi - i)^2(\Delta x)^2}} \tag{5.16}$$

with $i = 1, N^\varphi$ for the range $0 \leq \varphi_i \leq \pi/2$ and

$$v_i^\varphi = \cos(\varphi_i) = -\frac{(-i-1)\Delta y}{\sqrt{(-i-1)^2(\Delta y)^2 + (N^\varphi + i)^2(\Delta x)^2}} \tag{5.17}$$

with $i = -1, -N^\varphi$ for the range $\pi/2 \leq \varphi_i \leq \pi$. In the above Δx and Δy are the width of the cell in the X and Y directions respectively. Note that the change in the neutron direction from a reflection on a plane normal to the X-axis will result in a change in the integration angle from $\varphi_i \rightarrow \varphi_{-i}$. In DRAGON the quadrature points v_i^φ are evaluated in the subroutine `XELTSA`. The integration weights associated with these points are defined in such a way that:

$$\frac{2}{\pi}\sum_{i=1}^{N^\varphi} w_i (v_i^\varphi)^k = \frac{2}{\pi}\int_0^{\pi/2} \cos^{2k}(\varphi) d\varphi = \frac{(2k-1)!!}{(2k)!!} \tag{5.18}$$

where

$$(2k-1)!! = \frac{(2k-1)!}{2^{k-1}\,(k-1)!} = 1 \times 3 \times 5 \times \cdots \times (2k-1)$$

$$(2k)!! = 2^k\, k! = 2 \times 4 \times 6 \times \cdots \times (2k)$$

These weights are computed in DRAGON using the routine `XELTSW`.

For the h' integral, we will select a trapezoidal quadrature set. However this set will depend on the specific choice of φ_i because of the requirement that a given integration line must be able to return to its starting point. In order to illustrate this problem, let us consider Figure 17 where a basic cell has been unfolded to infinity using periodic boundary conditions. The tracking lines $L_{\pm 2}$ and $L_{\pm 3}$ represent respectively the case where the

quadrature points $i = \pm 2$ and $i = \pm 3$ have been selected (here $N^\varphi = 4$). For $1 \leq i \leq N^\varphi$, the number of surfaces perpendicular to the X-axis crossed by a track before returning to a location in the cell identical to the starting point is $N^\varphi - |i|$. The number of surfaces perpendicular to the Y-axis will be $|i| - 1$ for a total of $N^\varphi - 1$ surfaces. In the case where $i = 1$ and $i = N^\varphi$, the total number of surfaces becomes 2 these being perpendicular to the X-axis ($i = 1$) or the Y-axis ($i = N^\varphi$). We can also see that each tracking angle will generate parallel lines in the original cell which are separated by a distance $\delta_{i,j}$. The obvious choice for the h' quadrature is therefore to select, for a specific tracking direction, a track spacing $\Delta h'$ such that it generates lines for a startup position h'_i which coincide with those associated with a different startup position $h'_i + k\Delta h'$. Accordingly the maximum value of $\Delta h'$ which will satisfy this condition is:

$$\Delta h' = \frac{\Delta x \Delta y}{\sqrt{(i-1)^2(\Delta y)^2 + (N^\varphi - i)^2(\Delta x)^2}} \tag{5.19}$$

For the specific choice of integration points we will then follow a technique similar to that described in Section 5.4.2. Thus, for a specified tracking density d_h, we will first select the effective track multiplication factor as:

$$n^h = d_h \Delta h' + 1 \tag{5.20}$$

from which the effective track spacing is computed using

$$\delta^h = \frac{\Delta h'}{n^h} \tag{5.21}$$

which results in a maximum number of parallel tracks given by

$$N^h = \frac{h_+}{\delta^h} + 1 \tag{5.22}$$

and quadrature weights and points given by Eqs. (5.14) and (5.15) respectively.

In the case where the boundary conditions represent total reflection, the same technique will be used with the difference that selecting only the angles located in the range $0 \leq \varphi_i \leq \pi/2$ automatically produce the angles in the range $\pi/2 \leq \varphi_i \leq \pi$ by reflection as seen in Figure 18. In addition, the number of surface crossing in both the X and Y planes are doubled in this case for each angle. The cases where mixed boundary conditions are considered can also be treated in much the same way.

Again a tracking line will be associated with each quadrature point (v_i^φ, v_i^h) and followed as it travels through the cell. One will then identify the successive external surfaces (both the surface by which the neutron leaves the cell and reenters it) and regions crossed by this line and evaluate the distance the neutron will travel inside each region while following the track. Note that there will also be a track length of 0.5 associated with each external surface. This information will then be saved on a binary tracking file in the format described in Appendix D.1. In DRAGON, `XELTS2` is the main tracking routine associated with this type of geometry.

5.5 Hexagonal 2–D Geometries with embedded annular regions

Here we will consider only the cases where a 2–D geometry can be subdivided into a number N_H of hexagon which can contain centered annular subregions (see Figure 19). To each hexagon will be associated 6 surfaces as described in Figure 20. Because of the symmetry of this problem, both the integration over φ and h' described in Eqs. (3.8) to (3.11) will generally be evaluated numerically (except for the $J_\pm$ model where, in addition, the h' integration is evaluated analytically) Note that for such geometries an explicit treatment of the boundary conditions via cell unfolding is not permitted.

5.5.1 The $J_\pm$ model

Here we will first concentrate on the evaluation of $\tilde{p}^{00}_{\alpha\gamma}$ for pure hexagons which is given by Eq. (3.28). For the geometry described in Figure 21 only three contributions are independent, namely $\tilde{p}^{00}_{s_4 1, s_1}$, $\tilde{p}^{00}_{s_4, s_2}$ and $\tilde{p}^{00}_{s_4, s_3}$. The

transmission from surface S_4 to S_1 is possible only if $0 \leq \varphi \leq \pi/6$. In addition for each angle in this range, the neutron will be able to reach the surface S_1 only when $0 \leq h' \leq H^1$ such that:[25]

$$H^1(\varphi) = \frac{H}{2}\left(\cos(\varphi) - \sqrt{3}\sin(\varphi)\right).$$

The optical path traveled by the neutron is independent of h' and given by:

$$\tau_{4,1}(\varphi) = \frac{\sqrt{3}\Sigma H}{\cos(\varphi)}.$$

Accordingly we will have:

$$\tilde{p}^{00}_{s_4,s_1} = \frac{1}{2\pi}\int_0^{\pi/6} d\varphi \frac{H}{2}\left(\cos(\varphi) - \sqrt{3}\sin(\varphi)\right)\mathrm{Ki}_3\left(\frac{\sqrt{3}\Sigma H}{\cos(\varphi)}\right), \tag{5.23}$$

For the higher order contributions to $\tilde{p}^{\nu\mu}_{s_4,s_1}$, the main difference is the presence of the factor $v(\varphi) = w(\varphi) = \cos(\varphi)$.

The second term we wish to consider is $\tilde{p}^{00}_{s_4,s_2}$. According to Figure 21, the limits of integration over φ and h' now become:

$$\begin{aligned}\frac{\pi}{6} \leq &\varphi \leq \frac{\pi}{3}\\ 0 \leq &h' \leq H^2\end{aligned}$$

with

$$H^2(\varphi) = H\left(\cos(\varphi - \frac{\pi}{6}) - 2\sin(\varphi - \frac{\pi}{6})\right)$$

However, in this case, the optical path remains a function of h':

$$\tau_{4,2}(\varphi, h') = \frac{\Sigma}{\cos(\varphi)\sin(\varphi)}\left(\Delta x \sin(\varphi) - h'\right).$$

We can now integrate the expression for the collision probability over h' and obtain:

$$\tilde{p}^{00}_{s_4,s_2} = \frac{1}{2\pi\Sigma}\int_{\pi/6}^{\pi/3} d\varphi \cos(\varphi)\sin(\varphi)\left[\mathrm{Ki}_4(0) - \mathrm{Ki}_4\left(\frac{\Sigma\Delta x}{\cos(\varphi)}\right)\right], \tag{5.24}$$

Finally, let us consider $\tilde{p}^{00}_{s_4,s_3}$. The limits of integration over φ and h' are:

$$\begin{aligned}\frac{\pi}{3} \leq &\varphi \leq \frac{\pi}{2}\\ 0 \leq &h' \leq H^3\end{aligned}$$

with

$$H^3(\varphi) = H\left(\cos(\varphi - \frac{\pi}{3}) - \sqrt{3}\sin(\varphi - \frac{\pi}{3})\right)$$

The optical path remains a function of h':

$$\tau_{4,3}(\varphi, h') = \frac{\Sigma}{\cos(\varphi)\sin(\varphi)}\left(\Delta x \sin(\varphi) - h'\right).$$

We can now integrate the expression for the collision probability over h' and obtain:

$$\tilde{p}^{00}_{s_4,s_4} = \frac{1}{2\pi\Sigma}\int_{\pi/3}^{\pi/2} d\varphi \cos(\varphi)\sin(\varphi)\left[\mathrm{Ki}_4(0) - \mathrm{Ki}_4\left(\frac{\Sigma\Delta x}{\cos(\varphi)}\right)\right], \tag{5.25}$$

For the higher order contributions to $\tilde{p}^{\nu\mu}_{s_4,s_2}$ and $\tilde{p}^{\nu\mu}_{s_4,s_3}$, the main difference is the presence of the factor $v(\varphi) = \sin(\varphi)$ and $w(\varphi) = \cos(\varphi)$. Finally let us discuss the numerical quadrature used. Since the above function and their derivatives are all finite for the whole φ integration range we can use directly a Gauss–Legendre quadrature.

In the case where hexagonal cells containing annular regions are considered, the collision probabilities are computed in the following way. For the annular regions, the results of Section 5.2.1 are used while for the hexagonal ring one uses a technique similar to that described in the Section 5.5.2 with opaque annular regions (infinite cross sections in the annular regions). Then, using this collision probability and the conservation and symmetry relations described in Section 1.8, the required transmission probabilities can be obtained.

5.5.2 The standard model

In this case the tracking will be performed as described in Section 5.4.2 with the following differences. The integration range $0 \leq \varphi \leq \pi$ will be further subdivided into two region, namely $0 \leq \varphi \leq \pi/2$ and $\pi/2 \leq \varphi \leq \pi$. For the case where an N^φ points equal weight angle quadrature is specified in DRAGON we will have in fact $2N^\varphi$ weights (w_i^φ) and points u_i^φ defined as follows:[33]

$$w_i^\varphi = \frac{\pi}{2N^\varphi} \tag{5.26}$$

$$u_i^\varphi = \left(\frac{2i-1}{2}\right) w_i^\varphi \tag{5.27}$$

$$w_{N^\varphi+i}^\varphi = w_i^\varphi \tag{5.28}$$

$$u_{N^\varphi+i}^\varphi = \left(\frac{2i-1}{2}\right) w_i^\varphi + \frac{\pi}{2} \tag{5.29}$$

For the h' integral, we will also select a trapezoidal quadrature set. This set will again be made independent of the angular set in the following way. We will select the smallest circle surrounding the cell (see Figure 22), namely for an assembly made up of N_c rings of hexagon each having the same dimension H specified by the width of one of its sides, we will select r_h as follows

$$r_h = \frac{H\sqrt{1+3(2N_c-1)^2}}{2} \tag{5.30}$$

Selecting a tracking density of d_h will be equivalent to selecting N^h spatial points such that:

$$N^h = (d_h r_h) + 1 \tag{5.31}$$

As a result the effective spacing between the tracks will be given by:

$$\delta^h = \frac{r_h}{N^h} \tag{5.32}$$

and the quadrature weights and points will be given by:

$$w_i^h = \delta^h \tag{5.33}$$

$$u_i^h = \left(\frac{2i-1}{2}\right) \delta^h \tag{5.34}$$

The evaluation of the collision probability in this case proceeds as in Section 5.4.2, the main difference being that the tracking routine associated with this type of geometry is `TRKHEX`.

5.6 Cells Containing 2–D Pin Clusters

This case is similar to that described above with the additional possibility of having a second set of annular regions which are superimposed over the basic Annular, Cartesian/annular or hexagonal/annular geometry (see

Figure 23). These types of geometry can first be analyzed using the standard collision probability model using a technique similar to that described in Section 5.4.2. The main difference here is that the angles are selected in the range $0 \leq \varphi \leq 2\pi$. One also assumes in these cases that the origin of the h axis is located at the center of the cell, the quadrature being performed only over positive h values.

In addition, the Cartesian/annular cluster pin geometry can also be analyzed using the infinite collision probability method. In this case the technique is identical to that used in Section 5.4.3. For pin cluster geometry, the tracking in DRAGON is performed using the `XCWTRK` routine.

5.7 Cartesian 3–D Geometries with embedded annular regions

Here we will consider the case where a 3–D Cartesian region is subdivided into a number $N_x N_y N_z$ of smaller Cartesian sub-regions over which the cross sections are assumed uniform. The size of each of these regions does not need to be identical, however, they must be arranged in such a way as to form a regular mesh in both the X, Y and Z direction. To each Cartesian region will be associated 6 surfaces denoted respectively by $x_\pm$, $y_\pm$ and $z_\pm$ as described in Figure 24. In addition such geometries can contain embedded annular sub-regions similar to those described in Figure 25. Note that for such geometries an explicit treatment of the boundary conditions via cell unfolding is not permitted.

In this case we will evaluate $\tilde{p}_{ij}$, $\tilde{p}^0_{i\alpha}$ and $\tilde{p}^{00}_{\alpha\gamma}$ using Eq. (4.11), Eq. (4.18) and Eq. (4.21) directly. As one can see this involves a 4–D integration which will be performed numerically. For the integration over the solid angle Ω, we will consider only the upper half-sphere, namely

$$\begin{aligned} 0 \leq \varphi \leq 2\pi \\ 0 \leq \theta \leq \pi/2 \end{aligned}$$

for $\Omega = (\varphi, \theta)$. This is because the contributions to the integral arising from Ω directed towards the lower half-sphere will be associated with the probability $\tilde{p}_{ji}$ which are symmetric to $\tilde{p}_{ij}$. Here the integral over the solid angle Ω is discretized using the equal weight EQ_N quadrature technique developed for S_n method.[17,34] Each angle Ω_i will therefore be written in terms of is director cosines:

$$\Omega_i = (\cos(\Omega_{x,i}), \cos(\Omega_{y,i}), \cos(\Omega_{z,i})) = (u_{xi}, u_{yi}, u_{zi})$$

such that

$$u^2_{xi} + u^2_{yi} + u^2_{zi} = 1$$

For a N^Ω solid angle quadrature, $N^\Omega(N^\Omega + 2)/2$ weights and points will be selected in the upper half-sphere.

There still remains the problem of discretizing the dx' and dy' integral over a plane normal to the direction Ω (see Figure 26). The limits of integration for these integrals will be specified in such a way that they are independent of the specific integration direction. Accordingly, after locating the center of the cell (x_c, y_c, z_c), we will compute h_+, the radius of the smallest sphere centered at (x_c, y_c, z_c) surrounding the cell. Then the integration limits will be given by:

$$\begin{aligned} -h_+ \leq & x' \leq h_+ \\ -h_+ \leq & y' \leq h_+ \end{aligned}$$

Selecting a tracking density of d_h will be equivalent to selecting N^2 spatial points such that:

$$N = (2\sqrt{d_h} h_+) + 1 \tag{5.35}$$

As a result the effective spacing between the tracks will be given by:

$$\delta = \frac{2h_+}{N} \tag{5.36}$$

and the quadrature weights and points will be given by:

$$w_{ij} = \delta^2 \tag{5.37}$$

$$u_i^x = \left(\frac{2i-1}{2}\right)\delta^h \tag{5.38}$$

$$u_j^y = \left(\frac{2j-1}{2}\right)\delta^h \tag{5.39}$$

A final point concerns the specific location of the x' and y' axis. The (x', y') plane is defined arbitrarily with respect to the direction Ω which represents a z' axis. A rotation of the plane around the z' axis will yield a new plane which can also be used for the $dx'dy'$ integration. However the integration lines associated with this new plane will be located at different positions in space.

The explicit location of the x' and y' axis could be selected using various criteria. In DRAGON, because of the need to insure that this surface integral for a single cubic cell is invariant under a rotation of the integration plane, the following criteria has been selected. For each direction Ω three different integration planes were selected and tracked successively. As a result the weight associated with each track direction had to be reduced by a factor of 3. The plane were selected in such a way that the x' axis would lie successively in the (x, y), (z, x) and y, z planes (see Figure 26). Defining $\vec{\omega}'_x$, $\vec{\omega}'_y$ and $\vec{\omega}'_z$ to be the unit vectors defining the direction of the axis x', y' and z' respectively, we can then write:

$$\begin{aligned}
\vec{\omega}'_x &= \left(-\frac{u_{yi}}{\sqrt{1-u_{zi}^2}}\,,\frac{u_{xi}}{\sqrt{1-u_{zi}^2}}\,,0\right)\\
\vec{\omega}'_y &= \left(\frac{u_{xi}u_{zi}}{\sqrt{1-u_{zi}^2}}\,,\frac{u_{yi}u_{zi}}{\sqrt{1-u_{zi}^2}}\,,-\sqrt{1-u_{zi}^2}\right)\\
\vec{\omega}'_z &= (u_{xi}, u_{yi}, u_{zi})
\end{aligned}$$

in the case where the x' axis is in the $x-y$ plane, and

$$\begin{aligned}
\vec{\omega}'_x &= \left(-\frac{u_{zi}}{\sqrt{1-u_{yi}^2}}\,,0\,,\frac{u_{xi}}{\sqrt{1-u_{yi}^2}}\right)\\
\vec{\omega}'_y &= \left(\frac{u_{xi}u_{yi}}{\sqrt{1-u_{yi}^2}}\,,-\sqrt{1-u_{yi}^2}\,,\frac{u_{zi}u_{yi}}{\sqrt{1-u_{yi}^2}}\right)\\
\vec{\omega}'_z &= (u_{xi}, u_{yi}, u_{zi})
\end{aligned}$$

or

$$\begin{aligned}
\vec{\omega}'_x &= \left(0\,,-\frac{u_{zi}}{\sqrt{1-u_{xi}^2}}\,,\frac{u_{yi}}{\sqrt{1-u_{xi}^2}}\right)\\
\vec{\omega}'_y &= \left(-\sqrt{1-u_{xi}^2}\,,\frac{u_{yi}u_{xi}}{\sqrt{1-u_{xi}^2}}\,,\frac{u_{zi}u_{xi}}{\sqrt{1-u_{xi}^2}}\right)\\
\vec{\omega}'_z &= (u_{xi}, u_{yi}, u_{zi})
\end{aligned}$$

for the case where the x' axis is in the $z-x$ or $y-z$ planes respectively.

In DRAGON, the resulting tracking, which is performed by the `XELTI3` routine, proceeds as follows. For each quadrature directions, $\vec{\omega}'$ a set of parallel tracking lines will be followed at they travel through the cell. One will then identify the successive external surfaces and regions crossed by these lines and evaluate the distance the neutron will travel inside each region while following these tracks. This information will then be saved on a binary tracking file in the format described in Appendix D.1.

5.8 Hexagonal 3–D Geometries with embedded annular regions

Here we will consider only the cases where a 3–D geometry can be subdivided into a number N_H of hexagon which can contain centered cylinders (see Figure 27). In this case the tracking will be performed as described in Section 5.7 with the following differences. The EQ_N integration over the solid angle Ω will be replaced by double Gauss–Legendre quadrature over $0 \leq \theta \leq \pi/2$ and $0 \leq \varphi \leq 2\pi$. The surface integral $dx'dy'$ will be replaced by an integral over $dudh$. Here the dh integral is located in the 2–D $x - y$ plane as described in Figure 22 while the du integral defines the angle between the plane and the z axis (see Figure 28). The integration limits for the dh integration will be defined as in Section 5.5.2. For the du integration we will use

$$-\left(\frac{H}{2} + \frac{r_h}{\cos(\theta)}\right) \leq u \leq \left(\frac{H}{2} + \frac{r_h}{\cos(\theta)}\right)$$

where for N_c concentric rings of hexagon we will have:

$$r_h = \frac{H\sqrt{1 + 3(2N_c - 1)^2}}{2} \tag{5.40}$$

Namely, for the u integration limits, we will consider a projection on the plane $u-v$ centered at $u = 0$ of a cylinder of height H capped with hemispherical regions of radius r_h.[33]

6 COLLISION PROBABILITY INTEGRATION IN DRAGON

Once a specific geometry has been tracked in DRAGON, there still remains the problem of processing the resulting tracking file and to generate the multigroup collision probability matrices associated with a given problem. In the code DRAGON, this processing is generally divided into three steps. The first step consists in integrating explicitly the multigroup collision probabilities. This is followed by a normalization step where the conservation properties associated with the collision probabilities, (see Section 1.5) which may have been broken because of the use of a numerical integration procedure, are restored. Finally, the last calculation step that needs to be performed consists in building a complete collision probability matrix which includes the boundary conditions (see Section 1.7).

6.1 Collision Probability Integration Module

Here we will discuss only the collision probability integration module associated with the `EXCELT` tracking module of DRAGON. The reason for this restriction is that it is the most reliable collision probability integration technique of DRAGON. Moreover, it uses the standard `EXCELL` binary tracking file defined in Appendix D.1. It can also treat explicitly voided regions. Here we will discuss briefly the general technique used for the integration of collision probability in 2–D and 3–D geometries when isotropic boundary conditions are used. We will also present the integration method used when a 2–D specular tracking is considered.

In the following, we will use, for simplicity, the notation W^n=`WEIGHT` and $L^{n,m}$=`SEGLEN(II)` for the integration lines stored on the binary tracking file. The index $n = 1, N$ denotes the track line number and the index $m = 1, M$ a given segment of an integration line.

6.1.1 Isotropic Collision Probability in 2–D

In this case DRAGON uses the `PIJI2D` integration routine. The first step in this routine consists in scanning the integration line and computing the contributions to $\Sigma_i^2 \tilde{p}_{ii}$ proportional to $\mathrm{Ki}_2(0)$ (see Eq. (3.19)),

$$\frac{1}{2}\Sigma_i^2 \tilde{p}_{ii} = \sum_n W^n \mathrm{Ki}_2(0) \sum_{m \in i} \tau_i^{n,m}. \tag{6.1}$$

In the above, the presence of the factor 2 is justified by the fact that the W^n include, in addition to the angular and spatial integration integration weights, a factor of $1/(2\pi)$. Here we have used the following definition for $\tau_i^{n,m}$

$$\tau_i^{n,m} = \Sigma_i L^{n,m} \qquad \text{with } m \in i. \tag{6.2}$$

This is then followed in `PIJI2D` by a second scan of the integration line, where one adds to the collision probabilities associated with region i, the contributions proportional to $\tau_{i-\frac{1}{2},j\pm\frac{1}{2}}$ (see Eq. (3.15)):

$$\Sigma_i \Sigma_j \tilde{p}_{ij} = \sum_n \sum_{m \in j} \kappa_{ij}^{n,m}, \tag{6.3}$$

where

$$\kappa_{ij}^{n,m} = W^n \left(\mathrm{Ki}_3(\tau_{ij}^{n,m}) - \mathrm{Ki}_3(\tau_{ij}^{n,m-1}) \right), \tag{6.4}$$

with $\tau_{ij}^{n,0} = \tau_{ij}^{n,M+1} = 0$ and

$$\tau_{ij}^{n,m} = \sum_{l=1}^{m} \Sigma_k L^{n,l} \qquad \text{for } m > 0 \text{ and with } l \in k \text{ and } m \in j. \tag{6.5}$$

The same term also contributes to the leakage probability associated with the first surface α encountered by the track (see Eq. (3.23)):

$$\Sigma_j \tilde{p}_{j\alpha} = -\sum_n \sum_{m\in j} \kappa_{ij}^{n,m}. \tag{6.6}$$

Finally, once the last segment of the integration line is reached, one can compute the contribution to $\tilde{p}_{i\beta}$ and $\tilde{p}_{\alpha\beta}$ where β is associated with the last surface encountered by the track and i and α are the first region and surface encountered by this same track respectively. We will then have:

$$\Sigma_j \tilde{p}_{i\beta} = \sum_n \sum_{m\in j} \kappa_{ij}^{n,M+1}, \tag{6.7}$$

$$\tilde{p}_{\alpha\beta} = -\sum_n \sum_{m\in j} \kappa_{ij}^{n,M+1}. \tag{6.8}$$

The integration line will then be scanned a third time to compute the contributions to $\tilde{p}_{ij}$ corresponding to the remaining regions in the cell. In this case, a two levels sweep will be considered, namely, for an initial line segment m, the line will be analyzed for each segment $m' = m, M$. We will then compute:

$$\kappa_{ij}^{n,m,m'} = W^n \left(\mathrm{Ki}_3(\tau_{ij}^{n,m,m'}) - \mathrm{Ki}_3(\tau_{ij}^{n,m,m'-1}) \right), \tag{6.9}$$

where $\tau_{ij}^{n,m,m-1} = \tau_{ij}^{n,m,M+1} = 0$ and for $m' \leq M$ we have used

$$\tau_{ij}^{n,m,m'} = \sum_{l=1}^{m'-m+1} \Sigma_k L^{n,m-1+l} \qquad \text{for } m-1+l \in k, m \in i \text{ and } m' \in j. \tag{6.10}$$

The term $\kappa_{ij}^{n,m,m'}$ contributes to two different collision probabilities, namely

$$\Sigma_i \Sigma_j \tilde{p}_{ij} = \sum_n \sum_{m\in i} \sum_{m'\in j} \kappa_{ij}^{n,m,m'}, \tag{6.11}$$

$$\Sigma_{i'} \Sigma_j \tilde{p}_{i'j} = -\sum_n \sum_{m-1\in i'} \sum_{m'\in j} \kappa_{ij}^{n,m,m'}, \tag{6.12}$$

corresponding respectively to the terms $\tau_{i-\frac{1}{2},j\pm\frac{1}{2}}$ and $\tau_{i+\frac{1}{2},j\pm\frac{1}{2}}$ in Eq. (3.15). In addition the value of $\kappa_{ij}^{n,m,m'}$ associated with the last line segment $m' = M+1$ also contributes to the leakage probabilities $\tilde{p}_{i\beta}$ and $\tilde{p}_{i'\beta}$ where β is the last surface reached by the track:

$$\Sigma_i \tilde{p}_{i\beta} = \sum_n \sum_{m\in i} \kappa_{ij}^{n,m,M+1}, \tag{6.13}$$

$$\Sigma_{i'} \tilde{p}_{i'\beta} = -\sum_n \sum_{m-1\in i'} \kappa_{ij}^{n,m,M+1}. \tag{6.14}$$

Finally, the last line segment corresponding to $m = m' = M$ contributes an additional term to $\tilde{p}_{j\beta}$ of the form:

$$\Sigma_j \tilde{p}_{j\beta} = \sum_n \kappa_{ij}^{n,M,M+1}, \tag{6.15}$$

corresponding to $\tau_{i+\frac{1}{2},\alpha} = 0$ in Eq. (3.23).

Note that the above relations yield vanishing results for all the collision probabilities $\Sigma_i \Sigma_j \tilde{p}_{ij}$ when the cross sections associated with region i or j vanish. A similar result is also obtained for the leakage probabilities $\Sigma_j \tilde{p}_{j\alpha}$ when region j is voided. Accordingly, the above calculation will always be performed in DRAGON even if they are not strictly required for voided regions.

In the case where one or more region is voided, the integration process will be repeated but using a slightly different algorithm. Here we will consider only the two levels sweep of the track. For an initial line segment m, the line will first be analyzed for segment $m' = m$, then for the remaining segments $m' = m+1, M$ and $m' = m-1, 1$. For the case where $m = m'$ we will use (see Eq. (3.20)):

$$\frac{1}{2}\tilde{p}_{ii} = \sum_n W^n \frac{\mathrm{Ki}_1(0)}{2} \sum_{m\in i} (\tau_i^{n,m})^2 \,. \tag{6.16}$$

For the line segments $m' \neq m$ we will first compute:

$$\kappa_{ij}^{n,m,m'} = \begin{cases} \frac{1}{2} W^n \left(\tau_i^{n,m}\right)^2 \mathrm{Ki}_1(\tau_{ij}^{n,m,m'}) & \text{if region } i \text{ and } j \text{ are voided} \\ -W^n \tau_i^{n,m} \left(\mathrm{Ki}_2(\tau_{ij}^{n,m,m'}) - \mathrm{Ki}_2(\tau_{ij}^{n,m,m'-1})\right) & \text{if only region } i \text{ is voided} \end{cases}, \tag{6.17}$$

where we have used the definition of Eq. (6.2) for $\tau_i^{n,m}$, Eq. (6.10) for $\tau_{ij}^{n,m,m'}$ with $m' > m$ while in the case where $m' < m$ we will use:

$$\tau_{ij}^{n,m,m'} = \sum_{l=1}^{m-m'+1} \Sigma_k L^{n,m'-1+l} \qquad \text{for } m'-1+l \in k, m \in i \text{ and } m' \in j. \tag{6.18}$$

These will generate contributions to the collision probabilities of the form:

$$\tilde{p}_{ij} = \sum_n \sum_{m\in i} \sum_{m'\in j} \kappa_{ij}^{n,m'-m+1} \qquad \text{if region } i \text{ and } j \text{ are voided and}$$

$$\Sigma_j \tilde{p}_{ij} = \sum_n \sum_{m\in i} \sum_{m'\in j} \kappa_{ij}^{n,m'-m+1} \qquad \text{if only region } i \text{ is voided,}$$

while the contribution to the leakage probabilities associated with the first (α) or last (β) surface will be given by

$$\tilde{p}_{j\alpha} = \sum_n W^n \kappa_{ij}^{n,m,0},$$

$$\tilde{p}_{j\beta} = \sum_n W^n \kappa_{ij}^{n,m,M+1}.$$

A final comment here concerns the fact that the integration procedure we used above for computing the various probabilities is not complete since we have considered only the contributions with $m < m'$ or $m > m'$. As a result the collision probabilities will contain only half the possible contributions which should have been included. Since the probabilities $\tilde{p}_{ij}$ should be symmetric, then all the contributions added to $\tilde{p}_{ij}$ for $i \neq j$ should also have been included in $\tilde{p}_{ji}$. Moreover, there is a factor of 2 missing in the expressions we used here for $\tilde{p}_{ii}$. This task of completing the collision probability matrices for the isotropic 2–D integration module is performed in an independent routine called `PIJCMP`.

6.1.2 Isotropic Collision Probability in 3–D

The DRAGON integration routine used in this case is `PIJI3D`. The first step in this routine consists in scanning the integration line and computing the contributions to $\Sigma_i^2 \tilde{p}_{ii}$ (see Eq. (4.15)),

$$\frac{1}{2}\Sigma_i^2 \tilde{p}_{ii} = \sum_n W^n \sum_{m\in i} (\tau_i^{n,m} - \kappa_i^{n,m}) \,, \tag{6.19}$$

where

$$\kappa_i^{n,m} = (1 - \exp[-\tau_i^{n,m}]) \,, \tag{6.20}$$

$$\tau_i^{n,m} = \Sigma_i L^{n,m} \qquad \text{with } m \in i, \tag{6.21}$$

and the presence of the factor 2 above is justified by the fact that the W^n include here a factor of $1/(4\pi)$.

This is then followed in `PIJI3D` by a second scan of the integration line, to compute the contributions to $\tilde{p}_{ij}$ corresponding to the remaining regions in the cell. In this case, a two levels sweep will be considered, namely, for an initial line segment m, the line will be analyzed for each segment $m' = m+1, M$. We will then compute:

$$\Sigma_i \Sigma_j \tilde{p}_{ij} = \sum_n W^n \sum_{m \in i} \sum_{m' \in j} \kappa_i^{n,m} \kappa^{n,m+1,m'-1} \kappa_j^{n,m'}, \tag{6.22}$$

using

$$\kappa^{n,m,m'} = \prod_{l=m}^{m'} \exp\left[-\tau_i^{n,l}\right], \tag{6.23}$$

where $\kappa_i^{n,m}$ and $\tau_i^{n,l}$ are defined in Eqs. (6.20) and (6.21) respectively.

The contributions to the leakage and escape probabilities are also computed using similar relations:

$$\Sigma_i \tilde{p}_{i\alpha} = \sum_n W^n \sum_{m \in i} \kappa^{n,1,m-1} \kappa_i^{n,m}, \tag{6.24}$$

$$\Sigma_i \tilde{p}_{i\beta} = \sum_n W^n \sum_{m \in i} \kappa_i^{n,m} \kappa^{n,m+1,M}, \tag{6.25}$$

$$\tilde{p}_{\alpha\beta} = \sum_n W^n \kappa^{n,1,M}, \tag{6.26}$$

where α and β are respectively the initial and final surface associated with track n.

In `PIJI3D`, the case where one or more region is voided is treated independently. The general procedure is similar to that above with the following differences. For the evaluation of $\tilde{p}_{ii}$, where i is a voided region, instead of using Eq. (6.19), we will consider the following relation:

$$\frac{1}{2}\tilde{p}_{ii} = \sum_n \frac{W^n}{2} \sum_{m \in i} \left(\kappa_{i,v}^{n,m}\right)^2, \tag{6.27}$$

where

$$\kappa_{i,v}^{n,m} = L^{n,m} \qquad \text{with } m \in i. \tag{6.28}$$

For the remaining probabilities we will still use Eq. (6.22) or Eqs. (6.24) to (6.26), however for a voided region k the terms of the form $\kappa_k^{n,m}$ will now be replaced by $\kappa_{k,v}^{n,m}$.

This integration procedure is not complete since we have considered only the contributions with $m < m'$. The task of completing the collision probability matrices for the isotropic 3–D integration module is performed in this case directly in the routine `PIJI3D` using a procedure similar to that used in `PIJCMP`.

6.1.3 Specular Collision Probability in 2–D

The DRAGON integration routine used in this case is `PIJS2D`. The procedure used here is similar to that used for the 3–D isotropic collision probability integrator since the 2–D specular integration involves exponential terms rather than Bickley Nayler functions as is the case for the 2–D isotropic integrator. The first step in routine `PIJS2D` therefore consists in scanning the integration line and computing the contributions to $\Sigma_i^2 \tilde{p}_{ii}$,

$$\frac{1}{2}\Sigma_i^2 \tilde{p}_{ii} = \sum_n W^n \sqrt{1-(u^n)^2} \sum_{m \in i} \left(\tau_i^{n,m} - \kappa_i^{n,m}\right), \tag{6.29}$$

where u^n is the Gauss-Legendre integration point for the u integration in Eqs. (3.38) or (3.40) associated with this track (see Section 5.4.3) and

$$\kappa_i^{n,m} = \left(1 - \exp\left[-\tau_i^{n,m}\right]\right), \tag{6.30}$$

$$\tau_i^{n,m} = \frac{\Sigma_i L^{n,m}}{\sqrt{1-(u^n)^2}} \qquad \text{for } m \text{ in region } i. \tag{6.31}$$

One can note again the presence of the factor 2 that has been justified above. During this stage of the integration we will also compute the global attenuation factor Γ^n associated with a complete track cycle using:

$$\Gamma^n = \left[1 - \beta \exp\left(-\frac{\tau}{\sqrt{1-u^2}}\right)\right]^{-1} = \left(1 - \prod_{m=1}^{M} \gamma^{n,m}\right)^{-1}, \tag{6.32}$$

where

$$\gamma^{n,m} = \begin{cases} \exp\left[-\tau_i^{n,m}\right] & \text{for } m \text{ in region } i \\ \beta_\alpha & \text{for } m \text{ on surface } \alpha \end{cases}.$$

where β_α is the reflection (albedo) or transmission coefficient on surface α.

This is then followed by a second scan of the integration line, to compute the contributions to $\tilde{p}_{ij}$ corresponding to the remaining regions in the cell. In this case, a two levels sweep is considered, namely, for an initial line segment m, the line will be analyzed for each segment $m' = 1, M$. We will then compute:

$$\Sigma_i \Sigma_j \tilde{p}_{ij} = \sum_n W^n \sqrt{1-(u^n)^2} \sum_{m \in i} \sum_{m' \in j} \kappa_i^{n,m} \kappa^{n,m+1,m'-1} \kappa_j^{n,m'}, \tag{6.33}$$

using

$$\kappa^{n,m,m'} = \prod_{l=m}^{m'} \gamma^{n,m}, \tag{6.34}$$

where $\kappa_i^{n,m}$ and $\tau_i^{n,l}$ are defined in Eqs. (6.30) and (6.31) respectively.

Note that in the case where the line segments m' is located on surface α while m is still inside i, we will have:

$$\Sigma_i \tilde{p}_{i\alpha} = \sum_n W^n \sqrt{1-(u^n)^2} \sum_{m \in i} \sum_{m' \in \alpha} \kappa_i^{n,m} \kappa^{n,m+1,m'-1} \kappa_j^{n,m'}, \tag{6.35}$$

while if both m and m' are associated with surfaces we will compute:

$$\tilde{p}_{\alpha\beta} = \sum_n W^n \sqrt{1-(u^n)^2} \sum_{m \in \alpha} \sum_{m' \in \beta} \kappa_i^{n,m} \kappa^{n,m+1,m'-1} \kappa_j^{n,m'}. \tag{6.36}$$

In this routine the case where one or more regions are voided is treated in parallel with the non-voided regions. The general procedure is therefore similar to that described above with the following differences. For the evaluation of $\tilde{p}_{ii}$, where i is a voided region, instead of using Eq. (6.29), we will consider the following relation:

$$\frac{1}{2}\tilde{p}_{ii} = \sum_n \frac{W^n}{2} \sqrt{1-(u^n)^2} \sum_{m \in i} \left(\kappa_{i,v}^{n,m}\right)^2, \tag{6.37}$$

where

$$\kappa_{i,v}^{n,m} = \frac{L^{n,m}}{\sqrt{1-(u^n)^2}} \qquad \text{with } m \in i. \tag{6.38}$$

For the remaining probabilities we will still use Eq. (6.33) or Eqs. (6.35) to (6.36), however for a voided region k the terms of the form $\kappa_k^{n,m}$ will be replaced by $\kappa_{k,v}^{n,m}$.

As for the routine `PIJI2D`, the integration procedure we considered is not complete since we have considered only the contributions with $m < m'$. The task of completing the collision probability matrices for the specular 2–D integration module is performed directly in the routine `PIJS2D` using a procedure similar to that used in `PIJCMP`.

6.1.4 Additional Considerations

The three routines we described above are called directly by the routine `EXCELP` and read explicitly the tracking file described in Appendix D.1. In the case where the tracks are not stored in a file but are kept in memory, the

routines `QIJI2D`, `QIJI3D` and `QIJS2D` are called via the routine `EXCELL`. In fact only the routine `QIJI3D`, which has the same logical structure as `PIJI3D`, is available in the current version of DRAGON since the `EXCELL` module is currently restricted to 3–D geometries.

Note that the explicit form of the collision probability computed in the routine `PIJI2D`, `PIJI3D` and `PIJS2D` all depend on the presence or absence of voided region. In fact the collision and leakage probabilities associated with non-voided region will be restored to their explicit from ($\tilde{p}_{ij}$ instead of $\Sigma_i\Sigma_j\tilde{p}_{ij}$) directly in the routine `EXCELP` which calls these routines.

6.2 Collision Probability Normalization

Once the transmission, leakage and collision probabilities have been evaluated independently one can verify if the neutron conservation relations described in Eqs. (1.37) and (1.39) are satisfied numerically. In fact one will generally obtains:

$$R_j = \Sigma_j V_j - \sum_{\alpha=1}^{N_\alpha} \frac{S_\alpha}{4}\Sigma_i p^0_{\alpha j} - \sum_{i=1}^{N_i} \Sigma_j\Sigma_i V_i p_{ij},$$

$$R_\beta = \frac{S_\beta}{4} - \sum_{\alpha=1}^{N_\alpha} \frac{S_\alpha}{4} p^{00}_{\alpha\beta} - \sum_{i=1}^{N_i} \Sigma_i V_i p^0_{i\beta},$$

or

$$R_j = \tilde{P}_{0j} - \sum_{\alpha=1}^{N_\alpha} \tilde{P}_{\alpha j} - \sum_{i=1}^{N_i} \tilde{P}_{ij}, \tag{6.39}$$

$$R_\beta = \tilde{P}_{0\beta} - \sum_{\alpha=1}^{N_\alpha} \tilde{P}_{\alpha\beta} - \sum_{i=1}^{N_i} \tilde{P}_{i\beta}, \tag{6.40}$$

where R_i and R_α represent the numerical errors on the conservation law for regions and surfaces respectively and we have used

$$\begin{aligned}
\tilde{P}_{ij} &= \tilde{P}_{ji} = \Sigma_j\Sigma_i V_i p_{ij} \\
\tilde{P}_{\alpha j} &= \tilde{P}_{j\alpha} = \frac{S_\alpha}{4}\Sigma_i p^0_{\alpha j} \\
\tilde{P}_{i\beta} &= \tilde{P}_{\beta i} = \Sigma_i V_i p^0_{i\beta} \\
\tilde{P}_{\alpha\beta} &= \tilde{P}_{\beta\alpha} = \frac{S_\alpha}{4} p^{00}_{\alpha\beta} \\
\tilde{P}_{0j} &= \Sigma_j V_j \\
\tilde{P}_{0\beta} &= \frac{S_\beta}{4}
\end{aligned}$$

These conservation laws can be restored in DRAGON using different collision probabilities normalization schemes which we will now describe.

6.2.1 Diagonal Normalization

The simplest normalization scheme that can be used to restore the conservation laws above while preserving the symmetry relations consist in updating the diagonal entries of the collision and leakage matrices.[6,21] Using this scheme, one can redefine the diagonal elements of collision probability matrix ($\tilde{P}^D_{ii}$ and $\tilde{P}^D_{\alpha\alpha}$) as follows:

$$\tilde{P}^D_{ii} = \tilde{P}_{ii} - R_i, \tag{6.41}$$

$$\tilde{P}^D_{\alpha\alpha} = \tilde{P}_{\alpha\alpha} - R_\alpha. \tag{6.42}$$

Large changes implied by this normalization will result in large changes of the diagonal entries. For small values of p_{ii} this scheme may result in non-physical negative probabilities in the final collision probability matrix. Moreover, this scheme cannot be applied to problems involving voided zones where $\Sigma_i = 0$. This normalization is performed in DRAGON using the routine `PIJRDG`.

6.2.2 Gelbard Normalization

Gelbard suggested a different normalization scheme, which is based on a correction using the collision probabilities in the homogeneous limit.[21,35] This scheme has been generalized to

$$\tilde{P}^G_{ij} = \tilde{P}_{ij} - \frac{1}{\tilde{\Sigma}} \left(\tilde{P}_{0i} R_j + \tilde{P}_{0j} R_i - \tilde{P}_{0i} \tilde{P}_{0j} \tilde{R}_v \right), \tag{6.43}$$

$$\tilde{P}^G_{\alpha\alpha} = \tilde{P}_{\alpha\alpha} - \frac{1}{\tilde{S}} (\tilde{P}_{0\beta} R_\alpha + \tilde{P}_{0\alpha} R_\beta - \tilde{P}_{0\alpha} \tilde{P}_{0\beta} \tilde{R}_s), \tag{6.44}$$

where

$$\tilde{\Sigma} = \sum_i \tilde{P}_{0i},$$

$$\tilde{S} = \sum_\alpha \tilde{P}_{0\alpha},$$

$$\tilde{R}_v = \frac{1}{\tilde{\Sigma}} \sum_i R_i,$$

$$\tilde{R}_s = \frac{1}{\tilde{S}} \sum_\alpha R_\alpha.$$

This additive scheme can be applied even in voided zones. It will redistribute the corrections to the conservation laws over the complete collision probability matrix. Corrections on the diagonal entries are now weaker than for the previous scheme, but they may still produce negative probabilities. This normalization is performed in DRAGON using the routine `PIJRGL`.

6.2.3 Multiplicative Normalization

Another way to reestablish conservation laws is to define weighting factors w_i and w_α that will be applied to the collision probability matrix in a multiplicative manner as follows:[21]

$$\tilde{P}^N_{ij} = w_i w_j \tilde{P}_{ij}, \tag{6.45}$$

$$\tilde{P}^N_{\alpha\beta} = w_\alpha w_\beta \tilde{P}_{\alpha\beta}. \tag{6.46}$$

This results in a quadratic system that we can solve for the weights. The main advantages of this multiplicative normalization is to preserve the null probabilities as well as the relative size of the collision probability matrix entries (since we have $w_i \approx 1$) and the overall positivity of the matrix. However, solving the resulting set of quadratic equations for the weight factors is generally a CPU intensive task. This normalization is performed in DRAGON using the routine `PIJRNL`.

6.2.4 HELIOS type Normalization

Finally, there is also the possibility to use in DRAGON a simplified multiplicative normalization scheme which does not involve the solution of a system of non-linear equations.[36] Instead of using Eq. (6.45) which involves the

product of two weights functions, we will use:

$$\tilde{P}_{ij}^{H} = (w_i + w_j)\tilde{P}_{ij}, \tag{6.47}$$

$$\tilde{P}_{\alpha\alpha}^{H} = (w_\alpha + w_\beta)\tilde{P}_{\alpha\alpha}. \tag{6.48}$$

The conservation laws can be ensured by requiring that:

$$w_b\left(\tilde{P}_{bb} + \sum_a \tilde{P}_{ab}\right) = \tilde{P}_{0b} + w_b\tilde{P}_{bb} - \sum_a w_a\tilde{P}_{ab} = \tilde{P}_{0b} - \sum_{a\neq b} w_a\tilde{P}_{ab}, \tag{6.49}$$

where the generic indices a and b run over the regions and surfaces. This system is solved in DRAGON for w_b using an iterative process, namely, assuming that w_a^k at iteration k is known for $a \neq b$ we can write:

$$w_b^{k+1} = \frac{\tilde{P}_{0b} - \sum_{a\neq b} w_a^k \tilde{P}_{ab}}{\tilde{P}_{bb} + \sum_a \tilde{P}_{ab}},$$

For $k = 1$, the weights $w_a^k = 0.5$ are all identical, corresponding to the case where the collision probabilities are already normalized. The solution for w_a^{k+1} is assumed converged when:

$$\max\left(\frac{w_a^{k+1} - w_a^k}{w_a^{k+1}}\right) \leq \epsilon$$

This normalization is performed in DRAGON using the routine `PIJRHL`.

6.3 Boundary Conditions

The specular integration procedure described above is such that the collision probabilities computed include directly the effect of the boundary conditions (see Section 1.2). As a result, the leakage and escape probabilities which are computed are not required for further DRAGON processing even if they are saved on the ASMPIJ data structure.[15] However, in the case of the isotropic integration procedure, the collision probabilities evaluated are those associated with a cell isolated in space. For such cases, DRAGON follows explicitly the technique described in Section 1.7 and computes the complete collision probability matrix which takes into account the boundary conditions using the relation:

$$\mathbf{P}_{vv}^{c} = \mathbf{P}_{vv} + \mathbf{P}_{vs}\mathbf{P}_{ss}^{c}\mathbf{P}_{sv},$$

where

$$\mathbf{P}_{ss}^{c} = (\mathbf{I} - \mathbf{A}\mathbf{P}_{ss})^{-1}\mathbf{A} = \left(\mathbf{A}^{-1} - \mathbf{P}_{ss}\right)^{-1}, \tag{6.50}$$

and A is the reflection/transmission matrix.

The matrix $\mathbf{P}_{ss}^{c}$ is generally computed in routine `PIJABC` using the last form of the above equation. However, in the cases where vacuum boundary conditions are applied on different surfaces S_α, a slightly modified expression must be used. The need for this modification becomes evident if one realizes that for such problems the matrix $\mathbf{A}$ is singular and its inverse cannot be computed. These modifications can be illustrated in the following way.

If one assumes that vacuum boundary conditions are applied to the first n surfaces while for the remaining surfaces reflection or periodic boundary conditions are considered. The matrix $\mathbf{A}$ and $\mathbf{P}_{ss}$ can then be written in the form:

$$\mathbf{A} = \begin{bmatrix} \mathbf{0} & \mathbf{0} \\ \mathbf{0} & \mathbf{A}_{22} \end{bmatrix},$$

$$\mathbf{A} = \begin{bmatrix} \mathbf{P}_{11} & \mathbf{P}_{12} \\ \mathbf{P}_{21} & \mathbf{P}_{22}. \end{bmatrix}$$

We can therefore write:

$$(\mathbf{I} - \mathbf{A}\mathbf{P}_{ss})^{-1}\mathbf{A} = \left(\begin{bmatrix} \mathbf{I} & \mathbf{0} \\ \mathbf{0} & \mathbf{A}_{22}^{-1} - \mathbf{P}_{22} \end{bmatrix}\right)^{-1} \begin{bmatrix} \mathbf{0} & \mathbf{0} \\ \mathbf{0} & \mathbf{I} \end{bmatrix}. \tag{6.51}$$

Accordingly, in the case where vacuum boundary are considered, we will replace the relation for $\mathbf{P}_{ss}^{c}$ described in Eq. (6.50) by the form described in Eq. (6.51).

REFERENCES

[1] B. Davison, *Neutron Transport Theory*, Oxford University Press, London (1957).

[2] F.E. Driggers, *A Method for Calculating Neutron Absorption and Flux Spectra at Epithermal Energies*, Report AECL-1996, Atomic Energy of Canada Limited, Chalk River, Ontario (1964).

[3] A. Kavenoky, *Calcul et utilisation des probabilité de première collision pour des milieux hétérogènes à une dimension: Les programmes ALCOLL et CORTINA*, Note CEA-N-1077, Commissariat à l'énergie atomique, Saclay, France (1969).

[4] G. Bell and S. Glasstone, *Neutron Reactor Theory*, Robert E. Krieger Publishing Company, Malabar, Florida (1970).

[5] J.R. Askew, "Review of the Status of Collision Probability Methods", *Seminar on Numerical Reactor Calculations*, 185-196, International Atomic Energy Agency, Vienna, 1972.

[6] J.V. Donnelly, *WIMS–CRNL: A User's Manual for the Chalk River Version of WIMS*, Report AECL-8955, Atomic Energy of Canada Limited, Chalk River, Ontario (1986).

[7] D. Emendorfer, "Physics Assumptions and Applications of Collision Probabilities Methods", *ANS Conference on Mathematical Models and Computational Techniques for Analysis of Nuclear Systems*, Ann Arbor, Michigan, CONF-730414-P2, U.S. Atomic Energy Commission (1974).

[8] R. Sanchez, "Approximate Solutions of the Two-Dimensional Integral Transport Equation by Collision Probability Methods", *Nucl. Sci. Eng*, **64**, 384-404 (1977).

[9] A. Kavenoky, "Status of Integral Transport Theory", *ANS/ENS International Topical Meeting on Advances in Mathematical Methods for the Solution of Nuclear Engineering Problems*, Munich, Germany, April 27-29, 1981.

[10] R. Sanchez and N.J. McCormick, "A Review of Neutron Transport Approximations", *Nucl. Sci. Eng*, **80**, 481-535 (1982).

[11] R.J.J. Stamm'ler and M.J. Abbate, *Methods of Steady-State Reactor Physics in Nuclear Design*, Academic Press, London (1983).

[12] E.E. Lewis and W.F. Miller, Jr., *Computational Methods of Neutron Transport*, John Wiley and Sons, New York (1984).

[13] A. Hébert, *Neutronique*, École Polytechnique de Montréal, Institut de Génie Nucléaire (1983).

[14] G. Marleau, A. Hébert and R. Roy, *A User's Guide for DRAGON – Version DRAGON_000331 Release 3.04*, Report IGE-174 Rev. 5, École Polytechnique de Montréal, Institut de génie nucléaire (2000).

[15] A. Hébert, G. Marleau and R. Roy, *A Description of the DRAGON Data Structures – Version DRAGON_000331 Release 3.04*, Report IGE-232 Rev. 3, École Polytechnique de Montréal, Institut de génie nucléaire (2000).

[16] G. Marleau and A. Hébert, "An Integral Transport Method for Treating CANDU and GCR Clusters", *Progress in Nuclear Energy*, **18**, 197-206 (1986).

[17] R. Roy, A. Hébert and G. Marleau, "A Transport Method for Treating 3D Lattices of Heterogeneous Cells", *International Topical Meeting on Advances in Reactor Physics, Mathematics and Computation*, pp 665-679, Paris, France, April 27–30, 1987.

[18] R. Roy, A. Hébert and G. Marleau, "A Transport Method for Treating Three-Dimensional Lattices of Heterogeneous Cells", *Nucl. Sci. Eng.*, **101**, 217-225 (1989).

[19] G. Marleau, M.L. Vergain, A. Hébert and R. Roy, "Computation of the DP1 Collision Probabilities for Spherical and Cylindrical Geometries", *Ann. nucl. Energy*, **17**, 119-134 (1990).

[20] G. Marleau, R. Roy and A. Hébert, "Analytic Reductions for Transmission and Leakage Probabilities in Finite Tubes and Hexahedra", *Nucl. Sci. Eng*, **104**, 209-216 (1990).

[21] R. Roy and G. Marleau, "Normalization Techniques for Collision Probability Matrices", *PHYSOR-90*, pp IX.40-IX.49, Marseille, France, April 23–27, 1990.

[22] R. Roy, "Anisotropic Scattering for Integral Transport Codes. Part 1. Slab Assemblies", *Ann. nucl. Energy*, **17**, 379-388 (1990).

[23] R. Roy, "Anisotropic Scattering for Integral Transport Codes. Part 2. Cyclic Tracking and its Application to XY Lattices", *Ann. nucl. Energy*, **18**, 511-524 (1991).

[24] R. Roy, A. Hébert and G. Marleau, "A Cyclic Tracking Procedure for Collision Probability Calculations in 2-D Lattices", *International Topical Meeting on Advances in Mathematics, Computation and Reactor Physics*, pp 2.2.4.1-2.2.4.14, Pittsburgh, PA, April 28 – May 2, 1991.

[25] M. Ouisloumen, G. Marleau, A. Hébert and R. Roy, "Computation of Collision Probabilities for Mixed Hexagonal-Cylindrical Geometries Using the DP1 Approximation to the $J_{\pm}$ Technique", *International Topical Meeting on Advances in Mathematical, Computation and Reactor Physics*, pp 2.2.1.1-2.2.1.12, Pittsburgh, PA, April 28 – May 2, 1991.

[26] G. Marleau and A. Hébert, "New Computational Methods Used in the Lattice Code DRAGON", *Topical Meeting on Advances in Nuclear Physics*, pp 1.177-1.188, Charleston, SC, March 8–11, 1992.

[27] G. Marleau and A. Hébert, "Analysis of Cluster Geometries Using the DP1 Approximation of the $J_{\pm}$ Technique", *Nucl. Sci. Eng*, **111**, 257-270 (1992).

[28] G. Marleau and R. Roy, "Use of Specular Boundary Conditions for CANDU Cell Analysis", *Fourth International Conference on Simulation Methods in Nuclear Engineering*, pp. 5B.3.1-5B.3.13, Montréal, Canada, June 2-4, 1993.

[29] R. Roy, G. Marleau, J. Tajmouati and D. Rozon, "Modeling of CANDU Reactivity Control Devices with the Lattice Code DRAGON", *Ann. nucl. Energy*, **21**, 115-132 (1994).

[30] A. Hébert, G. Marleau and R. Roy, "Application of the Lattice Code DRAGON to CANDU Analysis", *Trans. Am. Nucl. Soc.*, **72**, 335-336 (1995).

[31] M. Abramowitz and I.A. Stegun, *Handbook of Mathematical Functions*, Dover Publications, Inc, New York (1972).

[32] W.G. Bickley and J. Nayler, "A Short Table of the Functions $\mathrm{Ki}_n(\mathrm{x})$, from $n = 1$ to $n = 16$", *Phil. Mag.*, **20**, 343-347 (1935).

[33] M. Ouisloumen, G. Marleau and R. Roy, "Applying the Collision Probability Method to Hexagonal Assemblies in Two and Three Dimensions", *Joint International Conference on Mathematical Methods and Supercomputing in Nuclear Applications*, pp 102-112, Karlsruhe, Germany, April 19–23, 1993.

[34] B.J. Carlson, *Tables of Equal Weight Quadrature EQ_N Over the Unit Sphere*, LA-4734, Los Alamos Scientific Laboratory (1971).

[35] E.M. Gelbard, "Refinements in the Computation of Collision Probabilities", *International Meeting on Advances in Nuclear Engineering Computational Methods*, Knoxville, Tennessee, April 9–11, 1989

[36] E.A. Villarino, R.J.J. Stamm'ler, A.A. Ferri and J.J. Casal, "HELIOS: Angularly Dependent Collision Probabilities", *Nucl. Sci. Eng.*, **112**, 16–31 (1992).

FIGURES

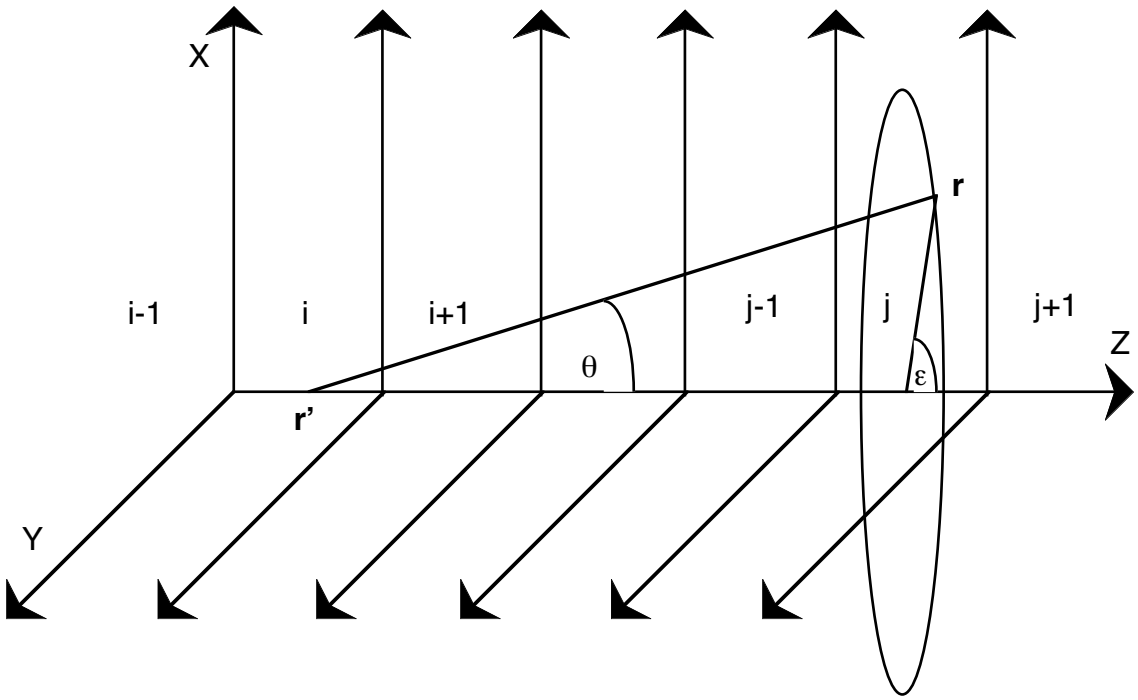

Figure 1: Example of a Cartesian 1–D geometry

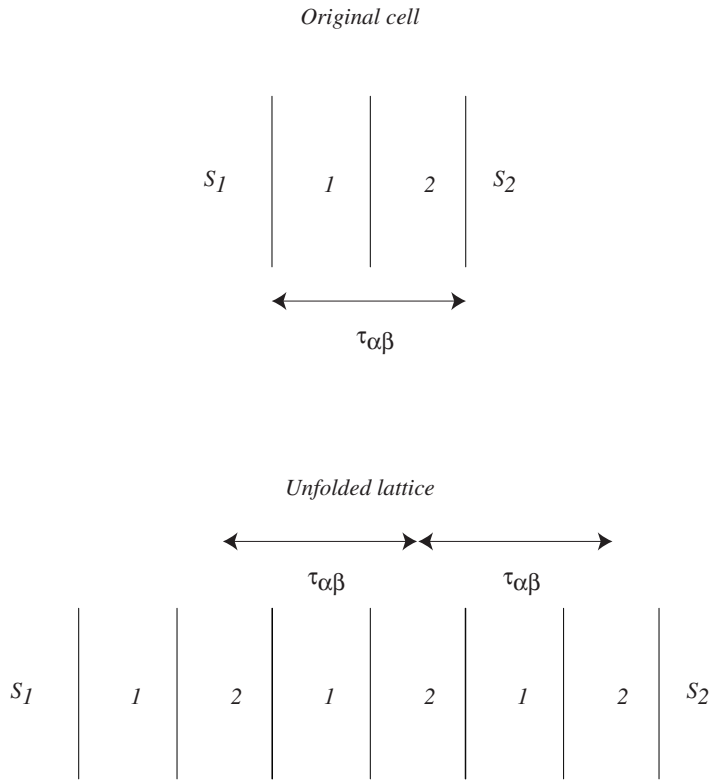

Figure 2: Example of a Cartesian 1–D geometry duplicated to infinity using periodic boundary conditions

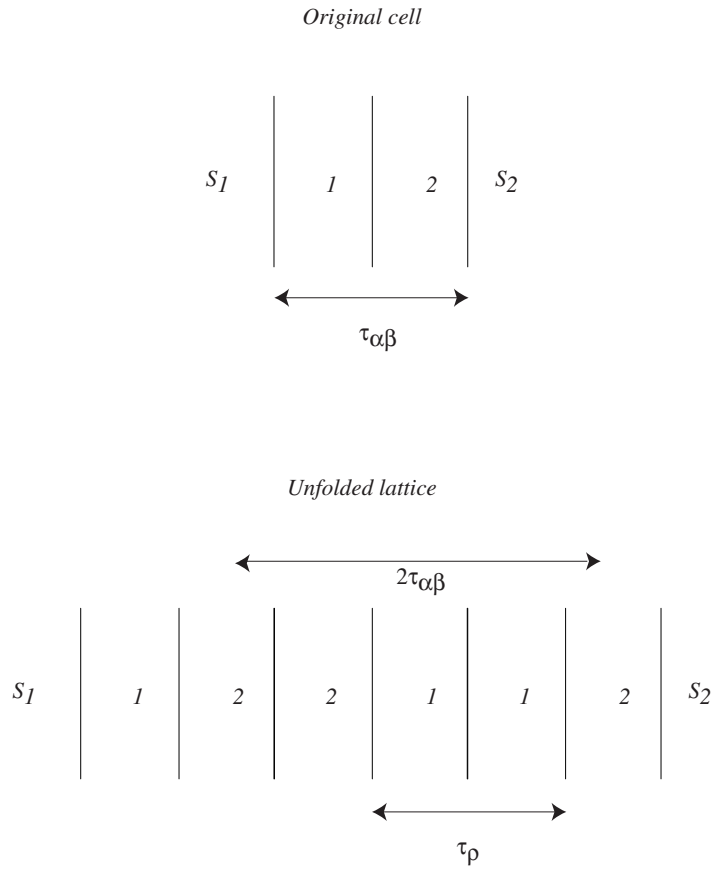

Figure 3: Example of a Cartesian 1–D geometry duplicated to infinity using reflection boundary conditions

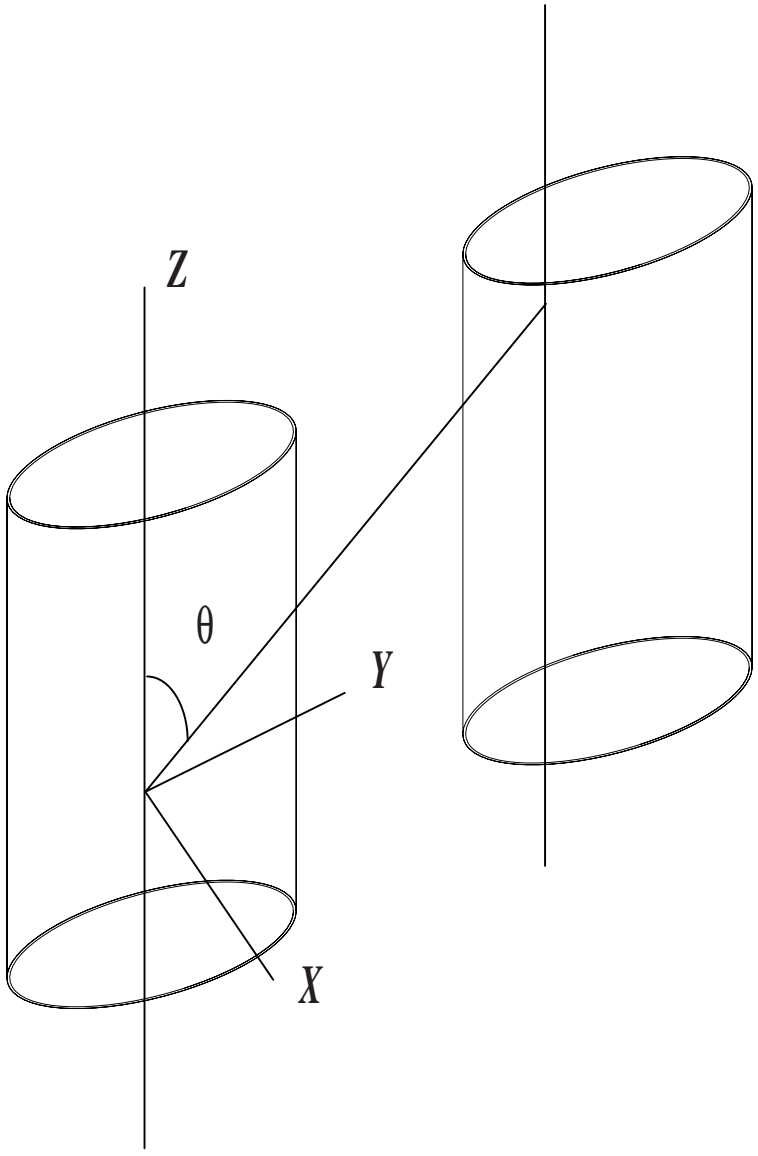

Figure 4: Example of a general 2–D geometry

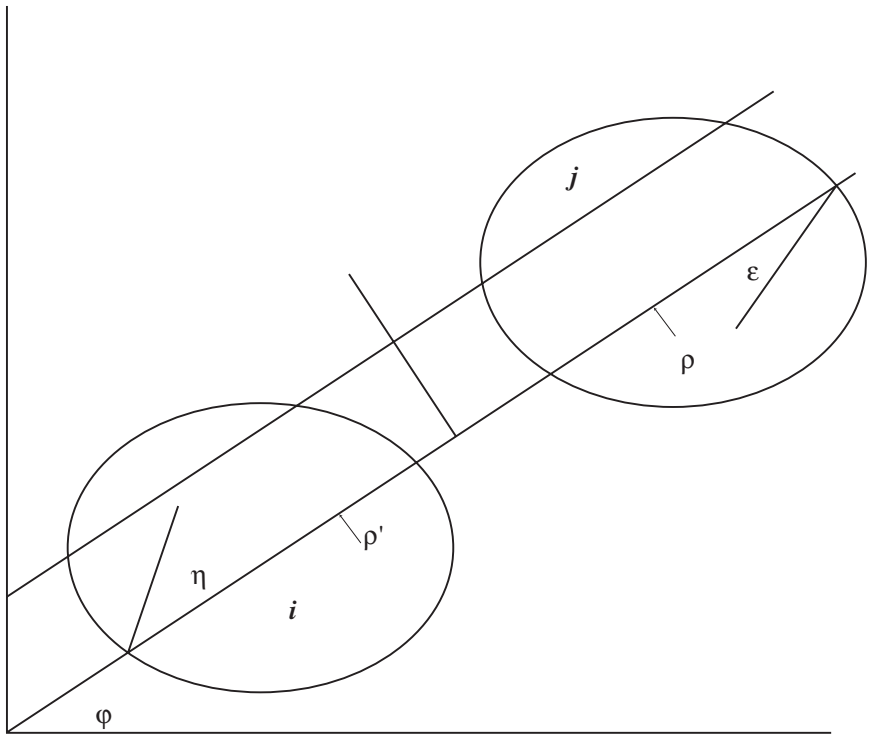

Figure 5: Projection in the $X - Y$ plane of the general 2–D geometry

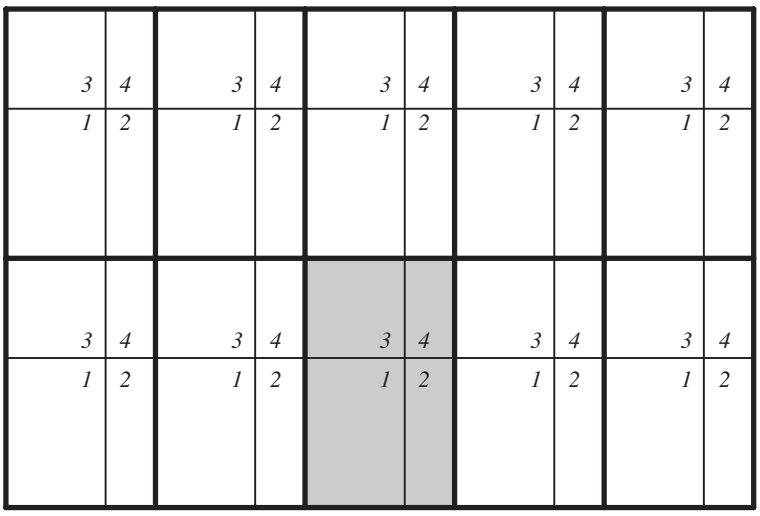

Figure 6: Example of a Cartesian 2–D geometry unfolded to infinity using periodic boundary conditions

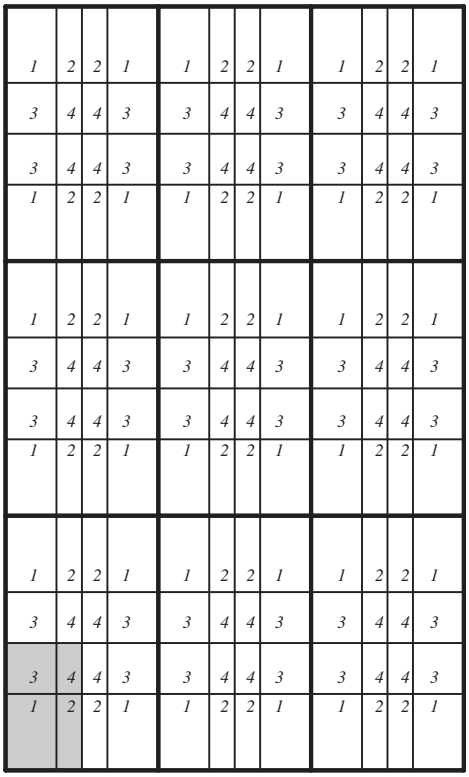

Figure 7: Example of a Cartesian 2–D geometry unfolded to infinity using reflection boundary conditions

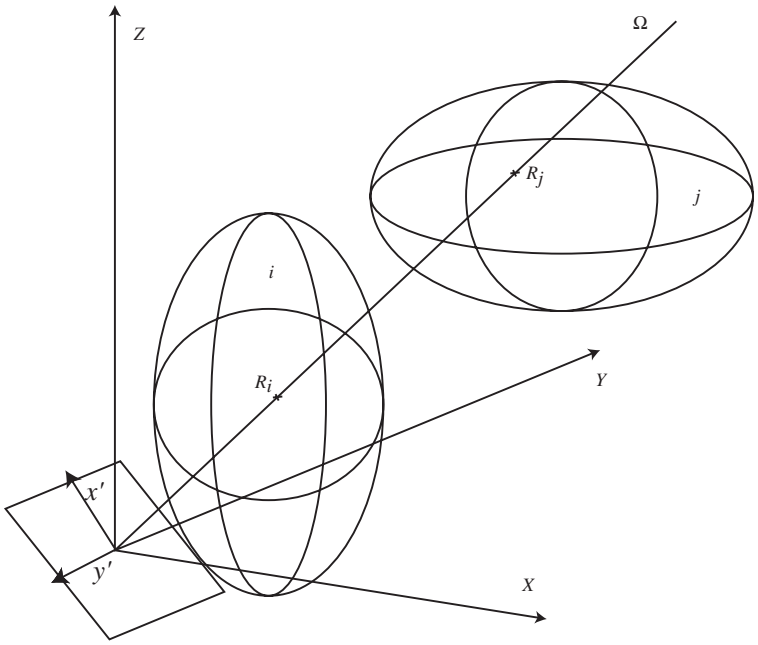

Figure 8: Example of a general 3–D geometry

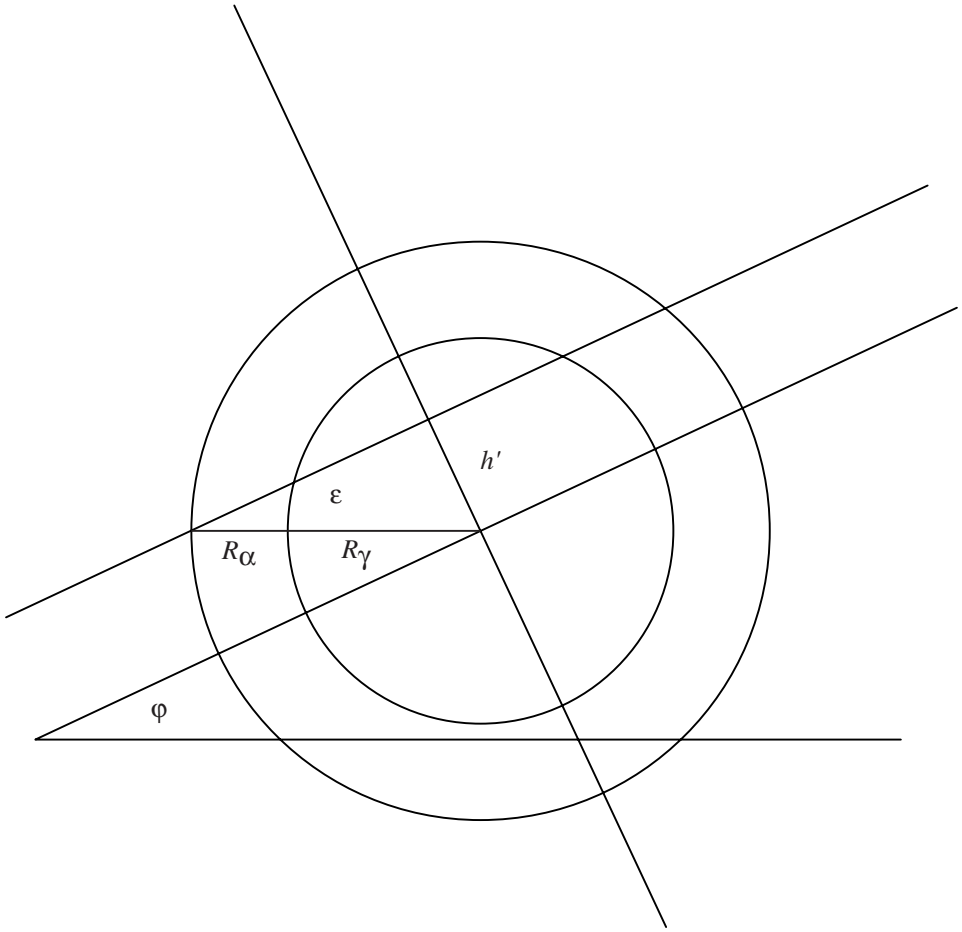

Figure 9: Integration variables for annular 1–D geometry in the $J_{\pm}$ model

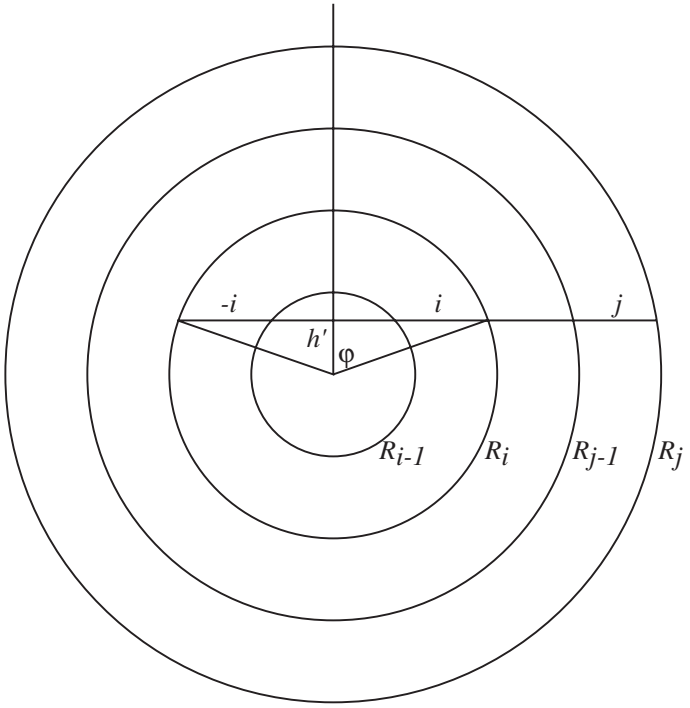

Figure 10: Integration variables for annular 1–D geometry in the standard model

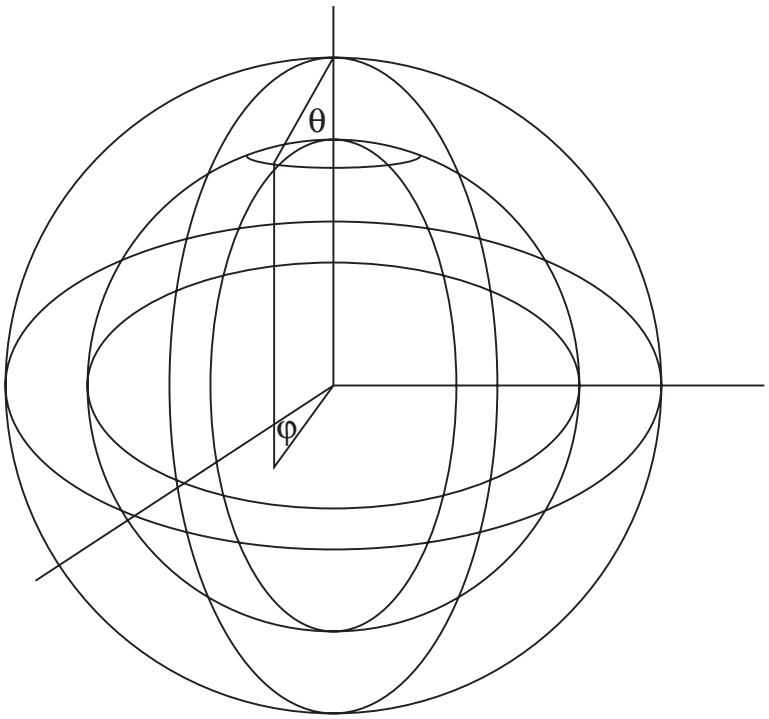

Figure 11: Integration variables for spherical 1–D geometry in the $J_{\pm}$ model

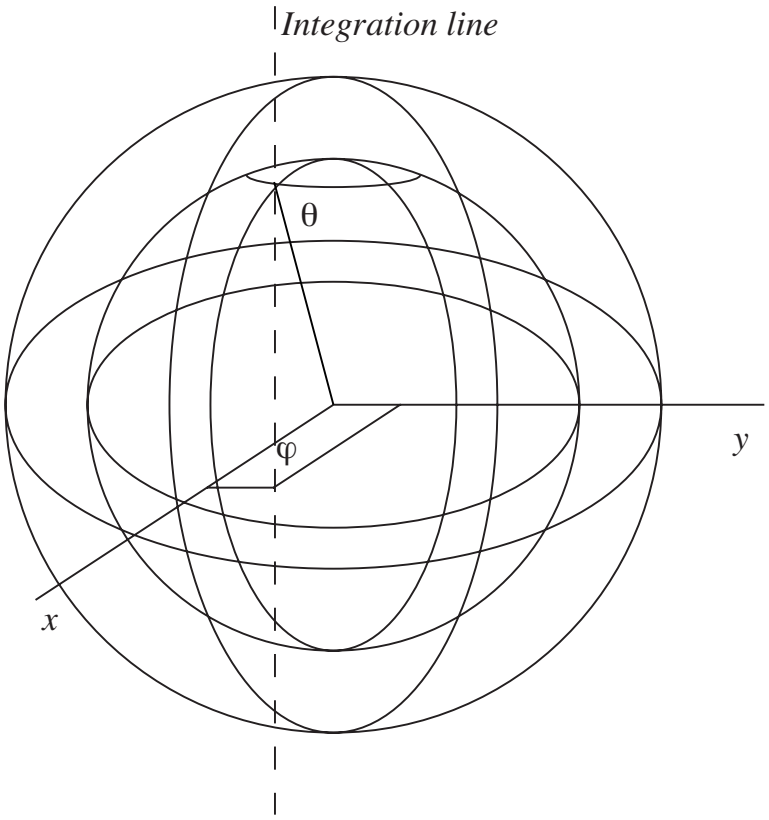

Figure 12: Integration variables for spherical 1–D geometry in the standard model

Allowed geometry

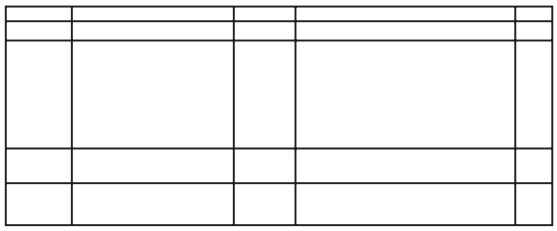

Forbidden geometries

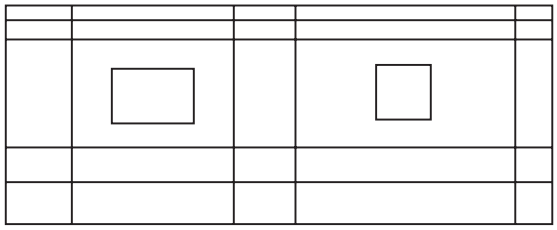

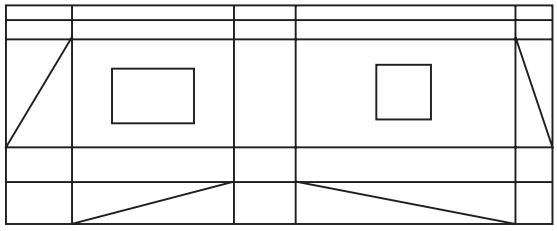

Figure 13: Pure Cartesian 2–D geometries allowed and forbidden in DRAGON

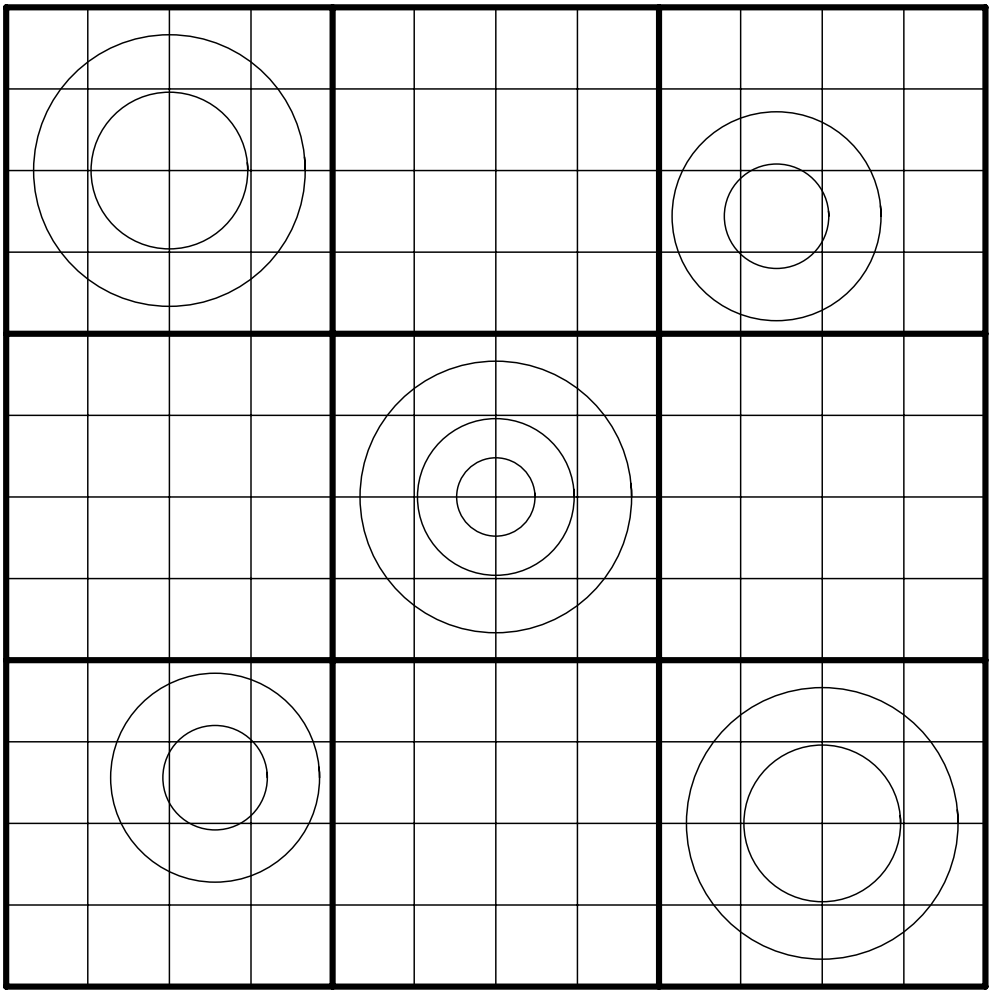

Figure 14: Cartesian 2–D geometry with embedded annular regions allowed in DRAGON

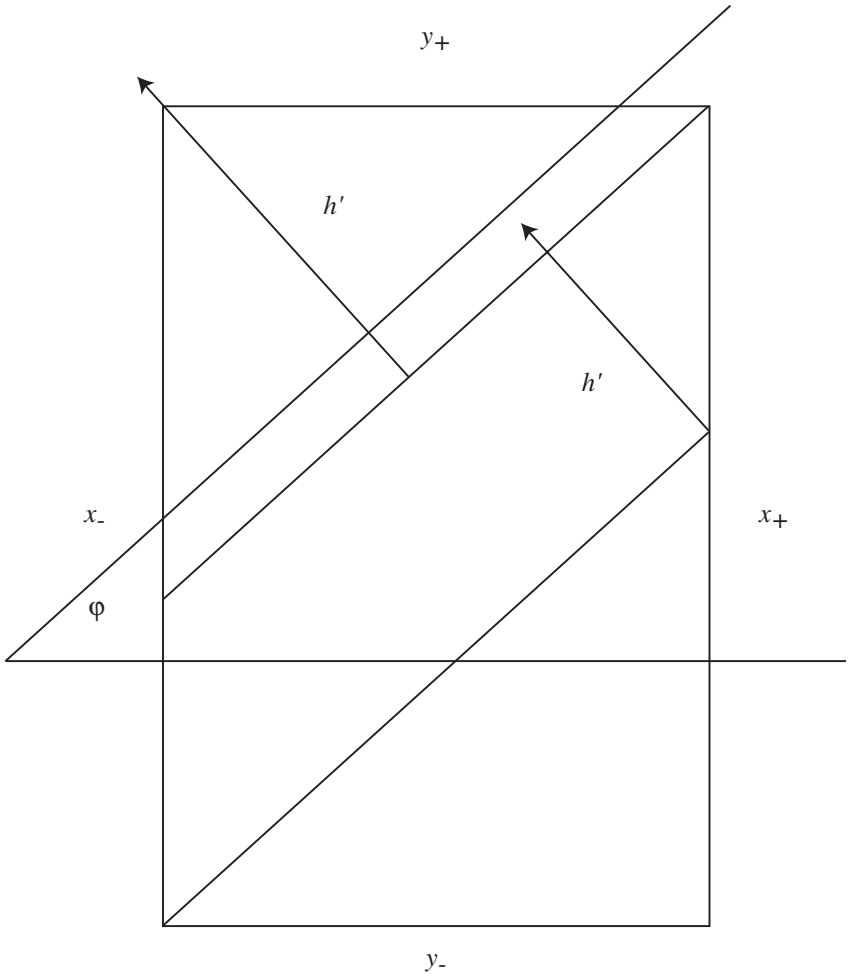

Figure 15: Integration variables for a pure Cartesian 2–D geometry in the $J_\pm$ model

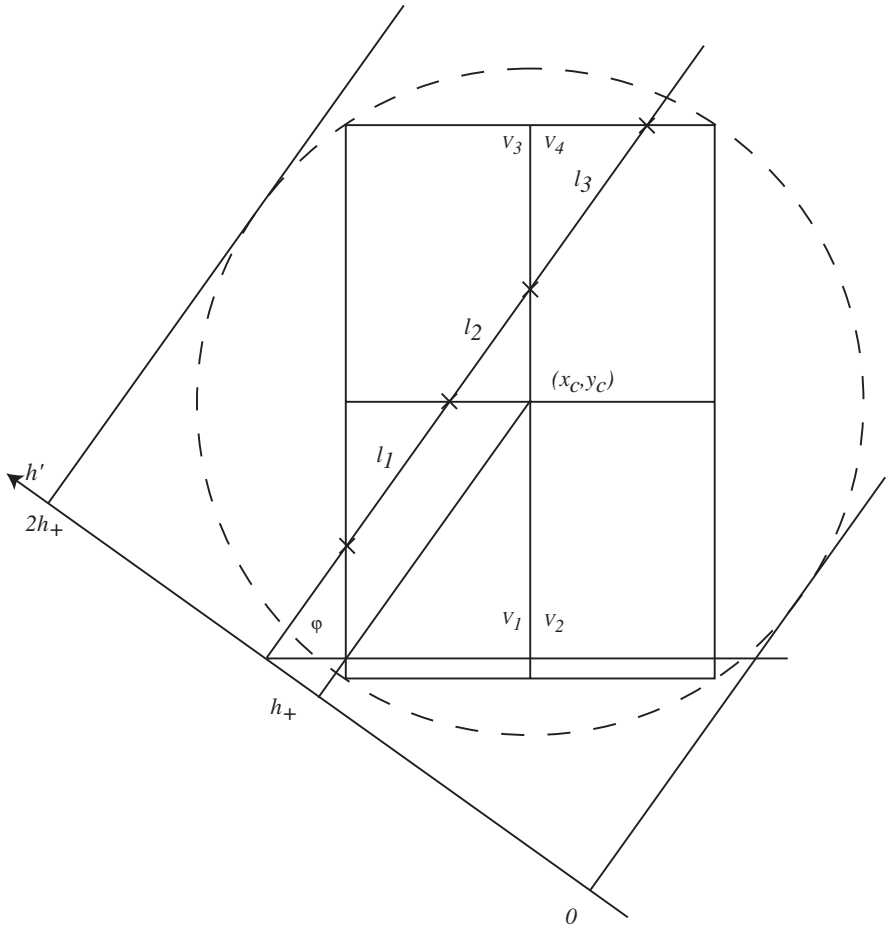

Figure 16: Integration variables for a pure Cartesian 2–D geometry in the standard model

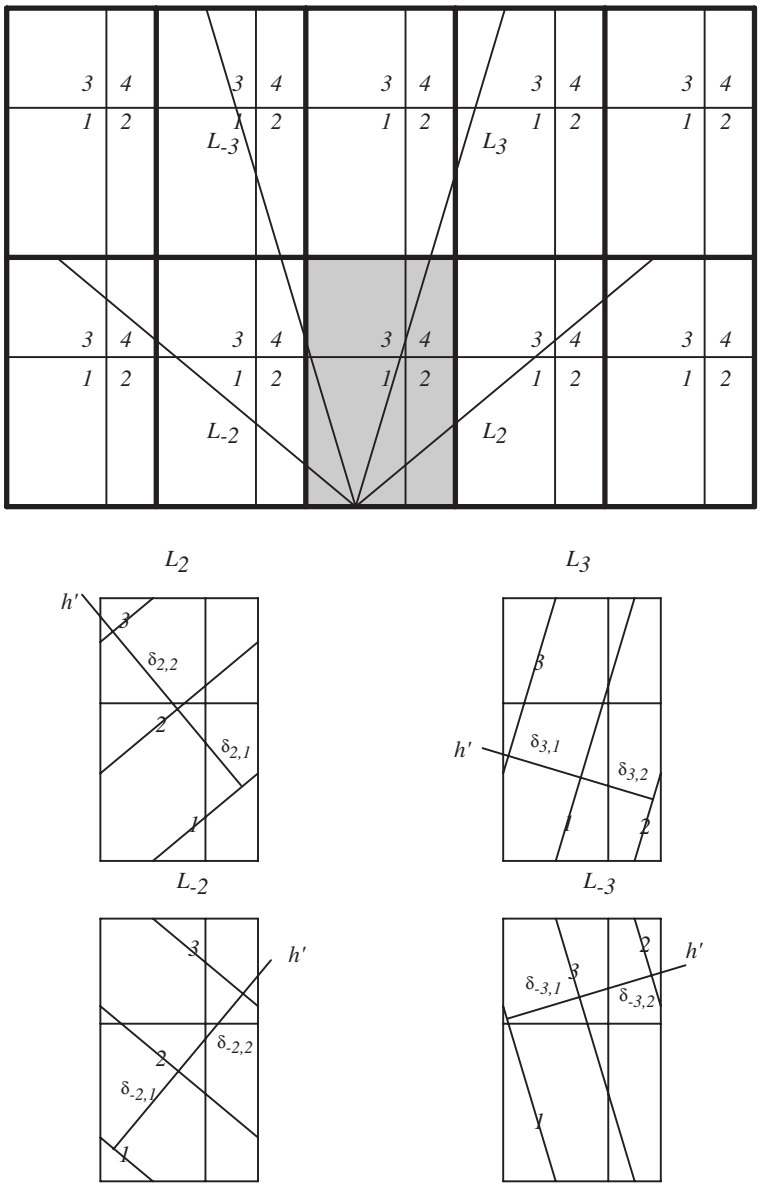

Figure 17: Tracking of an infinite Cartesian 2–D geometry with periodic boundary conditions

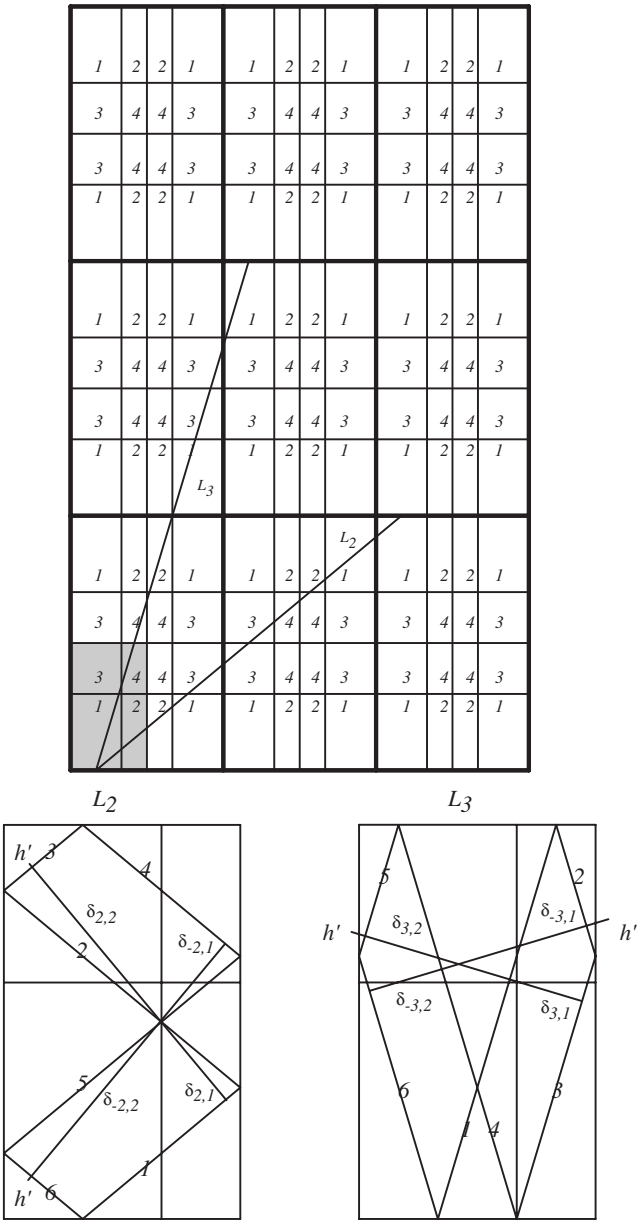

Figure 18: Tracking of an infinite Cartesian 2–D geometry with reflection boundary conditions

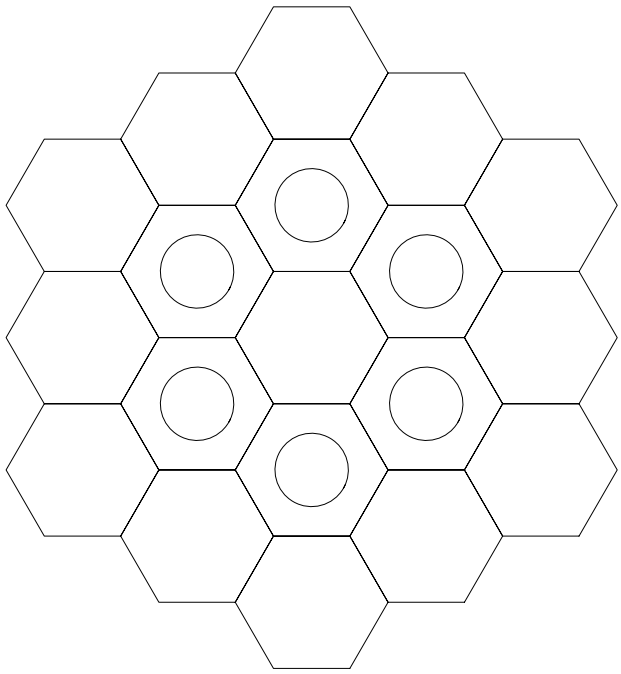

Figure 19: Example of a 2–D assembly composed of hexagon and allowed in DRAGON

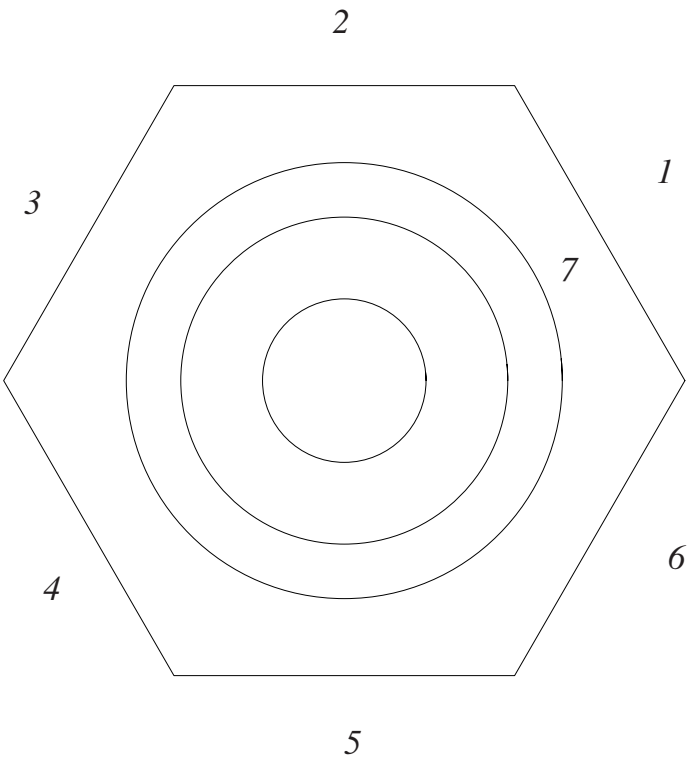

Figure 20: Surfaces definition for a 2–D hexagon in the $J_{\pm}$ model

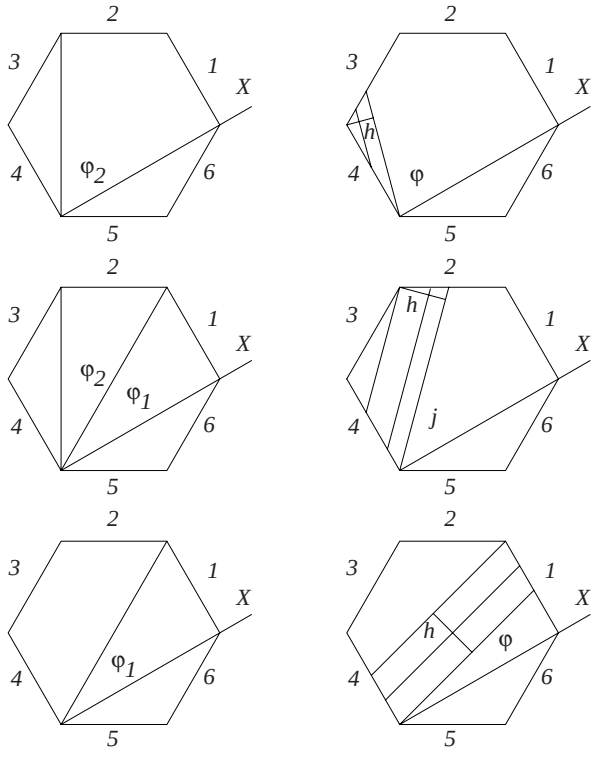

Figure 21: Integration variables for a 2–D hexagon in the $J_{\pm}$ model

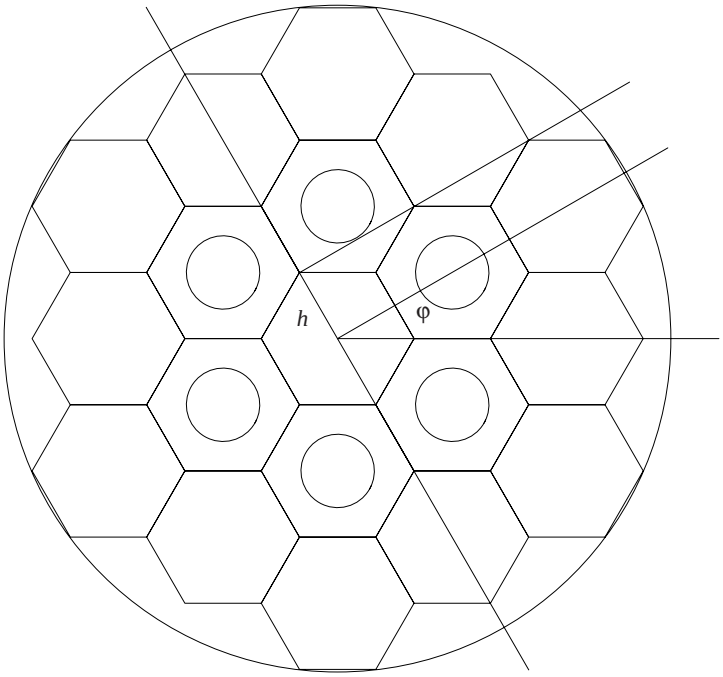

Figure 22: Integration variables for a 2–D hexagon in the standard model

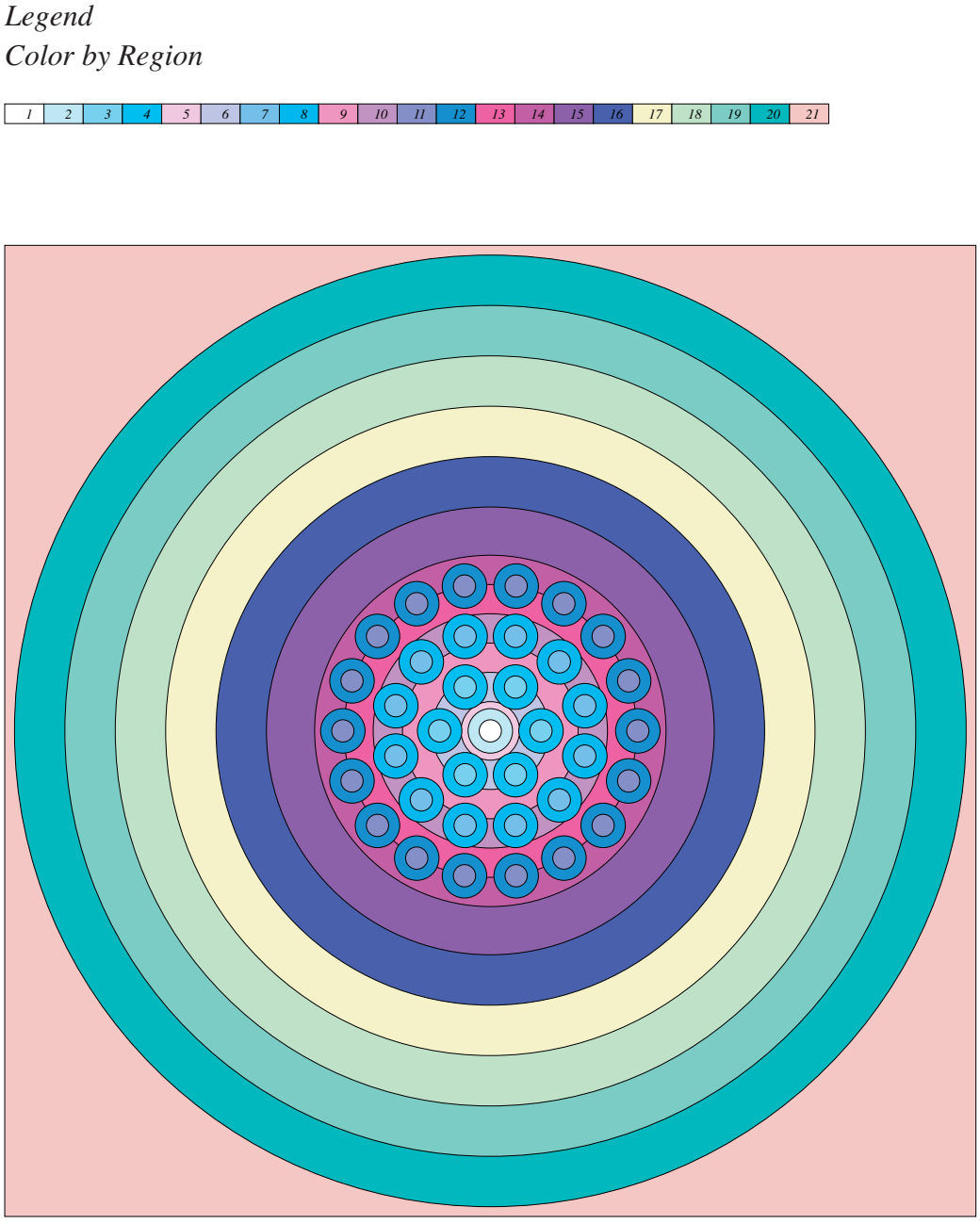

Figure 23: Cartesian 2–D geometry with pin clusters

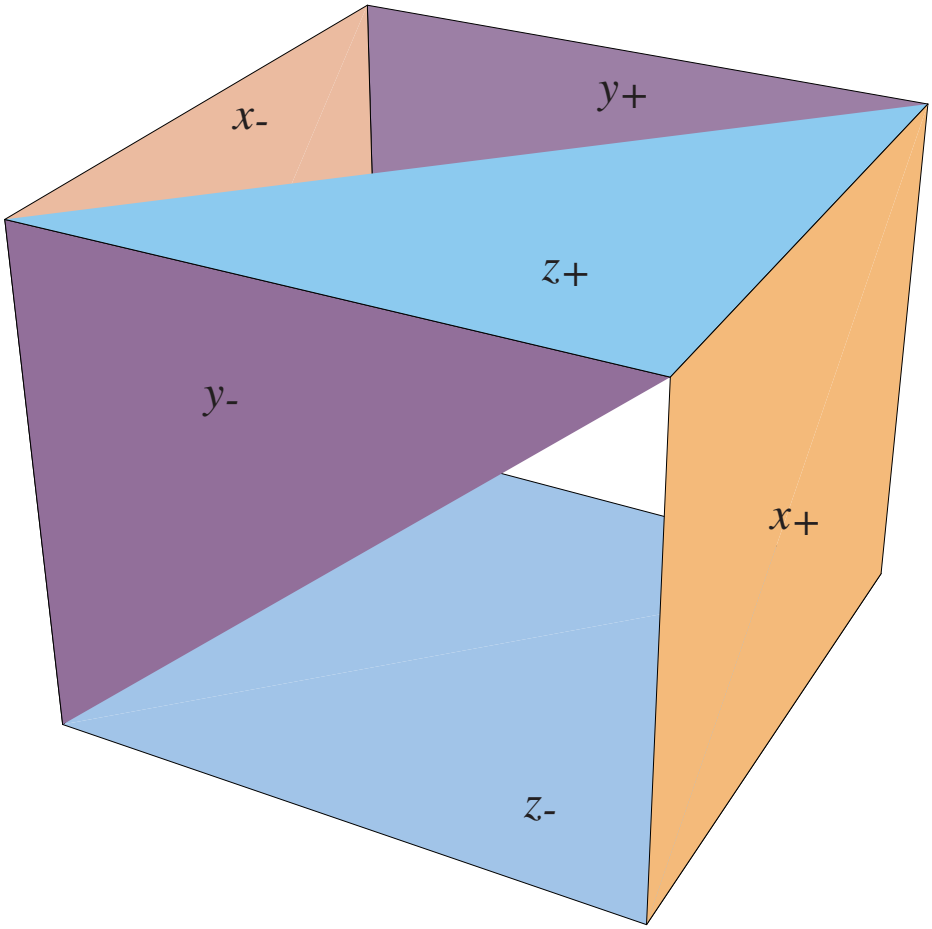

Figure 24: A simple 3–D Cartesian cell

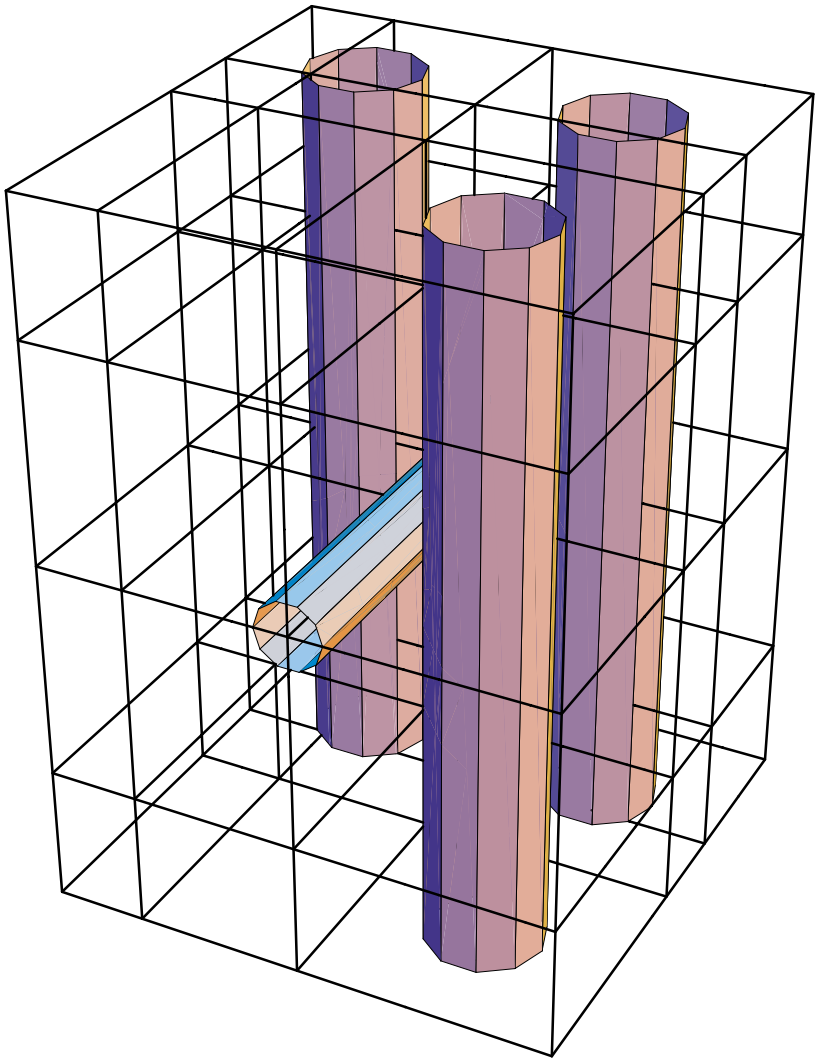

Figure 25: A general 3–D Cartesian assembly

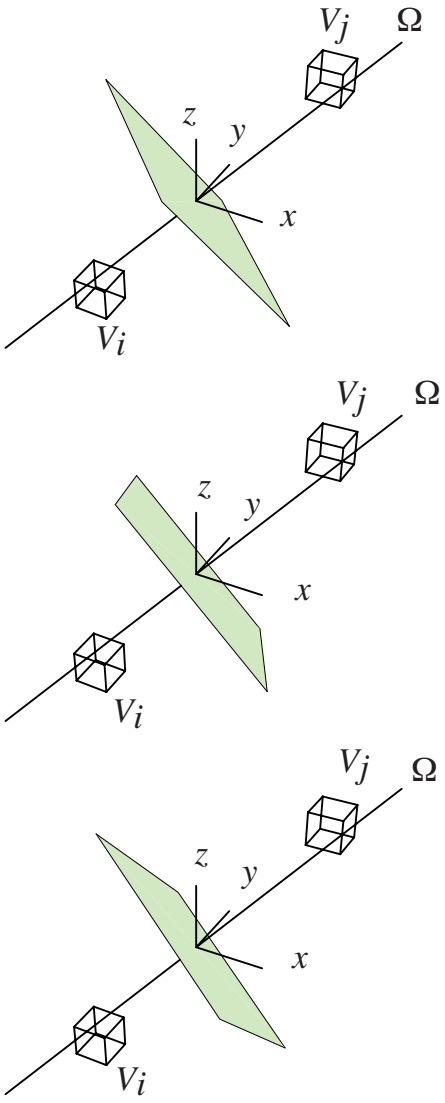

Figure 26: Tracking for Cartesian 3–D geometry

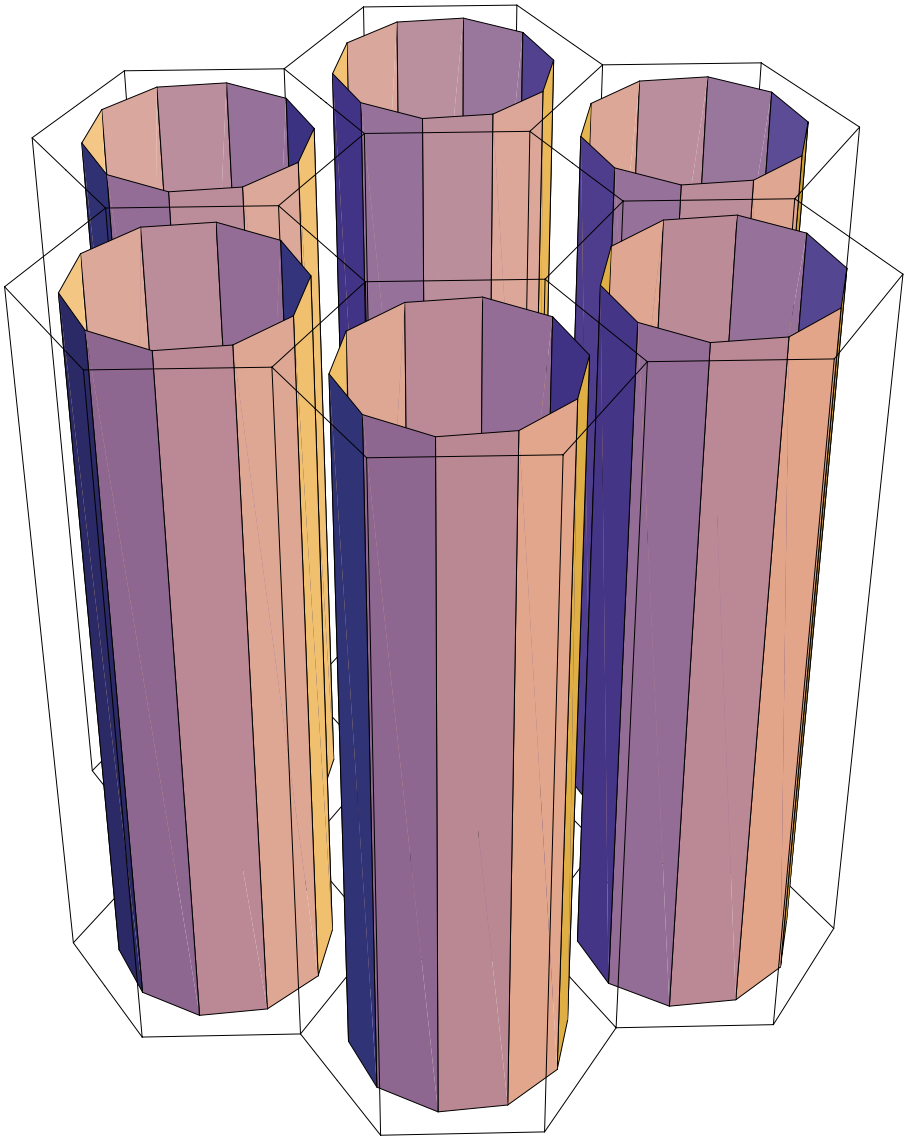

Figure 27: Example of a 3–D assembly composed of hexagon and allowed in DRAGON

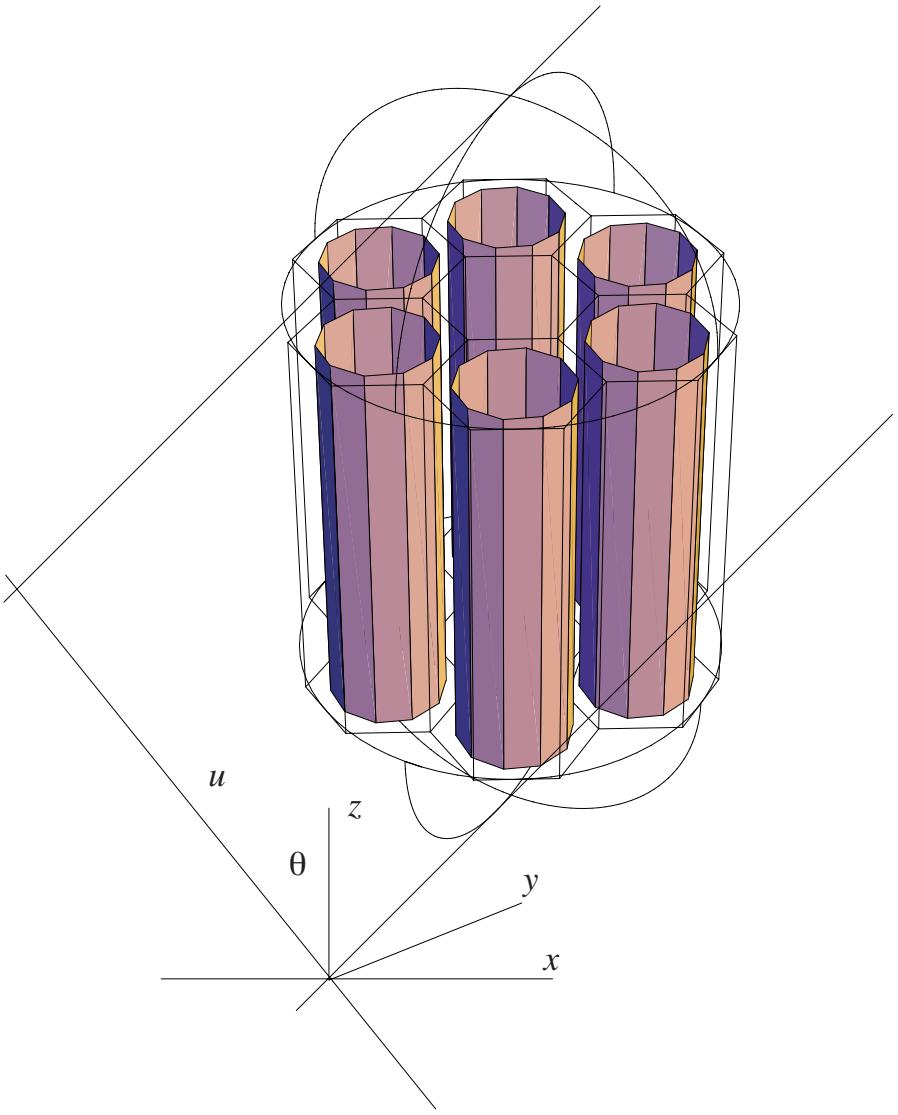

Figure 28: Integration variables for a 3–D hexagon

APPENDICES

APPENDIX A

PROPERTIES OF THE EXPONENTIAL INTEGRAL FUNCTIONS

A.1 Definition

The exponential integral functions are defined as:[31]

$$\begin{aligned} E_n(x) =& x^{n-1}\int_x^\infty \frac{e^{-t}}{t^n}dt = \int_1^\infty \frac{e^{-xt}}{t^n}dt \\ =& \int_0^1 t^{n-2}e^{-x/t}dt = x^{n-1}\int_0^{1/x} t^{n-2}e^{-1/t}dt \end{aligned}$$

for $n \geq 0$. In fact, in the case where $n = 0$ the integral above can be evaluated analytically and we will have:

$$E_0(x) = \frac{e^{-x}}{x}$$

They satisfy the following recurrence relations:

$$E_{n+1}(x) = \frac{1}{n}\left(e^{-x} - xE_n(x)\right)$$

for $n \geq 1$.

A.2 Differentiation and Integration Formulas

The derivative of an exponential integral function is given by

$$\frac{d}{dx}E_n(x) = -E_{n-1}(x)$$

for $n \geq 1$. This equation can be inverted to yield:

$$\int E_n(x)dx = -E_{n+1}(x)$$

for $n \geq 0$.

A.3 Series Expansion

The power series expansion for the exponential integral functions are of the form:

$$E_n(x) = \left[-\ln(x) - \gamma + \sum_{m=1}^{n-1}\frac{1}{m}\right]\frac{(-x)^{n-1}}{(n-1)!} - \sum_{m=1}^{n-2}\frac{(-x)^m}{(m-n+1)\,m!} - \sum_{m=n}^{\infty}\frac{(-x)^m}{(m-n+1)\,m!}$$

They can also be represented by the following incomplete Gamma function:

$$E_n(x) = x^{n-1}\Gamma(1-n, x)$$

and their asymptotic expansions are:

$$E_n(x) = \frac{e^{-x}}{x}\sum_{m=0}^{\infty}\frac{(-1)^m(n+m-1)!}{(n-1)!\,x^m}$$

A.4 Numerical Evaluation

In the case where $n > 1$, one can evaluate explicitly the exponential integral at $x = 0$ using their definition. This yields:

$$E_n(0) = \frac{1}{n-1}$$

For $0 < x < 1$, the following power series expansion can be used for numerical evaluation purpose:

$$E_1(x) = -\ln(x) + \sum_{i=0}^{5} a_i x^i + \epsilon(x)$$

where $\epsilon(x) < 2 \times 10^{-7}$ for all x in this range if

i	a_i
0	-0.57721566
1	$+0.99999193$
2	-0.24991055
3	$+0.05519968$
4	-0.00976004
5	$+0.00107857$

For $1 \leq x \leq \infty$, the following rational approximation can be used:

$$E_1(x) = \frac{e^{-x}}{x}\left(\frac{\sum_{i=0}^{4} b_i x^i}{\sum_{i=0}^{4} c_i x^i} + \epsilon(x)\right)$$

where $\epsilon(x) < 2 \times 10^{-8}$ for all x in this range if

i	b_i	c_i
0	0.2677737343	3.9584969228
1	8.6347608935	21.0996530827
2	18.0590169730	25.6329561486
3	8.5733287401	9.5733223454
4	1.0000000000	1.0000000000

Finally for $n > 1$, the numerical evaluation of the exponential integrals can be obtained using the above relations in conjunction with the recurrence relation described above.

APPENDIX B

PROPERTIES OF THE BICKLEY NAYLER FUNCTIONS

B.1 Definition

The Bickley Nayler functions are defined as:[12,32]

$$\begin{aligned}\mathrm{Ki}_n(x) &= \int_0^{\frac{\pi}{2}} d\theta \,(\sin\theta)^{n-1} \exp\left[\frac{-x}{\sin\theta}\right] \\ &= \int_0^1 du \left(\sqrt{1-u^2}\right)^{n-2} \exp\left(\frac{-x}{\sqrt{1-u^2}}\right),\end{aligned}$$

for all n. Here, $\mathrm{Ki}_0(x)$ and $\mathrm{Ki}_{-1}(x)$ are the modified Bessel functions of the second kind of order 0 and 1 respectively. They satisfy the following recurrence relations:

$$\mathrm{Ki}_n(x) = \left(\frac{n-2}{n-1}\right)\mathrm{Ki}_{n-2}(x) + \left(\frac{x}{n-1}\right)\left[\mathrm{Ki}_{n-3}(x) - \mathrm{Ki}_{n-1}(x)\right]$$

B.2 Differentiation and Integration Formulas

The derivative of a Bickley Nayler function is given by

$$\frac{d}{dx}\mathrm{Ki}_n(x) = -\mathrm{Ki}_{n-1}(x).$$

This equation can be inverted to yield:[12]

$$\mathrm{Ki}_n(x) = \int_x^\infty \mathrm{Ki}_{n-1}(y)dy$$

B.3 Series Expansion

The power series expansion for the Bickley Nayler functions are of the form:

$$\mathrm{Ki}_n(x) = \mathrm{Ki}_n(0) - x\mathrm{Ki}_{n-1}(0) + \frac{x^2}{2}\mathrm{Ki}_{n-2}(0) + \ldots$$

They also have asymptotic expansions of the form:

$$\mathrm{Ki}_n(x) = e^{-x}\sqrt{\frac{\pi}{2x}}\left\{1 - \frac{4n+1}{8x} + \frac{3(16n^2+24n+3)}{2!(8x)^2}\ldots\right\}$$

B.4 Numerical Values

In DRAGON the numerical value of the Bickley Nayler functions are evaluated using the subroutine `AKIN10` which is adapted from the `KIN` routine written by P. Christie for AELIB. It uses rational Chebyshev approximations for $\mathrm{Ki}_8(x)$, $\mathrm{Ki}_9(x)$ and $\mathrm{Ki}_{10}(x)$ with a backward recursion formula when $x > 6$ and rational Chebyshev approximations for $\mathrm{Ki}_1(x)$, $\mathrm{Ki}_2(x)$ and $\mathrm{Ki}_3(x)$ with a forward recursion formula when $0 \leq x \leq 6$.

APPENDIX C

GAUSSIAN QUADRATURES USED IN DRAGON

The general Gaussian quadrature methods are defined in the following way. One wants to select a set of N integration weights (w_i) and points (x_i) in such a way that the weighted integral of $f(x)$ over x given by:

$$\int_a^b f(x)g(x)dx = \sum_{i=1}^{N} w_i f(x_i),$$

is exact for the case where $f(x)$ is a polynomial of order $2 * N - 1$ or lower.[31] Here we will consider two special forms of the Gaussian quadrature corresponding to the case where the weight function takes the value $g(x) = 1$ and $g(x) = x$ corresponding to the Gauss–Legendre and Gauss–Jacobi quadrature respectively.

C.1 Gauss–Legendre quadrature

The integrations weights and points in the Gauss–Legendre quadrature are selected in such a way that:

$$\int_{-1}^{1} f(x)dx = \sum_{i=1}^{N} w_i f(x_i),$$

is exact when $f(x)$ is a polynomial of order $2 * N - 1$ or lower. This can be ensured by selecting the x_i for each order N as the zero's of the Legendre polynomials $P_N(x)$. Once the integration points have been computed, the associated weights can be obtained using:

$$w_i = \frac{2}{(1 - x_i^2)\left[P'_N(x_i)\right]^2}.$$

For the case where the lower and upper integration limits are a and b respectively one can use the following transformation:

$$\int_a^b f(x)dx = \sum_{i=1}^{N} w'_i f(x'_i),$$

such that

$$\begin{aligned} w'_i &= \frac{b-a}{2} w_i, \\ x'_i &= \frac{b-a}{2} x_i + \frac{b+a}{2} \end{aligned}$$

with the points x_i and the weight w_i as defined above. In DRAGON the Gauss–Legendre points and weights for arbitrary integration limits (x'_i and w'_i) can be obtained for values of N ranging from 2 to 20 and for 24, 28, 32, and 64 by calling the subroutine `ALGPT`.

C.2 Gauss–Jacobi quadrature

The integrations weights and points in the Gauss–Jacobi quadrature are selected in such a way that:

$$\int_0^1 x f(x)dx = \sum_{i=1}^{N} w_i f(x_i),$$

is exact when $f(x)$ is a polynomial of order $2 * N - 1$ or lower. This can be ensured by selecting the x_i for each order N as the zero's of the polynomials $q_N(x)$ which are defined in terms of the Jacobi polynomials $P_N^{(k,0)}(x)$ as follows:

$$q_N(x) = \sqrt{2n+2} P_N^{(1,0)}(1-2x)$$

Once the integration points have been computed, the associated weights can be obtained using:

$$w_i = \left(\sum_{j=0}^{N-1} \left[q_j(x_i) \right]^2 \right)^{-1}$$

For the case where the lower and upper integration limits are 0 and b respectively one can use the following transformation:

$$\int_0^b x f(x) dx = \sum_{i=1}^{N} w_i' f(x_i')$$

such that

$$\begin{aligned} w_i' &= b^2 w_i, \\ x_i' &= b x_i \end{aligned}$$

with the points and weight defined as above. In DRAGON the Gauss–Jacobi points and weights for the reference integration limits (x_i and w_i) can be obtained for values of N ranging from 1 to 8 by calling the subroutine `ALGJP`.

APPENDIX D

CONTENTS OF THE DRAGON BINARY TRACKING FILE

D.1 EXCELL Tracking File

The EXCELL tracking files are stored in a sequential binary format. They contain all the information required by the collision probability integrator to evaluate the collision probabilities associated with a geometry. In DRAGON, such files are generated indirectly, that is, first, a temporary tracking file is created by one of the DRAGON tracking options.[14] This temporary file is then processed by a track normalization routine which modifies the segment length associated with each region in such a way that the use of the normalized tracking file for regional volume evaluation results in the analytical volumes. The final tracking file is then written using the following FORTRAN instructions

```
      WRITE(IUNIT) '$TRK',NCOMNT,NBTR
      DO 100 ICOM=1,NCOMNT
        WRITE(IUNIT) COMNT(ICOM)
 100  CONTINUE
      WRITE(IUNIT) NDIM,ISPEC,NREG,NSOUT,NALBG,NCOR,NANGL,MXSEG
      WRITE(IUNIT) (VOLSUR(II),II=-NSOUT,NREG)
      WRITE(IUNIT) (MATALB(II),II=-NSOUT,NREG)
      WRITE(IUNIT) (ICODE(II),II=1,NALBG)
      WRITE(IUNIT) (GALBED(II),II=1,NALBG)
      WRITE(IUNIT) ((ANGLE(II,JJ),II=1,NDIM),JJ=1,NANGL)
      WRITE(IUNIT) (DENSTY(JJ),JJ=1,NANGL)
      DO 110 ILINE=1,NBTR
        IF(NSEG .GT. 0) THEN
          WRITE(IUNIT) IANGL,NSEG,WEIGHT,
     >               (NRSEG(II),II=1,NSEG),
     >               (SEGLEN(II),II=1,NSEG)]
        ENDIF
 110  CONTINUE
```

where

`IUNIT`	FORTRAN unit associated with this file
`$TRK`	Character*4 keyword to identify a tracking file
`NCOMNT`	Number of comment records.
`NBTR`	Total number of tracks records. In the initial pass generating the temporary tracking file, `NBTRK`=0. It is reset to the exact number of tracks before being transferred to the final track file.
`COMNT`	Character*80 comment line.
`NDIM`	Dimension of problem (2 for 2-D geometry and 3 for 3-D geometry).
`ISPEC`	Type of tracking. `ISPEC`=0 for normal tracking and `ISPEC`=1 for specular tracking.
`NREG`	Number of regions.
`NSOUT`	Number of outer surfaces.
`NALBG`	Number of geometric albedos.

NCOR	Number of initial and final surfaces that can be crossed by a track.
NANGL	Number of track direction angles considered in the integration.
MXSEG	Maximum number of line segments per track.
VOLSUR	Surface-volume vector.
MATALB	Surface direction and region material identification vector.
ICODE	Albedo number associated with a face. Negative values for ICODE refers to a geometric albedo while positive values refers to a physical albedo.
GALBED	Geometric albedos.
ANGLE	Tracking angle directions. For 2-D geometry they represent the cosine and sine of the tracking angles respectively while for 3-D geometries, they represent the 3 director cosines associated with the track direction.
DENSTY	Density associated with each tracking angle. For 2-D geometries, this is a linear density while for 3-D geometries it is a surface track density.
IANGL	Angle number for this track.
NSEG	Number of segments for this track.
WEIGHT	Integration weight factor associated with this track.
NRSEG	Surface (negative) and region (positive) numbers crossed by track. When ISPEC=0, the first and the last elements of this vector are associated with the external surfaces, all the other elements being associated with region numbers. When ISPEC=1, NRSEG starts and finishes with a surface number. In addition the surface numbers will be mixed with the region numbers in the remaining elements of the vector NRSEG.
SEGLEN	Length of segment crossing a region. Elements of the vector SEGLEN associated with surfaces are set to 1.0 for isotropic scattering and 0.5 for specular tracking.